CHARACTERIZATION OF NOVEL WNT/β-CATENIN PATHWAY TARGETS

by

İzzet Akiva

B.S., Molecular Biology and Genetics, Boğaziçi University, 2006

M.S., Molecular Biology and Genetics, Boğaziçi University, 2009

Submitted to the Institute for Graduate Studies in
Science and Engineering in partial fulfillment of
the requirements for the degree of
Doctor of Philosophy

Graduate Program in Molecular Biology and Genetics

Boğaziçi University

2016

CHARACTERIZATION OF NOVEL WNT/β-CATENIN PATHWAY TARGETS

APPROVED BY:

Assist. Prof. Necla Birgül İyison .....

(Thesis Supervisor)

Prof. Kuyaş Buğra .....

Prof. Nesrin Özören .....

Prof. Uğur Sezerman .....

Prof. Eda Tahir Turanlı .....

DATE OF APPROVAL: 22.09.2016

To my mother and father...

ACKNOWLEDGEMENTS

First and foremost, I would like to express my sincere gratitude to my thesis advisor Assist. Prof. Necla Birgül İyison for her constant support in many aspects, for being considerate and insightful. I would also like to thank her for her guidance, valuable criticism, motivation and encouragement throughout this study.

I would like to extend my thanks to my thesis committee members Prof. Kuyaş Buğra, Prof. Nesrin Özören, Prof. Uğur Sezerman and Prof. Eda Tahir Turanlı for their helpful suggestions and for sharing their valuable time to evaluate, criticize and improve this thesis.

I would like to add my appreciations to all current and former CSL Lab members for creating such a fun and warm lab environment which always motivated me during the course of my study. Especially, I want to thank Tuncay Şeker M.Sc., Burçin Duan M.Sc., Tolga Aslan M.Sc., Aida Shahraki M.Sc. and Ali İşbilir M.Sc., for their both scientific and nonscientific discussions, for coloring up the laboratory life with their sense of humor and miscellaneous attractions. I would also like to thank them for sharing their experience, improving my knowledge in various aspects and providing unending support.

I would like to thank the members of AKIL, Yamanlab, Genreg, Retina and Kommagene groups for their help and support both experimentally and theoretically. I want to thank specially to Neslihan Zohrap Ph.D., Elif Eren Ph.D., Ayşin Demirkol M.Sc., Aslı Uğurlu and Mustafa Yalçınkaya M.Sc., for sharing their knowledge on different experimental techniques.

Furthermore, I want to thank to Serkan Uğurlu M.D., Ph.D., for providing me plasmids for luciferase experiments, Mehmet Can Demirler for sharing his time and effort in obtaining confocal microscopy images, Aybüke Garipcan M.Sc., for her assistance in FACS analysis, Yeşerin Yıldırım Ph.D. and Esra Yıldız for their help and patience during my real-time PCR experiments.

I would like to thank all the Vivarium staff, especially to Arzu Temizyürek DVM, and Ersin Eruz for their assistance and guidance with in vivo xenograft experiments and mice injections. They contributed a lot in this study and I really appreciate all they have done. Without their help, support and patience, I certainly would not be able to handle these kind of experiments by myself.

I would like to honor my closest friends Yusuf Ergen and Enver Çıracı for their friendship and help whenever I need most.

I am very thankful to Selgin Deniz Çakal, who has always been very affectionate. I am very happy to have her support which is a great source of motivation for me all the time.

I want to appreciate our department's faculty members and graduate students for raising me academically and taking care of all the questions, problems and hardships that I encountered during my study.

This study has been supported by funding from TUBITAK (The Scientific and Technological Research Council of Turkey) - 108T183 and BAP (Boğaziçi University Research Projects) 08B101, 6734P and 15B01D3.

Finally, I am very grateful to TUBITAK-BIDEB for awarding and supporting me with BIDEB 2211 Scholarship program during my graduate study.

ABSTRACT

CHARACTERIZATION OF NOVEL WNT/BETA-CATENIN PATHWAY TARGETS

The Wnt/β-catenin signaling pathway is an evolutionary conserved pathway which has important functions in vertebrate early development such as axis formation, cellular proliferation and morphogenesis. The activation of this pathway leads to translocation of the transcriptional activator β-catenin into the nucleus where it activates T-cell factor/Lymphoid enhancer factor (Tcf/Lef) family of transcription factors, which regulate expression of developmental and cell cycle-related genes. Apart from its roles in various cellular processes, Wnt/β-catenin signaling pathway is also one of the most important intracellular pathways implicated cancer progression. A significant number of identified target molecules of this pathway, are known to have tumorigenic characters when mutated.

Previous studies confirmed BRI3 (Brain protein I3) gene to be one of the transcriptional target genes of Wnt/β-catenin pathway. We used various approaches for the functional characterization of its novel targets. As a first step in our study, IFITM3 and MGAT1 proteins were confirmed as interaction partners for BRI3 by Yeast-two Hybrid and Co-IP techniques. BRI3 was found to be upregulated in response to TNF-α treatment and overexpression of BRI3 resulted in an increase in NFkB promoter activity. On the other hand, MGAT1 is a putative novel target of Wnt/β-catenin signaling pathway and determined to be upregulated in response to β-catenin activation. Cell proliferation and migration assays showed that, Huh7 cells stably expressing each of the BRI3 and MGAT1 genes have greater proliferative and invasive capabilities compared to control Huh7 cells. Furthermore, *in vivo* xenograft experiments were performed and it was determined that the stable overexpression of both of these genes in Huh7 cell lines lead to increased rate of tumor growth in NUDE/SCID mice. The resulting tumors were subjected to transcriptomic analyses using RNA-Sequencing technique in order to determine which pathways and biological processes take part in the cancer initiation process.

ÖZET

WNT/BETA-KATENIN YOLAĞININ YENİ HEDEF GENLERİNİN KARAKTERİZASYONU

Evrimsel süreçte korunmuş bir yolak olan Wnt/β-katenin sinyal yolağının omurgalı erken gelişiminde, eksen oluşumunda, hücresel farklılaşma ve morfojenezde önemli görevleri vardır. Bu yolağın aktifleşmesi, β-catenin molekülünün hücre çekirdeğine taşınmasını ve orada T-hücresi faktörü/Lenfoid arttırıcı faktör (Tcf/Lef) ailesinden olan transkripsiyon faktörlerini aktifleştirerek gelişimsel ve hücre döngüsüyle alakalı genlerin anlatımlarını düzenler. Birçok farklı hücresel süreçteki görevinin dışında, Wnt/β-katenin sinyal yolağı aynı zamanda kanser gelişiminde de kritik öneme sahip hücre içi yolaklarından bir tanesidir. Bu yolağın açığa çıkarılan hedef moleküllerinden çok önemli bir kısmının mutasyona uğradıkları taktirde tümör oluşturucu karakterde oldukları bilinmektedir.

Laboratuarımızda yapılan çalışmalarda, BRI3 geninin bu yolağın transkripsiyonel hedef genleri arasında bulunduğu doğrulanmıştır. Yeni hedef genlerin karakterizasyonu amacıyla birçok farklı yaklaşımdan faydalanılmıştır. Çalışmamızın ilk aşaması olarak, Maya ikili hibrit ve Co-IP teknikleri sayesinde IFITM3 ve MGAT1 proteinleri BRI3'ün bağlanma partnerleri olarak belirlenmiştir. BRI3 protein seviyesinin TNF-α muamelesine bağlı olarak yükseldiği görülmüş ve BRI3'ün yüksek anlatımının NFkB promotor aktivitesinde artışa yol açtığı belirlenmiştir. Öte yandan, Wnt/β-katenin sinyal yolağının varsayılan hedef genlerinden biri olan MGAT1'ın β-katenin aktifleşmesi sonucu anlatımının arttığı saptanmıştır. Yapılan hücre çoğalması ve yerdeğiştirimi deneylerinde BRI3 ve MGAT1 genlerinin yüksek anlatımları sağlanan Huh7 hücrelerinin kontrol Huh7 hücrelerine göre proliferatif ve invazif kapasitelerinin daha yüksek olduğu belirlenmiştir. *In vivo* ksenograft deneylerinde ise bu genlerin her birinin yüksek anlatımları sağlanan Huh7 hücre hatlarının NUDE/SCID farelerin deri altlarına enjekte edilmesi sonucunda tümör büyüme hızında artış görülmüştür. Oluşan tümörler RNA sekanslama yöntemi kullanılarak transkriptomik analize tabi tutulmuş ve bu sayede kanserin oluşma sürecinde hangi genlerin ve sinyal yolaklarının rolü olduğunun belirlenmesi amaçlanmıştır.

TABLE OF CONTENTS

ACKNOWLEDGEMENTS iv

ABSTRACT vi

ÖZET vii

TABLE OF CONTENTS viii

LIST OF FIGURES xiii

LIST OF TABLES xvii

LIST OF SYMBOLS xx

LIST OF ACRONYMS/ABBREVIATIONS xxi

1. INTRODUCTION 1

1.1. Cancer: Overview 1

1.2. Hepatocellular Carcinoma 1

1.2.1. Treatment of Hepatocellular Carcinoma 4

1.3. Wnt Signaling Pathway 5

1.4. The canonical Wnt/β-catenin signaling pathway 7

1.4.1. Major components of the Canonical Wnt pathway 7

1.4.2. The On/Off States of the Canonical Wnt pathway 10

1.5. Wnt/β-catenin pathway and Cancer 11

1.5.1. The Role of Wnt/β-catenin pathway in Hepatocellular Carcinoma 12

1.6. Identification of novel Wnt/β-catenin target genes 12

1.6.1. BRI3 as a novel Wnt/β-catenin pathway target gene 13

1.6.2. MGAT1 15

1.7. NFkB Signaling Pathway 16

1.8. NFkB and cancer 18

1.9. Crosstalk between Wnt/β-catenin and NFkB Signaling 18
2. PURPOSE 20
3. MATERIALS 21
3.1. General Kits, Enyzmes and Reagents 21
3.2. Chemicals 22
3.3. Biological materials 24
3.3.1. Yeast Strains 24
3.3.2. Bacterial Strains 24
3.3.3. Mammalian Cell Lines 24
3.3.4. NUDE/SCID mice in Xenografting 24
3.4. Buffers and Solutions 25
3.4.1. DNA Gel Electrophoresis 25
3.4.2. RNA Gel Electrophoresis 26
3.4.3. Western Blotting Buffers and Solutions 26
3.4.4. Immunoprecipitation Buffers and Solutions 28
3.4.5. Polymerase Chain Reaction 29
3.4.6. Restriction Enzyme Analysis 29
3.4.7. Bacterial Culture Solutions and Antibiotics 30
3.5. Yeast Growth Media 31
3.6. Nucleic Acids 32
3.6.1. Plasmids 32
3.6.2. Oligonucleotides 32
3.7. Antibodies 34
3.8. Disposable Labware 36
3.9. General Equipment 37
4. METHODS 40
4.1. Molecular Cloning 40

4.1.1. PCR Reaction 40
4.1.2. Restriction digestion of plasmids and PCR products 40
4.1.3. Agarose Gel Electrophoresis 41
4.1.4. PCR Purification and Agarose Gel Extraction 41
4.1.5. Ligation of DNA molecules 41
4.1.6. Preparation of Chemically Competent Cells 42
4.1.7. Transformation of the Chemically Competent Cells 42
4.1.8. Colony PCR 42
4.1.9. Plasmid DNA Purification and Sequencing 43
4.2. Cell Culture Experiments 43
4.2.1. Maintenance of Cells 43
4.2.2. Cell Freezing 44
4.2.3. Cell Thawing 44
4.2.4. Transfection of Mammalian Cell Lines 44
4.2.5. TNF-α treatment of HEK293-4KB-GFP cell lines 45
4.3. Yeast Two Hybrid Screening 45
4.4. SDS/PAGE and Western Blotting 46
4.4.1. Cell Lysis and Protein Extraction from HEK293FT Cell Line 46
4.4.2. Quantification of Protein Lysates 46
4.4.3. SDS/PAGE 47
4.4.4. Western Blotting 47
4.5. Total RNA Isolation 48
4.6. Reverse Transcription PCR (RT-PCR) 49
4.7. Coimmunoprecipitation 49
4.8. Generation of Stable Cell Lines 50
4.9. PI Staining and FACS Analysis 50
4.10. Wound Healing Assay 51

4.11. XTT Cell Proliferation Assay 51
4.12. Luciferase Reporter Assay 52
4.13. Lithium Treatment Assay 52
4.14. Confocal Microscopy 53
4.15. Quantitative Polymerase Chain Reaction 53
4.16. Xenograft on NUDE/SCID mice 54
4.17. RNA Sequencing 54
5. RESULTS 56
5.1. Identification of Interaction Partners of BRI3 56
5.1.1. Co-Immunoprecipitation of BRI3 and its isoform with the candidate interaction partners 59
5.1.2. Colocalization Assay in Huh7 cell lines 61
5.2. MGAT1 and IFITM3 as potential targets of the Wnt/β-catenin pathway 62
5.2.1. LiCl treatment leads to MGAT1 upregulation in Huh7 cells 64
5.2.2. Analysis of MGAT1 and IFITM3 promoter activities 65
5.2.3. Analysis of MGAT1 protein levels in response to β-catenin overexpression 68
5.2.4. Determination of MGAT1 mRNA levels in the presence of Wnt agonists and GSK-3β inhibitor 70
5.3. BRI3 and the NFkB pathway 71
5.3.1. BRI3 might be involved in a complex with TRAF2/TRAF6 heterodimers 71
5.3.2. Analysis of NFkB promoter activity in response to BRI3 overexpression 72
5.3.3. BRI3 protein expression correlates with TNFα levels 73
5.4. Assessing the tumorigenic potentials of BRI3 and MGAT1 74
5.4.1. Generation of stable cell lines overexpressing BRI3 and MGAT1 75

5.4.2.Comparison of migration and proliferation abilities of stable cell lines....75
5.4.3. In vivo analysis of tumorigenesis....80
5.5. Transcriptomic analysis via RNA Sequencing....84
5.5.1. Pathway enrichment analysis via PANOGA....89
5.5.2. Gene Ontology Enrichment Analysis via GOrilla....91
5.5.3. Candidate Gene Selection for Further Analysis....93
6. DISCUSSION....95
REFERENCES....105
APPENDIX A: PLASMID MAPS....119
APPENDIX B: QUANTITATIVE REAL-TIME PCR ANALYSIS OF MGAT1 AND BRI3 IN ISOLATED TUMOR SAMPLES....122
APPENDIX C: COUNT NUMBERS OF MGAT1 AND BRI3 IN TUMOR SAMPLES AS DETECTED BY RNA SEQUENCING....123
APPENDIX D: RNA INTEGRITY NUMBERS (RIN) AND SPECTROPHOTO-METRIC ABSORBANCE RATIOS OF THE TOTAL RNA ISOLATED FROM TUMORS....124
APPENDIX E: RNA INTEGRITY ANALYSES BY AGILENT BIOANALYZER....125

LIST OF FIGURES

Figure 1.1. Major risk factors for developing HCC (Hepatocellular Carcinoma). 2

Figure 1.3. Genetic, epigenetic and genomic contributions to HCC development. 3

Figure 1.4. Wnt/β-catenin signaling cascade in its 'inactive' and 'active' states. 8

Figure 1.5. Experimental flowchart showing the techniques being employed for the identification of novel Wnt/β-catenin pathway targets. 13

Figure 1.6. BRI3 was determined to be a novel target of Wnt/β-catenin pathway by means of several approaches 15

Figure 1.7. Overview of the canonical NFkB Signaling pathway. 17

Figure 5.1. Yeast mating and subsequent screening of the resulting colonies 57

Figure 5.2. Identification of candidate cDNA clones by colony PCR, sequencing and confirmation by co-transformation into yeast cells. 58

Figure 5.3. Alignment and comparison of the aminoacid sequences for the two isoforms of BRI3. Pairwise Sequence Alignment was performed by using EMBOSS Needle tool. 58

Figure 5.4. Western Blot of immunoprecipitated samples from HEK-293T cells transfected with the indicated constructs. 59

Figure 5.5. Coimmunoprecipitation of BRI3 a-isoform together with the candidate proteins from HEK-293T cells 60

Figure 5.6. Coimmunoprecipitation of BRI3 b-isoform together with the candidate proteins from HEK-293T cells.....60

Figure 5.7. Colocalization Assay in Huh7 cells expressing GFP-tagged BRI3 (isoform a) together with either MGAT1-dsRED or IFITM3-dsRED.....61

Figure 5.8. Colocalization Assay in Huh7 cells expressing GFP-tagged BRI3 (isoform b) together with either MGAT1-dsRED or IFITM3-dsRED. 62

Figure 5.9. Basal expression levels of the indicated proteins for various cell lines. 63

Figure 5.10. Western blotting for the expression levels of indicated proteins upon NaCl and LiCl treatment of Huh7 cells. 65

Figure 5.11. Luciferase reporter assay on Huh7 cells in the presence of S33Y-β-catenin overexpression.....66

Figure 5.12. Luciferase reporter assay on Huh7 cells overexpressing S33Y-β-catenin in combination with either TCF4 or dN-TCF4.....67

Figure 5.13. Luciferase reporter assay on Huh7 cells overexpressing S33Y-β-catenin in combination with either TCF4 or dN-TCF4.....68

Figure 5.14. Overexpression of wild-type and mutant β-catenin in Huh7 cells and western blotting to detect the protein levels of the indicated proteins 69

Figure 5.15. Quantitative real-time PCR analysis for the determination of MGAT1 mRNA levels in Huh7 cells treated with different concentrations of Wnt agonist and TWS 119 70

Figure 5.16. Coimmunoprecipitation from HEK293-FT cells transfected with the indicated constructs 72

Figure 5.17. Luciferase reporter assay for the determination of NFkB promoter activity. . 73

Figure 5.18. Time-course TNFα treatment of stable HEK293 cells and determination of the expression levels of indicated proteins by Western Blotting 74

Figure 5.19. Stable Huh7 cells visualized by the fluorescent microscope and determination of RNA and protein levels by RT-PCR and WB..... 75

Figure 5.20. Wound healing assay for the stable cells overexpressing the indicated genes 77

Figure 5.21. Cell cycle profiles of BRI3, MGAT1 and GFP overexpressing stable cells are demonstrated as histograms..... 78

Figure 5.22. Relative absorbance values for the indicated stable cell lines as measured by XTT cell proliferation assay..... 79

Figure 5.23. MGAT1 overexpressing stable cells are subcutaneously injected into the left flank region of each mouse 80

Figure 5.24. BRI3 overexpressing stable cells are subcutaneously injected into the left flank region of each mouse 81

Figure 5.25. Representative tumor images were obtained for comparison. 82

Figure 5.26. Average weights of tumors are plotted for BRI3 vs GFP and MGAT1 vs GFP tumors. 83

Figure 5.27. Overview of the strategy employed for RNA-Sequencing procedure 84

Figure A.1. Restriction map and Multiple Cloning Site (MCS) of pGBKT7 vector used in Yeast-two Hybrid screening for the cloning and expression of the bait protein. 119

Figure A.2. Restriction map and Multiple Cloning Site (MCS) of pACT2 vector which is used in Yeast-two Hybrid screening for the expression of cDNA library proteins.....120

Figure A.3. Restriction map and Multiple Cloning Site (MCS) of pIRES2-EGFP vector which is used for the cloning and stable expression of the genes in mammalian cells. 121

Figure B.1. Determination of MGAT1 and BRI3 mRNA levels in isolated tumors samples.....122

Figure E.1. Agilent Bioanalyzer results of total RNA extractions from MGAT1 and GFP tumor replicates. 125

Figure E.2. Agilent Bioanalyzer results of total RNA extractions from BRI3 and GFP tumor replicates. 125

LIST OF TABLES

Table 1.1. Mutation rates in tumor suppressor genes and oncogenes in Hepatocellular Carcinoma. 6

Table 1.2. Fold changes for the selected candidate genes with respect to SAGE, Microarray and Q-RTPCR results. 14

Table 3.1. List of kits, enzymes and reagents. 21

Table 3.2. Chemicals used in this study. 22

Table 3.3. DNA Gel Electrophoresis buffers and solutions. 25

Table 3.4. RNA Gel Electrophoresis buffers and solutions. 26

Table 3.5. SDS-PAGE and Western Blotting buffers and solutions. 26

Table 3.6. Immunoprecipitation buffers and solutions. 28

Table 3.7. Polymerase chain reaction buffers and solutions. 29

Table 3.8. Buffers used in Restriction Enzyme Analysis. 29

Table 3.9. Solutions and Antibiotics used for the growth and maintenance of 30

Table 3.10. Primers used throughout this study for cloning and diagnostic purposes. 33

Table 3.11. Antibodies used throughout this study. 34

Table 3.12. List of disposable labware used in this study. 36

Table 3.13. Equipment used in this study. 37

Table 4.1. PCR protocol using the Phusion High-Fidelity DNA Polymerase 40

Table 4.2. Reagents used to prepare SDS/PAGE gels 47

Table 5.1. The percentage of cells in each phase of cell cycle. 78

Table 5.2. Weights of the isolated tumors. 82

Table 5.3. Significantly upregulated genes in BRI3 overexpressing tumors in comparison with the GFP overexpressing tumors. 85

Table 5.4. Significantly downregulated genes in BRI3 overexpressing tumors in comparison with the GFP overexpressing tumors. 86

Table 5.5. Significantly upregulated genes in MGAT1 overexpressing tumors in comparison with the GFP overexpressing tumors. 87

Table 5.6. Significantly downregulated genes in MGAT1 overexpressing tumors in comparison with the GFP overexpressing tumors. 88

Table 5.7. List of enriched pathways associated with the differentially expressed genes in BRI3 vs. GFP samples as determined by the PANOGA analysis software. 90

Table 5.8. List of enriched pathways associated with the differentially expressed genes in MGAT1 vs. GFP samples as determined by the PANOGA analysis

software. 90

Table 5.9. GO enrichment analysis (Biological Process) for differentially expressed genes in BRI3 vs. GFP samples as determined by GOrilla analysis. 91

Table 5.10. GO enrichment analysis (Biological Process) for the differentially expressed genes in MGAT1 vs. GFP samples as determined by GOrilla analysis. 92

Table 5.11. List of candidate genes selected for further verification. 94

Table C.1. RNA-Seq count numbers of MGAT1 in three pairs of biological replicates... 123

Table C.2. RNA-Seq count numbers of BRI3 in three pairs of biological replicates. 123

Table D.1. RIN numbers and spectrophotometric absorbance ratios for the MGAT1 and GFP replicates. 124

Table D.2. RIN numbers and spectrophotometric absorbance ratios for the BRI3 and GFP replicates. 124

LIST OF SYMBOLS

A	Adenine
C	Cytosine
°C	Centigrade Degree
G	Guanine
g	Gravity
m	Meter
M	Molar
mg	Miligram
ml	Mililiter
mM	Millimolar
ng	Nanogram
P	Proline
pmol	Picomole
S	Serine
T	Thymine
V	Volt
v	Volume
w	Weight
Y	Tyrosine
u	Unit
α	Alpha
β	Beta
γ	Gamma
Δ	Delta
κ	Kappa
µg	Microgram
µl	Microliter
µM	Micromolar

LIST OF ACRONYMS/ABBREVIATIONS

ActD	Actinomycin D
AD	Activator domain
Amp	Ampicillin
APC	Adenomatous Polyposis Coli
APS	Ammonium persulfate
ATP	Adenosine Triphosphate
BCA	Bicinchoninic Acid Assay
BD	Binding Domain
BLAST	Basic Local Alignment Search Tool
bp	Base pair
BPB	Bromophenol blue
BRI3	Brain protein I3
BRI3BP	BRI3 binding protein
BSA	Bovine Serum Albumine
$CaCl_2$	Calcium chloride
cDNA	Complementary deoxyribonucleic acid
ChIP	Chromatin immunoprecipitation
CKIα	Casein Kinase Iα
CO_2	Carbondioxide
DAPI	4', 6-Diamidino-2-phenylindole
DEPC	Diethylpyrocarbonate
dH_2O	Distilled water
DMEM	Dulbecco's modified Eagle's medium
DMSO	Dimethyl sulfoxide
DNA	Deoxyribonucleic Acid
dNTP	Deoxyribonucleosidetriphosphate
DO	Dropout medium
Dsh	Dishevelled
DsRED	*Discosoma sp*. Red Fluorescent Protein
DTT	Dithiothreitol

Dvl	Dishevelled
EB	Elution Buffer
ECL	Enhanced Chemiluminescence
EDTA	Ethylenediaminetetraacetate
EGFP	Enhanced Green Fluorescent Protein
EpCAM	Epithelial cell adhesion molecule
ERK	Extracellular-signal-regulated kinase
EtBr	Ethidium Bromide
EtOH	Ethanol
FACS	Fluorescence-activated cell sorting
FAP	Familial Adenomatous Polyposis
FBS	Fetal Bovine Serum
FC	Fold Change
Fz	Frizzled
GO	Gene Ontology
GPCR	G-protein Coupled Receptor
GSEA	Gene Set Enrichment Analyses
GSK3β	Glycogen Synthase Kinase 3β
HA	Hemagglutinin
HCC	Hepatocellular Carcinoma
HCl	Hydrochloric Acid
HEK	Human Embryonic Kidney
hiNOS	Human inducible Nitric Oxide Synthase
His	Histidine
HRP	Horse radish peroxidase
hrs	Hours
Huh	Human hepatoma
IFITM3	Interferon induced transmembrane protein 3
Ig	Immunoglobulin
IKBα	Inhibitor of Kappa B α
IRES	Internal Ribosome Entry Site
Kan	Kanamycin
kb	Kilobase

kDa	Kilodalton
LB	Luria-Bertani
LDL	Low density lipoprotein
LEF	Lymphoid Enhancer Factor
Leu	Leucine
LiAc	Lithium Acetate
LiCl	Lithium Chloride
LRP	Low density lipoprotein receptor-related protein
Luc	Luciferase
MGAT1	α-1,3-mannosyl-glycoprotein 2-β-N-acetylglucosaminyltransferase
$MgCl_2$	Magnesium chloride
min	Minute
MOPS	Morpholinopropane sulfonic acid
mRNA	Messenger Ribonucleic Acid
NaCl	Sodium chloride
NaF	Sodium Flouride
NaOH	Sodium hydroxide
Na_3VO_4	Sodium orthovanadate
NCBI	National center for biotechnology information
NEAA	Non-Essential Amino-Acid
NFκB	Nuclear Factor Kappa B
NP-40	Nonidet P-40
OD	Optical density
ORF	Open Reading Frame
pAb	Polyclonal antibody
PAGE	Polyacrylamide gel electrophoresis
PBS	Phosphate buffered saline
PCP	Planar Cell Polarity
PCR	Polymerase Chain Reaction
PEG	Polyethylene glycol
PI	Propidium Iodide
PMSF	Phenylmethylsulfonyl fluoride

PVDF	Polyvinylidene Difluoride
QDO	Quadruple Dropout
Q-RTPCR	Quantitative Reverse transcriptase mediated polymerase chain reaction
RE	Restriction Enzyme
RIPA	Radio Immunoprecipitation Assay
RNA	Ribonucleic acid
RNA-Seq	RNA Sequencing
ROS	Reactive Oxygen Species
rpm	Revolutions per minute
RPMI	Roswell Park Memorial Institute medium
RT-PCR	Reverse-transcriptase mediated polymerase chain reaction
SAGE	Serial Analysis of Gene Expression
SCID	Severe combined immunodeficiency
SD	Synthetically defined medium
SD	Standard Deviation
SDS	Sodium Dodecyl Sulphate
sec	Second
SOC	Super optimal catabolite repressed broth
TAE	Tris-Acetic acid EDTA
Taq	Thermus Aquaticus
TBE	TCF binding element
TBS	Tris Buffered Saline
TBST	Tris Buffered Saline Tween
TCF	T-cell factor
TE	Tris-EDTA (buffer)
TEMED	N, N, N, N-tetramethylethylenediamine
TFBE	Transcription Factor Binding Element
TM	Transmembrane
TNFα	Tumor Necrosis Factor α
TRAF	TNF Receptor Associated Factor
Trp	Tryptophan

TSS	Transcriptional Start Site
UV	Ultraviolet
v/v	Volume to volume
w/v	Weight to volume
WB	Western Blot
WCL	Whole Cell Lysate
WT	Wild-Type
YPD	Yeast extract-peptone-dextrose medium
YPDA	Yeast extract-peptone-dextrose medium supplemented with adenine

1. INTRODUCTION

1.1. Cancer: Overview

Cancer is a large family of diseases that is characterized by abnormal cell growth and has the potential to invade or spread from the initial tumor site to other parts of the body. It is mainly based on genetic and epigenetic alterations that lead to loss of control in critical cellular events. In order for a normal cell to transform into a cancer cell, especially the genes that regulate cell growth, differentiation and programmed cell death must be altered (Croce, 2008).

There are two broad categories of genes that are affected by these alterations. Oncogenes may be normal genes that are expressed at inappropriately high levels, or altered genes by dominant gain-of-function mutations in protooncogenes. In either case, expression of these genes promotes the malignant phenotype of cancer cells. On the other hand, tumor suppressor genes are genes that inhibit cell division, survival or other properties of cancer cells. Tumor suppressor genes are often inactivated by cancer-promoting genetic changes, i.e. recessive loss-of-function mutations in both copies of these genes. Typically, changes in many genes are required to transform a normal cell into a cancer cell (Knudson, 2001).

All tumor cells exhibit the six hallmarks of cancer. These characteristics are required to produce a malignant tumor. They include; self-sufficiency in growth signals, insensitivity to anti-growth signals, avoidance of programmed cell death, limitless number of cell division potential, stimulation of the growth of blood vessels and finally invasion of the local tissue and formation of metastases (Weinberg *et al.*, 2000).

1.2. Hepatocellular Carcinoma

The liver contains the main liver cells called hepatocytes, further it contains the liver bile ducts, blood vessels and fat-storing cells. 80% of the liver tissue is made of

hepatocytes. 90-95% of the primary liver cancers are caused by the hepatocytes, that become malignant.

Hepatocellular Carcinoma (HCC) is the most frequent primary liver cancer. Another type of cancer formed by liver cells is hepatoblastoma, which is specifically formed by immature liver cells. Liver cancer can also develop from other structures within the liver such as the bile duct, blood vessels and immune cells. Cancer of the bile duct (cholangiocarcinoma and cholangiocellular cystadenocarcinoma) account for approximately 6% of primary liver cancers (Dileep *et al.*, 2009).

Hepatocellular Carcinoma is the sixth most common cancer worldwide and the third leading cause of cancer death (Dhanasekaran *et al.*, 2012). HCC affect 5 out of 100.000 people in the European, and 20 out of 100.000 people in the Asian continents. It is one of the most deadly cancers with approximately 600.000 deaths per year (Llovet *et al.*, 2003).

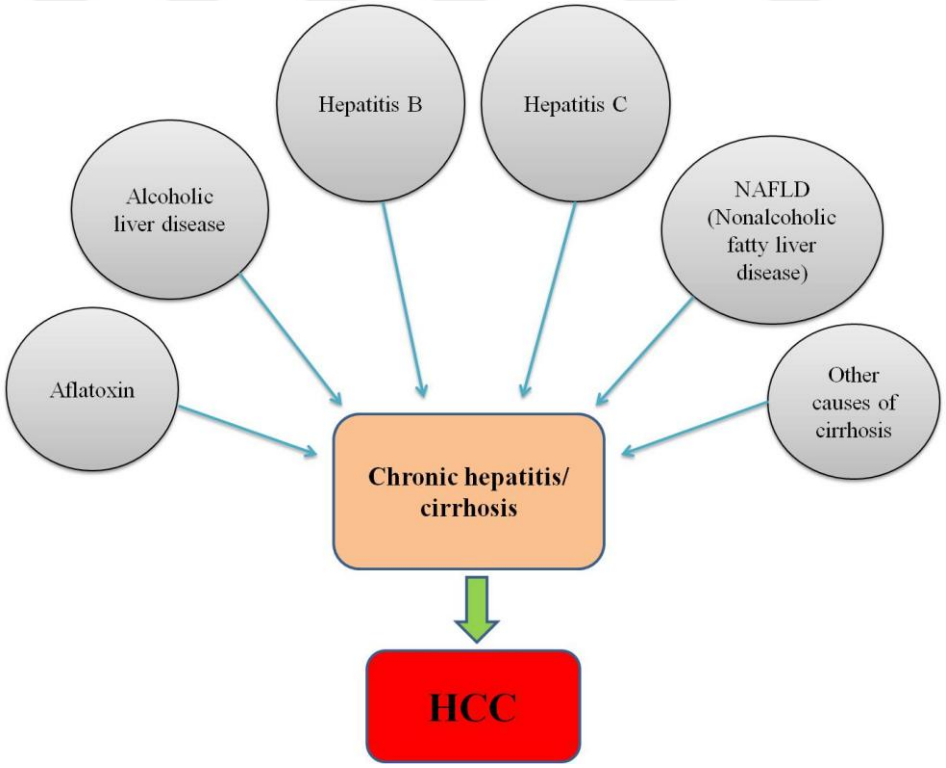

Figure 1.1. Major risk factors for developing HCC (Hepatocellular Carcinoma) (modified from Cabrera *et al.*, 2012).

Hepatocarcinogenesis nearly always develops in the setting of chronic hepatitis or cirrhosis; conditions in which many hepatocytes are killed, inflammatory cells invade the liver and connective tissue (Thorgeirsson and Grisham, 2002).

Infection with hepatitis B virus (HBV), hepatitis C virus (HCV) and chronic exposure to aflatoxin B1 (AFB1) are responsible for about 80% of all Hepatocellular carcinomas in humans (Bosch et al, 1999). Major risk factors for developing hepatocellular carcinoma are illustrated in Figure 1.1. In addition to these, diabetes is another factor that increases the risk of Hepatocellular Carcinoma. Smoking also increases the risk of HCC compared to non-smokers and previous smokers (Chuang *et al.* 2009).

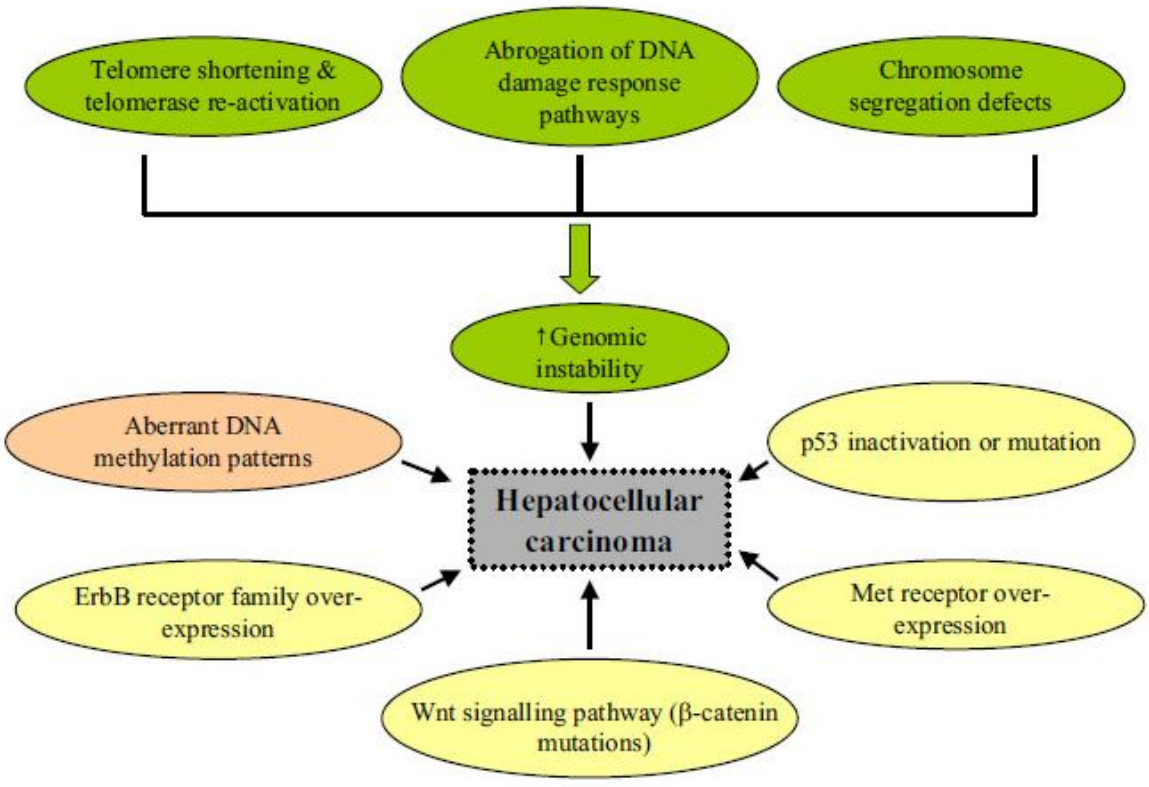

Figure 1.2. Genetic, epigenetic and genomic contributions to HCC development. (Wittekind *et al.*, 2002).

Development of Hepatocellular carcinoma is a relatively slow process requiring 10-30 years from the initiation to the fully malignant phenotype. During the long preneoplastic stage, in which the liver is often the site of chronic hepatitis, cirrhosis, or both, hepatocyte cycling is accelerated by upregulation of mitogenic pathways. The accumulation of irreversible structural alterations in genes and chromosomes also takes place throughout this process (Thorgeirsson and Grisham, 2002).

The sequential events leading to hepatocellular carcinoma may be summarized in 5 steps: chronic liver injury that produces inflammation, cell death, cirrhosis and regeneration, DNA damage, dysplasia and finally hepatocellular carcinoma (Wittekind et al, 2002).

Hepatocellular carcinoma symptomatically presents itself as an abdominal mass, abdominal pain, nausea and liver dysfunction. Furthermore; anemia, fever, decreased apetite, weight loss, and jaundice (yellowing of the eyes and skin) can be listed among the symptoms of hepatocellular carcinoma (Sun and Sarna, 2008).

More than 60-80% of Hepatocellular carcinoma cases arise in liver cirrhosis. At later stages of hepatocellular carcinogenesis, increased expression of TGF-β is thought to promote angiogenesis and metastasis (Greenbaum *et al.*, 2004).

The genetic and epigenetic alterations generally result in disruption of p53, Wnt or Rb-p16 pathways in Hepatocellular Carcinoma. Additionally, aberrant DNA methylation patterns and genomic instability, especially telomerase reactivation, are common factors in the development of Hepatocellular Carcinoma (Figure 1.2). Table 1.1 shows the mutation rates of various tumor suppressor genes and oncogenes in Hepatocellular Carcinoma.

1.2.1. Treatment of Hepatocellular Carcinoma

Liver transplantation can be curative for the early stages of HCC. However, if the liver tumor has metastasized, the immuno-suppressant post-transplant drugs decrease the

chance of survival (Obed *et al.,* 2009). Furthermore, there is a limited supply of good quality deceased donor organs which prompts the usage of alternative methods.

Surgical resection is another option in which the tumor is removed together with the surrounding liver tissue while preserving enough liver for normal body function at the same time. Surgical resection offers the best prognosis for long-term survival, but only 10-15% of patients are suitable for the usage of this technique. This is mostly because of extensive disease or poor liver function (Kaido *et al.*, 2011).

Systemic treatment is recommended for patients with advanced hepatocellular carcinoma and patients who are not candidates for liver transplantation or surgical resection. In clinical trials some agents such as tamoxifen and ketoconazole were tested for advanced HCC but the trials were terminated, because of their toxic effects without any survival benefit (Zhu, 2006). The only drug with proven survival benefit for advanced stage of HCC is sorafenib, which is also approved by FDA (Llovet *et al.*, 2008). Sorafenib is a receptor tyrosine kinase inhibitor with antiangiogenic and proapoptotic properties. It is unique in its ability to target multiple pathways by blocking RAF/MEK/ERK signaling at the level of Raf-kinase, as well as by inhibiting vascular endothelial growth factor receptor (VEGFR) and platelet-derived growth factor receptor beta (PDGFR-β) (Liu *et al.,* 2006). Combination therapies of sorafenib with other small molecules or chemicals (such as doxorubicin) are still in progress.

1.3. Wnt Signaling Pathway

The Wnt Signaling pathway is conserved in various organisms from worms to mammals, and plays important roles in development, differentiation, cellular proliferation, morphology, motility and fate. Wnt proteins constitute a large family of secreted cysteine-rich glycoproteins that exhibit distinct expression patterns in embryo and adult organisms (Cadigan and Nusse, 1997). Functions of the Wnt proteins have been extensively investigated through genetic studies in *Drosophila melanogaster*, *Caenorhabditis elegans*,

mouse, zebrafish, and through biochemical and cell biology studies in *Xenopus laevis*, sea urchin, chicken embryos and mammalian cultured cells (Wodarz and Nusse, 1998).

Binding of the Wnt protein to its receptors stimulates 3 different pathways; which are canonical Wnt pathway, planar cell polarity pathway (PCP) and Wnt/calcium pathway. The canonical Wnt pathway involves the protein β-catenin as the main executer, whereas planar cell polarity and Wnt/calcium pathways operate independent of β-catenin. The planar cell polarity pathway controls the temporal and spatial tissue arrangement during embryonic development, but its role in carcinogenesis is unclear (Lustig and Behrens, 2003). On the other hand, the Wnt/calcium pathway regulates calcium release from the endoplasmic reticulum (ER) in order to control intracellular calcium levels (Komiya and Habas, 2008).

Table 1.1. Mutation rates in tumor suppressor genes and oncogenes in Hepatocellular Carcinoma.

Gene(s)	Mutation rate	Reference(s)
p53	28-50 %	Oda *et al.* (1992); Öztürk *et al.* (1997)
M6P/IGF2R	25-55 %	De Souza *et al.* (1995); Yamada *et al.* (1997)
β-catenin	18-41 %	Nhieu *et al.* (1999); Terris *et al.* (1999)
p16	10 %	Liew *et al.* (1999)
Axin1 & Axin2	5-10 %	Taniguchi *et al.* (2002)
Smad2 & Smad4	3-6 %	Yakicier *et al.* (1999)
BRCA2	5 %	Katagiri *et al.* (1996)
Rb	rare	Zhang *et al.* (1994)
Ras	rare	Ong *et al.* (1996)

1.4. The canonical Wnt/β-catenin signaling pathway

Wnt/β-catenin signaling pathway has important roles in several cellular functions during embryonic development, maintenance of organs, cell proliferation and differentiation, adult tissue homeostasis, cell fate determination, and angiogenesis.

The classical, also called canonical Wnt/β-catenin signaling pathway is the best understood Wnt signaling pathway. β-catenin, which is localized with the membrane bound E-cadherin or is free in the cytoplasm, plays a major role in the transduction of the canonical Wnt/β-catenin signal (Takeichi *et al.*, 1991; Ikeda *et al.*, 1998). Without Wnt signaling, cytoplasmic β-catenin levels are normally kept low through continuous proteasome-mediated degradation, which is mediated by a multiprotein complex mainly consisting of GSK-3β/APC/Axin - also called the destruction complex. The canonical Wnt/β-catenin signaling is initiated by the binding of a Wnt ligand to Frizzled and LRP5/6 as its coreceptors and progresses through dissociation of the destruction complex, leading to the stabilization and translocation of β-catenin into the nucleus. Once in the nucleus, β-catenin acts as a transcriptional coactivator by interacting with the TCF/LEF family of transcription factors in order to activate target gene expression (Yamamoto *et al.*, 1999; MacDonald *et al.*, 2009). A variety of Wnt/β-catenin target genes have been identified which include regulators of cell proliferation, developmental control genes and genes implicated in tumor progression. The canonical Wnt/β-catenin signaling pathway is summarized in Figure 1.3.

1.4.1. Major components of the Canonical Wnt pathway

A total of 19 highly conserved Wnt genes were identified in the human genome. These genes control the synthesis of secreted signaling molecules that regulate cell differentiation during development and tissue homeostasis, stem cell number in adult organism. Wnt proteins that are released from the surface of signaling cells act on target cells by binding to the receptor complex of Frizzled (Fz)/ Low density lipoprotein (LDL) receptor-related protein (LRP) at the cell surface. These receptors transduce a signal to several intracellular proteins including Dishevelled (Dsh), Glycogen Synthase Kinase-3β

(GSK-3β), Axin, APC and the transcriptional coactivator β-catenin (Clevers and Nusse, 2012).

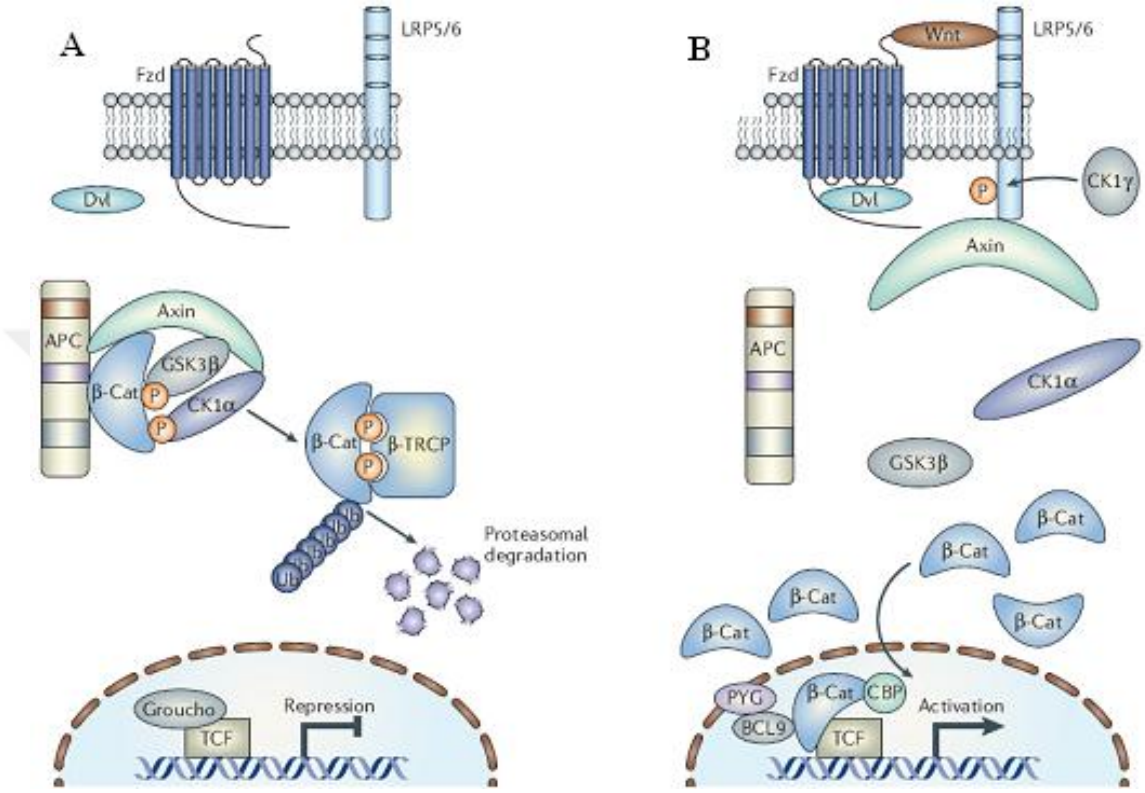

Figure 1.3. Wnt/β-catenin signaling cascade in its 'inactive' (A) and 'active' (B) states (Adopted from Barker and Clevers, 2006).

Frizzled (Fz) is the main receptor of Wnt ligands. It is a seven-transmembrane receptor with a highly conserved amino-terminal cysteine rich domain (CRD). On the other hand, the Wnt co-receptors LRP5/6 contain a long single-pass transmembrane domain. LRP5/6 is phosphorylated in a Wnt-induced manner on the intracellular domain by GSK-3β and CKIγ. The phosphorylated LRP5/6 intracellular domain then recruits Axin to the membrane, which results in the dissociation of the destruction complex (Mao *et al.*, 2001).

Axin is the core scaffold protein of the β-catenin destruction complex. It possesses separate binding sites for APC, GSK-3β, β-catenin, Dishevelled, and PP2A. Axin inhibits Wnt signaling by facilitating the GSK-3β-dependent phosphorylation of β-catenin. In the Axin complex, GSK-3β efficiently phosphorylates β-catenin, APC and Axin itself, whereas

in the absence of Axin, GSK-3β phosphorylates β-catenin at a very low rate (Kishida *et al.*, 1998).

Adenomatous Polyposis Coli Gene Product (APC) is an important component of the β-catenin destruction complex. Within the destruction complex, APC interacts with both Axin and β-catenin, leading to the proteasomal degradation of β-catenin. APC protein includes regions containing three 15-amino acid and seven 20-amino acid repeats. Both of these domains are known to bind β-catenin and the 20-amino acid repeats have an important function in downregulating β-catenin levels in the cell (Wands *et al.*, 2006).

The serine/threonine kinase Glycogen Synthase Kinase 3 beta (GSK-3β) is another crucial component of the β-catenin destruction complex. Phosphorylation of β-catenin by GSK-3β is essential for down regulation of Wnt signaling. GSK-3β dependent phosphorylation of β-catenin takes place at the serine 33, serine 37 and threonine 41 residues (Behrens *et al.*, 1998). Thus, β-catenin can be stabilized by point mutations of these serine and threonine residues in the N-terminal region, so that it can avoid phosphorylation and becomes resistant to degradation, hence leading to an overall increase in Wnt signaling (Aberle *et al.*, 1997). Furthermore, inhibition of GSK-3β via activation of Wnt/β-catenin pathway by using a recombinant Wnt ligand or treatment of the cells with lithium chloride (LiCl) to inactivate GSK-3β, can be considered as alternative approaches to stabilize β-catenin.

Dishevelled (Dvl) is a mammalian homolog of fly dishevelled (dsh) and it is an immediate downstream molecule of Frizzled. When a Wnt ligand binds to Frizzled and LRP5/6, Dvl is phosphorylated and in turn recruits Axin to the membrane. The destruction complex cannot be formed in the absence of Axin, thus the phosphorylation of β-catenin by GSK-3β is inhibited, and β-catenin starts to accumulate in the cytoplasm (Li *et al.*, 1999).

β-catenin has dual functions in cells. First of all, it has a role in cadherin-based cell adhesion system. It binds to the cytoplasmic domain of the transmembrane protein E-cadherin and regulates actin filament assembly by linking E-cadherin to α-catenin. Additionally, it is the key component of the canonical Wnt/β-catenin signaling pathway

through its role as a transcriptional activator. In the absence of Wnt signals, free β-catenin in the cytosol is constitutively phosphorylated and subsequently degraded in the proteasome, whereas in their presence, β-catenin is stabilized and translocated into the nucleus where it can associate with members of the T cell factor/Lymphoid enhancer factor (TCF/LEF) family of transcription factors and act as transcriptional activators of the Wnt target genes (van de Wetering *et al.*, 1997). β-catenin contains a large central region composed of 12 repeats of three helices each (called the armadillo repeats), forming a superhelix of helices (Huber *et al.*, 1997). This central region forms a rigid scaffold and contains binding sites for many factors, including TCF/LEF, the cell adhesion protein E-cadherin, APC, Axin and GSK-3β (Polakis, 1999).

1.4.2. The On/Off States of the Canonical Wnt pathway

β-catenin is detained in the Axin complex in the absence of a Wnt signal. In this complex, cytosolic β-catenin, but not the cadherin-bound β-catenin, is continuously phosphorylated, ubiquitinated and degraded by proteasome. The multiprotein complex that is responsible for β-catenin degradation is assembled around the scaffold protein Axin. Within this "destruction complex" complex, β-catenin is firstly phosphorylated by casein kinase Iα (CKIα) at serine 45 and then by GSK-3β on its serine/threonine residues 33, 37 and 41. Subsequently, β-catenin is targeted for degradation via the ubiquitin-proteasome pathway, after it is ubiquitinated by β-transduction repeat containing protein (β-TrCP), which is an E3 ubiquitin ligase (Rubinfeld *et al.*, 1996).

The "on" state of the canonical Wnt/β-catenin signaling pathway is initiated by the binding of a Wnt ligand to Frizzled (Fz) and LRP5/6 co-receptors. In this case, it is hypothesized that Dishevelled binds to Axin and antagonizes Axin activity in response to Wnt. Thus, Dishevelled is thought to inhibit GSK-3β dependent phosphorylation of β-catenin and APC through a still unclear mechanism. As a consequence, β-catenin is able to escape from the degradation and begins to accumulate in the cytosol. The accumulated β-catenin is then translocated into the nucleus, and binds to and activates TCF/LEF family of transcription factors that results in the expression of target genes (Behrens *et al.*, 1996).

Overall, in the absence of Wnt signaling, Wnt/Wingless (Wg) target genes are being repressed by the protein complex of TCF and several transcriptional co-repressors such as Groucho/TLE1 (Transducin-like Enhancer of split 1) and C-terminal binding protein (CtBP) (Cavallo *et al.*, 1998; Fang *et al.*, 2006). Once in the nucleus, β-catenin is thought to convert the TCF repressor complex into a transcriptional activation complex which possibly occurs via displacement of Groucho from TCF/LEF and recruitment of the histone acetylase CBP/p300 (CREB-binding protein) and the chromatin remodeling SWI/SNF complex (Daniels and Weis, 2005; Cadigan *et al.*, 2007).

1.5. Wnt/β-catenin pathway and Cancer

Wnt signaling had been associated with cancer since its initial discovery. Wnt1, when first discovered, was identified to be a proto-oncogene in a mouse model for breast cancer. Wnt1 is a homolog of Wg and it is involved in embryonic development, where it mostly requires rapid cell division and migration. Misregulation of these processes is very likely to result in tumor development via excess cell proliferation (Nusse, 2005).

In various types of cancers (colon, liver, prostate, blood, skin) Wnt/β-catenin associated molecules, such as proto-oncogene CTNNB1 (β-catenin), and tumor suppressor genes such as APC or AXIN show alterations. Mutations of CTNNB1 gene are commonly found in a variety of cancers including primary hepatocellular carcinoma, colorectal cancer, ovarial carcinoma, breast cancer, lung cancer and glioblastoma. Increased expression of Wnt ligand proteins such as Wnt1, Wnt2 and Wnt7A were observed in the development of glioblastoma, oesophageal cancer and ovarian cancer, respectively (Anastas and Moon, 2013). Nevertheless, in general, hepatocellular carcinoma and colorectal carcinoma harbor the highest rate of Wnt pathway gene mutations (Giles *et al.*, 2003).

In addition to these mutations, the nuclear accumulation of β-catenin due to aberrant activation of Wnt signaling is mainly observed in hepatocellular tumors, colorectal tumors, gastrointestinal tumors and breast tumors.

1.5.1. The Role of Wnt/β-catenin pathway in Hepatocellular Carcinoma

The Wnt/β-catenin signaling pathway plays a critical role in hepatic homeostasis, especially in liver development, regeneration and cancer; furthermore loss of β-catenin signaling is associated with increased apoptosis and knockdown of β-catenin using antisense treatment resulted in decreased liver regeneration (Nejak-Bowen *et al.* 2013).

Almost a third of Hepatocellular Carcinoma cases display constitutive activity of canonical Wnt signaling caused by mutations in CTNNB1 (β-catenin) or Axin1 genes (Clevers *et al.*, 2005). Additionally, the finding of mutated β-catenin in early stages of human HCC and rapid development of hepatomegaly in mutated β-catenin expressing transgenic mice suggest that aberrations in Wnt pathway can be considered as an early event in hepatocarcinogenesis (Jeng *et al*., 2000; Cadoret *et al*., 2001).

1.6. Identification of novel Wnt/β-catenin target genes

Identification of novel transcriptional targets of Wnt/β-catenin signaling pathway is crucial with respect to cancer research and several clinical research fields, since genes regulated by this pathway can be considered as potential drug and gene therapy targets.

In order to identify novel targets, transcriptome-profile analyses were recently performed in our laboratory using stable Huh7 (hepatocellular carcinoma) cell lines overexpressing a degradation-resistant, mutant form of β-catenin. Figure 1.4. represents the general workstream employed in order to determine the novel molecules involved in response to pathway activation. Among the transcriptome-profile analyses, both SAGE (Serial Analysis of Gene Expression) and genome-wide microarray screens were used to determine differential expression of potential target genes (Table 1.2).

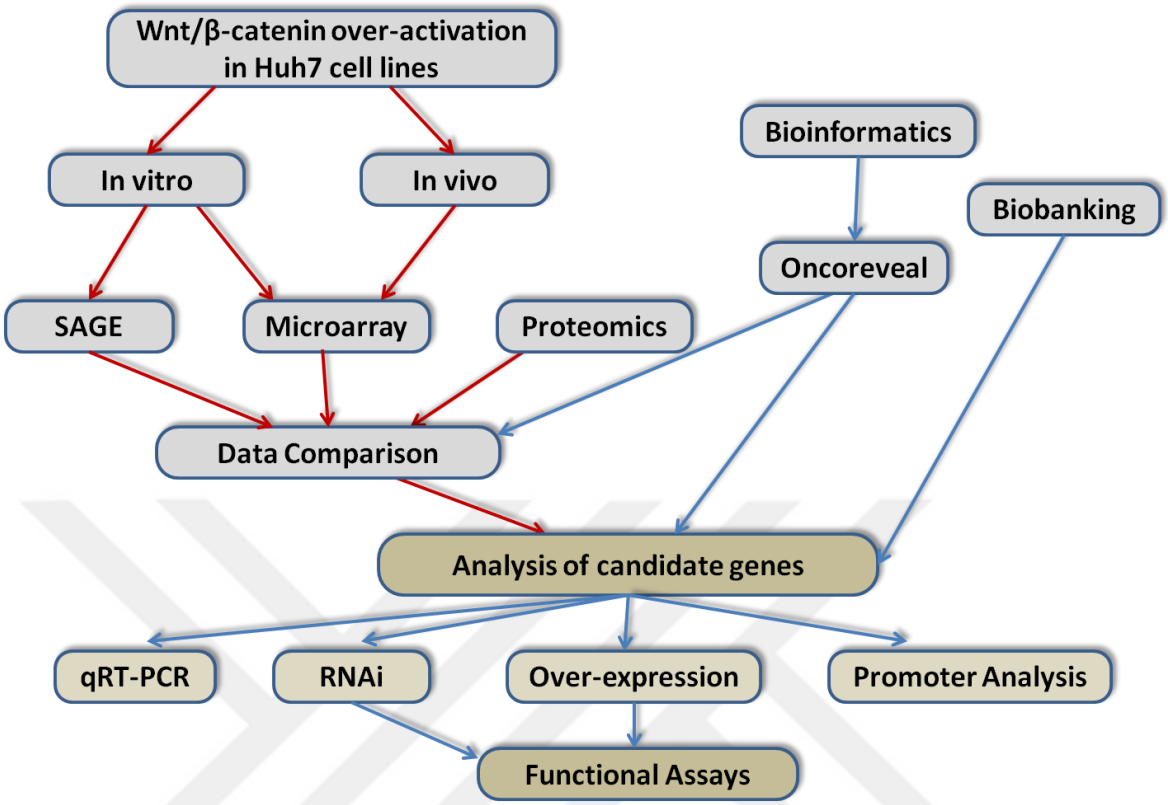

Figure 1.4. Experimental flowchart showing the techniques being employed for the identification of novel Wnt/β-catenin pathway targets.

1.6.1. BRI3 as a novel Wnt/β-catenin pathway target gene

BRI3 (Brain protein I3) has been selected among the potential Wnt/β-catenin signaling pathway targets based on the SAGE screen and an equivalent microarray screen (Kavak *et al.*, 2010). Moreover, lithium treatment of Huh7 cell lines and overexpression of the Wnt ligands in the same cell lines resulted in the upregulation of BRI3 gene expression, as determined by quantitative RT-PCR (Kavak *et al.*, 2010). The results obtained from luciferase reporter gene assay, in which BRI3 promoter activity was found to be increased due to overexpression of β-catenin, also supported the former data. Additionally, chromatin immunoprecipitation assays (ChIP) indicated that β-catenin interacts with BRI3 promoter region in Huh7 cell lines and in mouse liver tissue (Figure 1.5).

Table 0.2. Fold changes for the selected candidate genes with respect to SAGE, Microarray and Q-RTPCR results. SAGE and Microarray folds are denoted as ratio of Huh7-S33Y-β-catenin/Huh7-vector (ND: non-detected) (Kavak *et al.*, 2010).

Gene	Microarray Fold	SAGE *p value*	SAGE Fold	Q-RTPCR or RTPCR result
TINP1	0.97	0.46	-1.02	1.31
CLU	1.29	0.00	1.97	1.78
MGC40157	1.46	0.01	2.50	2.13
BRI3	**1.01**	**0.01**	**2.36**	**2.99**
NES	0.81	0.00	-3.38	0.40
SEC31L1	0.89	0.00	-5.33	1.09
APOA2	0.78	0.00	-2.45	1.07
MGAT1	**1.17**	**0.04**	**3.00**	**Up**
KIAA1924 (WDR90)	1.01	0.02	-6.00	Down
ATP5G1	0.78	0.00	-5.00	Down
TPT1	1.10	0.00	1.73	Up
BLP1 (tm2d2)	0.95	0.01	6.00	Up
MMP7	ND	ND	ND	No Change
MYC	1.13	ND	ND	Up
HSF2	1.24	ND	ND	2.10 (alpha isoform) 1.3 (beta isoform)

BRI3 was originally identified as a 125 amino acid transmembrane protein that is overexpressed in TNFα treated L929 -murine fibrosarcoma- cells (Wu *et al.*, 2003). The blocking of new BRI3 protein synthesis by using BRI3-antisense RNA, resulted in increased resistance of these cells to TNF-induced cell death at greater than 1000-fold. Although the exact action mechanism of BRI3 within the TNF-induced cell death pathway still remains unknown, it is hypothesized that, BRI3 synthesis acts as a negative checkpoint of this pathway (Wu *et al.*, 2003).

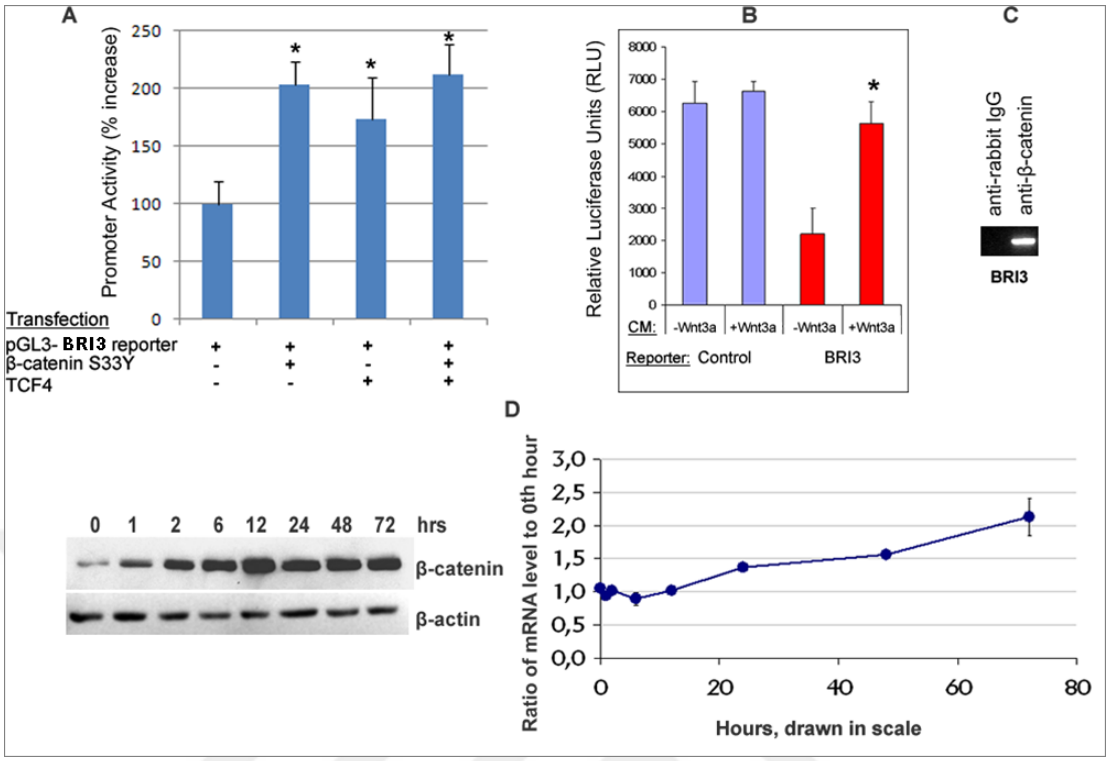

Figure 1.5. BRI3 was determined to be a novel target of Wnt/β-catenin pathway by means of several approaches. (A) Luciferase reporter assay, (B) Wnt ligand overexpression, (C) Chromatin immunoprecipitation and (D) β-catenin activation by lithium treatment (Kavak *et al.*, 2010).

1.6.2. MGAT1

MGAT1 (Mannosyl (alpha-1,3-)-glycoprotein beta-1,2-N-acetylglucosaminyl-transferase) is a medial Golgi enzyme which catalyzes the first step in the conversion of oligomannose-type N-glycans into complex and hybrid N-glycans (Yip *et al.*, 1997). The deduced protein sequence of MGAT1 is of 445 aa in length, and it is typical of other Golgi transferases that are type II transmembrane proteins (Kumar *et al.*, 1990).

Previous studies in our laboratory determined MGAT1 to be one of the genes that is upregulated upon β-catenin activation, as it is included among the list of differentially expressed genes with respect to transcriptomic analyses (Table 1.2). According to SAGE

results, MGAT1 displayed a significant increase in mRNA level upon stable overexpression of degradation-resistant β-catenin mutant (S33Y-β-catenin) in Huh7 cell lines compared to control cell lines (Huh7-vector). This upregulation was also confirmed by RT-PCR.

MGAT1 is essential for normal embryogenesis in the mouse. Previous studies showed that mice lacking a functional MGAT1 gene die at approximately 10 days after fertilization with multiple developmental abnormalities, indicating the importance of complex and hybrid type N-glycans in cell-cell interactions (Ioffe *et al.*, 1997).

Null mutations in Drosophila MGAT1 have been shown to produce defects in adult locomotory activitiy when compared to wild type flies. Moreover, the null mutant males are sterile and determined to have a severely reduced mean life span. Thus it is stated that, MGAT1-dependent N-Glycans are required for locomotory activity, life span and brain development in flies (Sarkar *et al.*, 2006).

1.7. NFkB Signaling Pathway

The NFkB transcription factor is rapidly activated by diverse stimuli that mostly alert a cell to stressful or infectious conditions. Known inducers of NFkB activity include reactive oxygen species (ROS), UV-irradiation, tumor necrosis factor alpha (TNFα), interleukin 1-beta (IL-1β), bacterial/viral products (LPS, dsRNA), isoproterenol and apoptotic or necrotic stimuli (Gilmore, 2006).

Mammalian cells express 5 NFkB members: Rel A (p65), Rel B, c-Rel, NFkB1 p50 and NFkB2 p52, which usually form p50/Rel or p52/Rel heterodimers. NFkB dimers are normally sequestered as latent complexes in the cytoplasm by the IkB inhibitors such as IkBα or IkB-like inhibitors such as p100. Therefore, NFkB induction is mainly based on inducible IkB degradation, which is named as canonical or classical pathway, or p100 processing, which is the non-canonical pathway.

Activation of the NFkB occurs primarily via activation of a kinase called the IkB kinase (IKK). IKK is composed of a heterodimer of the catalytic IKKα and IKKβ subunits and a master regulatory protein named as NEMO (NFkB essential modulator) or IKKγ. The activatory signals are transduced mainly by the adaptor protein family of TRAFs (TNF receptor associated factors). Upon activation by TRAFs, the IKK complex phosphorylates two serine residues (serine 32 and 36) located in the regulatory domain of IkB. This in turn, leads to the ubiquitination and subsequent degradation of IkB through proteasome. With the degradation of IkB, the NFkB complex is free to enter the nucleus where it can activate the expression of its target genes (Figure 1.6).

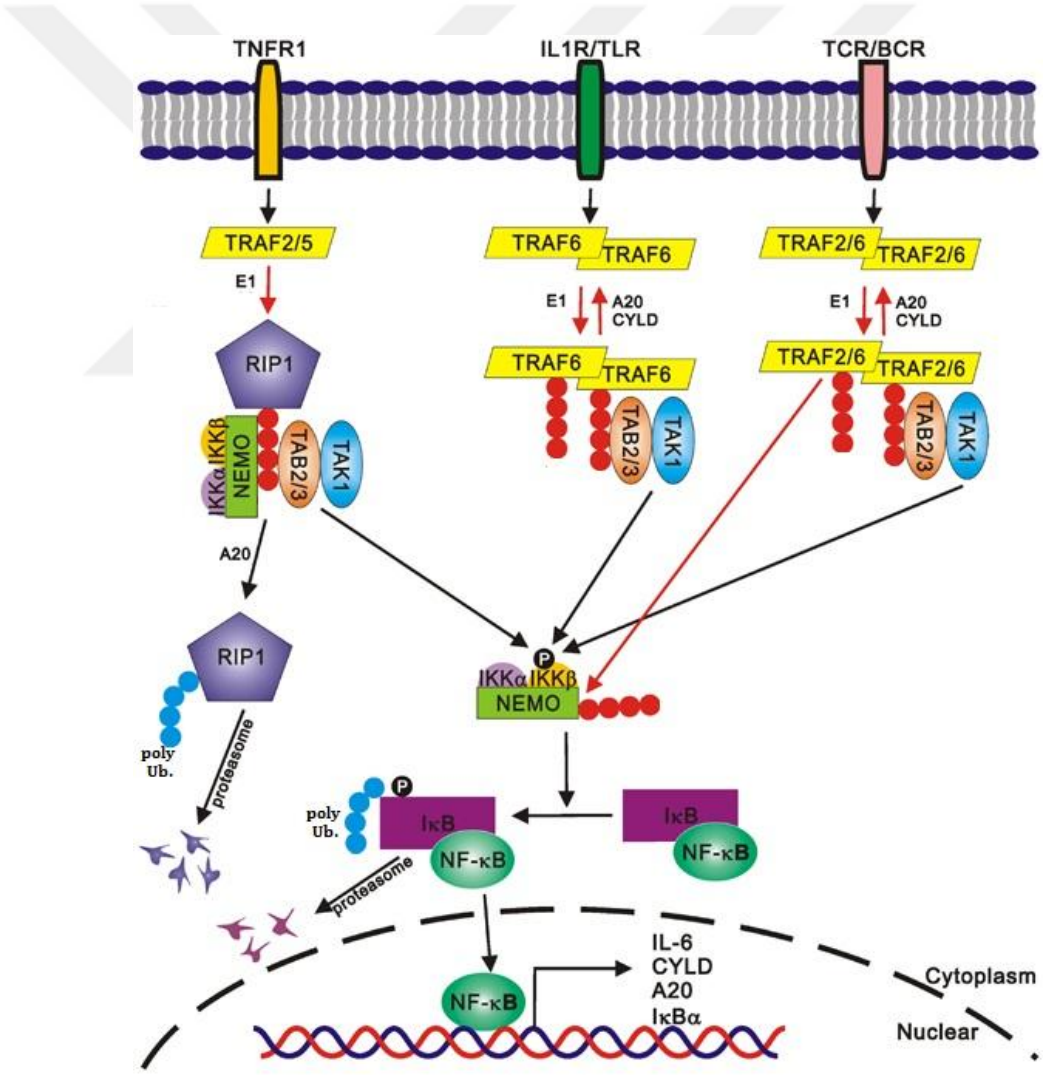

Figure 1.6. Overview of the canonical NFkB Signaling pathway (adapted and modified from Adhikari *et al.*, 2006).

1.8. NFkB and cancer

The genes that are regulated by NFkB are involved in the development and function of immune response, inflammation, cell growth control, differentiation, cell survival and proliferation. The tight control of NFkB is essential for normal cellular function. Defects in its activation lead to developmental deficiencies or even death, whereas persistent activation of NFkB pathway may result in various pathogenesis, particularly immune-related disorders and cancer (Xiao *et al.*, 2007).

In fact, aberrant or constitutive activation of NFkB is frequently observed in many cancers. This activation is either due to mutations in genes encoding the NFkB transcription factors themselves or in genes that control NFkB activity, such as IkB genes. Active NFkB turns on the expression of genes that keep the cell proliferating and protect the cell from committing programmed cell death. On the other hand, suppression of NFkB signaling limits the proliferation of cancer cells, induce their apoptosis or make them more sensitive to the action of anti-tumor agents (Escarcega *et al.*, 2007).

1.9. Crosstalk between Wnt/β-catenin and NFkB Signaling

There exist several studies to demonstrate the direct interaction between these two signaling pathways with respect to cancer development and apoptosis.

Deng *et al.* first showed that β-catenin inhibited NFkB activity in human colon and breast cancer cell lines (Deng *et al.*, 2002). Additionally, direct interaction between β-catenin and both p50 and p65 proteins, which are the subunits of NFkB, was confirmed via coimmunoprecipitation (Du *et al.*, 2009).

The *in vivo* tumor findings suggest that the crosstalk between Wnt/β-catenin and NFkB signaling occurs in the setting of inflammation-associated liver cancer and has also been reported in breast cancer specimens.

Sun *et al.* also reported a cross-talk between β-catenin and NFkB in bacterial-colonized HCT116 intestinal epithelial cells (Sun *et al.*, 2005). The findings suggest that, constitutively expressed β-catenin indirectly stabilized IkBα and thereby inhibited NFkB.

It was shown that β-catenin inhibited TNFα or TNFα/ActD mediated apoptosis, but it is unclear how Wnt/β-catenin pathway exerts its effects on TNFα pathway (Liu *et al.*, 2013).

High levels of β-catenin antagonized TNFα induced NFkB target gene expression and decreased NFkB-dependent hiNOS expression levels (Du *et al.*, 2009). Conversely, NFkB signaling was shown to suppress Wnt/β-catenin mediated transcription even in the case of cells expressing mutant stable forms of β-catenin (Masui *et al.*, 2002).

2. PURPOSE

Identification and characterization of novel targets of the Wnt/β-catenin pathway serves an important purpose for many clinical research fields, especially for the cancer research field, since genes regulated by this pathway are potential drug and gene therapy targets. The results of genome-wide microarray and SAGE screens performed previously in our laboratory have revealed several candidate target molecules of the Wnt/β-catenin pathway.

In this study, the major objective was to characterize the selected candidate target molecules in order to elucidate their biological roles and eventual implications in cancer. As a starting point, BRI3 has been selected as one of the Wnt/β-catenin pathway target genes, mainly based on its differential expression upon β-catenin activation, the presence of a putative TCF4-binding site in its promoter and the degree of characterization of its functions. Novel binding partners of BRI3 were tried to be identified in the first step. MGAT1 and IFITM3 were the two proteins we obtained from the screenings. Among these, MGAT1 was also worth focusing on, since it was one of the genes with differential expression in response to β-catenin activation. Therefore, another objective of this study was to confirm that MGAT1 is indeed regulated by Wnt/β-catenin signaling and also to reveal whether it has any role in cancer progression.

By means of employing a series of *in vitro* and *in vivo* techniques in order to further characterize these genes, we were able to expose their tumorigenic potentials. As a final step in this study, transcriptomic analysis by RNA-Sequencing method was carried out in order to identify the pathways and biological processes leading to tumorigenesis through the overexpression of these genes.

3. MATERIALS

3.1. General Kits, Enyzmes and Reagents

Table 3.1. List of kits, enzymes and reagents.

Name	**Supplier**
BCA Protein Assay Kit	Thermo, USA
Complete Mini PI (Protease Inhibitor) Cocktail	Roche, Switzerland
Dulbecco's Modified Eagle Medium (DMEM)	Hyclone, USA
DNA Molecular Weight Marker	GeneRuler 1 kb DNA Ladder, Fermentas, USA
Dual-Glo Luciferase Assay System	Promega, USA
Fetal Bovine Serum (FBS)	Gibco, USA
GeneJET Plasmid Midiprep Kit	Thermo, USA
Genopure Plasmid Midi Kit	Roche, Switzerland
High Pure Plasmid Isolation Kit	Roche, Switzerland
High Pure RNA Isolation Kit	Roche, Switzerland
ImProm-II Reverse Transcription System	Promega, USA
Matchmaker GAL-4 Yeast Two-Hybrid System	Clontech, USA
Maxima SYBR Green/ROX qPCR Master Mix (2x)	Thermo, USA
MinElute Gel Extraction Kit	Qiagen, Germany
MinElute PCR Purification Kit	Qiagen, Germany
Penicillin/Streptomycin (10X)	Hyclone, USA

Table 3.1. List of kits, enzymes and reagents (cont.).

Phusion High-Fidelity DNA Polymerase	NEB, USA
Protein Molecular Weight Marker	PageRuler Prestained Protein Ladder, Thermo, USA
QIAquick Gel Extraction Kit	Qiagen, Germany
Restriction Enzymes	Thermo, USA
RNase A	Roche, Switzerland
RNAstable	Biomatrica, USA
RPMI 1640 Medium	Hyclone, USA
T4 DNA Ligase	NEB, USA
Taq DNA polymerase	Thermo, USA
Trypsin-EDTA (0.5 mM EDTA, 0.025% Trypsin)	Hyclone, USA
Turbofect Transfection Reagent	Thermo, USA
Western Blotting Luminol Reagent	Super Signal West Femto Maximum Sensitivity Kit, Thermo, USA
RNeasy Mini Kit	Qiagen, USA
Vectashield Antifade Mounting Medium	Vector Laboratories, USA
XTT Cell Proliferation Assay kit II	Roche, Switzerland

3.2. Chemicals

Table 3.2. Chemicals used in this study.

Name	**Supplier**
Acetic Acid	Merck, USA
Acrylamide	AppliChem, Germany
Agar	Conda, Spain
Agarose E	Conda, Spain
Ammonium Persulfate (APS)	Sigma-Aldrich, USA

Table 3.2. Chemicals used in this study (cont.).

β-Mercaptoethanol	Merck, USA
Boric Acid	Sigma-Aldrich, USA
Ampicillin	Roche, Switzerland
Bovine Serum Albumin (BSA)	AppliChem, Germany
Bromophenol Blue	Fluka, USA
Calcium chloride dehydrate	AppliChem, Germany
DMSO	Sigma-Aldrich, USA
EDTA	AppliChem, Germany
Ethanol	Emsure, Germany
Ethidium Bromide	Sigma-Aldrich, USA
Tryptone	Sigma-Aldrich, USA
Formaldehyde	Sigma-Aldrich, USA
Geneticin (G418)	Hyclone, USA
Glycerol	Sigma-Aldrich, USA
Glycine	Fisher Scientific, USA
Isopropanol	Emsure, Germany
Kanamycin	Fluka, USA
Lithium Chloride	Fisher Scientific, USA
Methanol	Emsure, Germany
N, N, N', N'-tetramethylethylenediamine (TEMED)	AppliChem, Germany
N,N'-Methylenebisacrylamide	Sigma-Aldrich, USA
NP-40	Roche, Switzerland
Paraformaldehyde	Sigma-Aldrich, USA
Phosphate Saline Buffer (PBS) - Mol. Biology Grade	Gibco, UK
Propidium Iodide	Sigma-Aldrich, USA
Sodium Chloride (NaCl)	Fisher Scientific, USA
Sodium Deoxycholate	Sigma-Aldrich, USA
Sodium Fluoride	Merck, USA
Sodium Hydroxide	Sigma-Aldrich, USA
Sodium Dodecyl Sulfate (SDS)	AppliChem, Germany
TNF-α	Santa Cruz, USA
Tris Base	AppliChem, Germany
Tris Hydrochloride	AppliChem, Germany
Triton X-100	AppliChem, Germany
Tween 20	Sigma-Aldrich, USA
Xylene Cyanol	Sigma-Aldrich, USA
Yeast Extract	Conda, Spain

3.3. Biological materials

3.3.1. Yeast Strains

The yeast host strains used in this study were obtained from Clontech (CA, USA). These are AH109 (genotype: MATa, trp1-901, leu2-3, 112, ura3-52, his3-200, gal4Δ, gal80Δ, LYS2 : : GAL1UAS-GAL1TATA-HIS3, GAL2UAS-GAL2TATA-ADE2, URA3 : : MEL1UAS-MEL1TATA-lacZ) and Y187 (genotype: MATα, ura3-52, his3-200, ade2-101, trp1-901, leu2-3, 112, gal4Δ, met–, gal80Δ, URA3 : : GAL1UAS-GAL1TATA-lacZ).

3.3.2. Bacterial Strains

E. coli bacterial strain TOP10 (genotype: F- mcrA Δ (mrr-hsdRMS-mcrBC) φ80lacZΔM15 ΔlacX74 recA1 araD139 Δ (araleu) 7697 galU galK rpsL (Str^R) endA1 nupG, λ^-) or DH5α (genotype: F^- endA1 glnV44 thi-1 recA1 relA1 gyrA96 deoR nupG purB20 φ80dlacZΔM15 Δ(lacZYA-argF)U169, hsdR17($r_K^- m_K^+$), λ^-) were routinely used for cloning purposes.

3.3.3. Mammalian Cell Lines

Huh7, Hep3B, HepG2, Hep40, Mahlavu, SNU449 (human hepatocellular carcinoma; kindly provided by Dr. Mehmet Öztürk), U373-MG (human astrocytoma; kindly provided by Dr. P.O. Couraud), HCT116 (human colon carcinoma; kindly provided by Dr. Nesrin Özören), HeLa (human cervical carcinoma; kindly provided by Dr. Nesrin Özören) and HEK 293-FT (human embryonic kidney; kindly provided by Dr. Nesrin Özören) cell lines were used.

3.3.4. NUDE/SCID mice in Xenografting

Female NUDE/SCID mice 4-6 weeks of age were obtained from Boğaziçi University Vivarium department. The maintenance and breeding of animals were

established under pathogen free conditions. The animals were handled according to the university guidelines and with the approval of the local ethics committee BUHADYEK.

3.4. Buffers and Solutions

3.4.1. DNA Gel Electrophoresis

Table 3.3. DNA Gel Electrophoresis buffers and solutions.

Solution/Buffer	**Content**
50X Tris-acetic acid EDTA (TAE)	2M Tris-acetate 50mM EDTA pH 8.5
TE Buffer	10mM Tris–HCl 1mM EDTA, pH 8.0
Ethidium bromide (EtBr)	10 mg/ml (stock solution) 30 ng/ml (working solution)
10X Tris Borate EDTA (TBE)	108 g Tris base 55 g Boric acid 9.3 g EDTA Double distilled water up to 1 L
6X Loading Buffer	2.4 ml dH2O 0.1 ml 1M Tris-HCl, pH 7.6 0.3 ml 1% Bromophenol Blue (BPB) 6 ml 100 per cent glycerol 1.2 ml 0.5M EDTA distilled water up to 10 ml

3.4.2. RNA Gel Electrophoresis

Table 3.4. RNA Gel Electrophoresis buffers and solutions.

Solution/Buffer	**Content**
Diethylpyrocarbonate treated water	1 per cent (v/v) Diethylpyrocarbonate
10X Morpholino Propane Sulfonic Acid (MOPS)	41.8 g MOPS 20ml 0.5M EDTA 16.8ml 3M NaOAc DEPC treated water upto 1L. pH 7.00
EtBr RNA loading buffer	0.72 ml formamide 0.16 ml 10X MOPS 0.26 ml formaldehyde 0.18 ml DEPC treated water 0.1 ml 80% Glycerol 0.08 ml Bromophenol blue 50 µg EtBr

3.4.3. Western Blotting Buffers and Solutions

Table 3.5. SDS-PAGE and Western Blotting buffers and solutions.

Solution/Buffer	**Content**
10 % SDS-PAGE gel (separating gel)	10% Acrylamide : Bisacrylamide (37.5:1) 375mM Tris-HCl (pH 8.8) 0.1% SDS 0.1% APS 0.1% TEMED

Table 3.5. SDS-PAGE and Western Blotting buffers and solutions (cont.).

5 % SDS- PAGE gel (stacking gel)	5% Acrylamide : Bisacrylamide (37.5:1) 125mM Tris-HCl (pH 6.8) 0.1% SDS 0.1% APS 0.1% TEMED
5X SDS-PAGE Loading Dye	250 mM Tris-HCl (pH 6.8) 10% SDS 50% Glycerol 5% β-mercaptoethanol 0.1% Bromophenolblue
10X SDS Running Buffer	30.3 g Tris base 144 g Glycine 10 g SDS distilled water up to 1 L
10X Transfer Buffer	30.3 g Tris base 144 g Glycine distilled water up to 1 L
1X Transfer Buffer	100 ml 10X Transfer Buffer 200 ml Methanol 700 ml distilled water
10X TBS (Tris Buffered Saline)	24.23 g Tris Base 80.06 g NaCl distilled water up to 1 L pH 7.4 - 7.6
1X TBST (Tris Buffered Saline with Tween-20)	100 ml 10X TBST 900 ml distilled water 10 ml 10% Tween-20

Table 3.5. SDS-PAGE and Western Blotting buffers and solutions (cont.).

Blocking Solution	5% non-fat milk powder in 1X TBST or 3% BSA (Bovine Serum Albumin) in 1X TBST
Stripping Solution	62.5 mM Tris-HCl, pH 6.8 2% SDS 0.7% β-mercaptoethanol

3.4.4. Immunoprecipitation Buffers and Solutions

Table 3.6. Immunoprecipitation buffers and solutions.

Solution/Buffer	**Content**
Protein A/G Plus Agarose Beads	0.5 ml agarose in 2.0 ml PBS buffer with 0.02% azide purchased from Santa Cruz, USA
IP Lysis Buffer	137 mM NaCl 20 mM Tris-HCl (pH 8.0) 2 mM EDTA 0.2 % NP40 1 mM PMSF 1X PI Cocktail
1X PBS (Phosphate Buffered Saline)	8 g NaCl 0.2 g KCl 1.44 g Na_2HPO_4 0.24 g KH_2PO_4

3.4.5. Polymerase Chain Reaction

Table 3.7. Polymerase chain reaction buffers and solutions.

Solution/Buffer	**Content**
10X Taq Polymerase Buffer	750 mM Tris-HCl (pH 8.8) 200 mM $(NH_4)_2SO_4$ 0.1% (v/v) Tween 20 Thermo, USA
Magnesium Chloride ($MgCl_2$)	25 mM, Thermo, USA
Deoxyribonucleotides (dNTPs)	100 mM of each dNTP
Dimethylsulphoxide (DMSO)	Applichem, Germany

3.4.6. Restriction Enzyme Analysis

Table 3.8. Buffers used in Restriction Enzyme Analysis.

Buffer	**1X Buffer Composition**
Buffer Tango	33 mM Tris-acetate (pH 7.9) 10 mM magnesium acetate 66 mM potassium acetate 0.1 mg/ml BSA
Buffer B	10 mM Tris-HCl (pH 7.5) 10 mM $MgCl_2$ 0.1 mg/ml BSA
Buffer O	50 mM Tris-HCl (pH 7.5) 10 mM $MgCl_2$ 100 mM NaCl 0.1 mg/ml BSA

Table 3.8. Buffers used in Restriction Enzyme Analysis (cont.).

Buffer R	10 mM Tris-HCl (pH 8.5) 10 mM $MgCl_2$ 100 mM KCl 0.1 mg/ml BSA

3.4.7. Bacterial Culture Solutions and Antibiotics

Table 3.9. Solutions and Antibiotics used for the growth and maintenance of bacterial cultures.

Solution	**Content**
Luria-Bertani medium (LB)	10 g tryptophan 5 g yeast extract 10 g NaCl Distilled water up to 1 L, autoclaved
Luria-Bertani Agar	10 g tryptophan 5 g yeast extract 10 g NaCl 15 g Agar Distilled water up to 1 L, autoclaved
Ampicillin stock	100 mg/ml in 50 % Ethanol Filter-sterilized and stored at -20°C 100 μg/ml (working concentration)
Kanamycin stock	50 mg/ml in distilled water Filter-sterilized and stored at -20°C 50 μg/ml (working concentration)
Chloramphenicol stock	30 mg Chloramphenicol in 1 ml Absolute Ethanol Filter-sterilized and stored at -20°C 30 μg/ml (working concentration)

Table 3.9. Solutions and Antibiotics used for the growth and maintenance of bacterial cultures (cont.).

SOC medium	20 g Tryptone 5 g Yeast Extract 2 ml of 5M NaCl 2.5 ml of 1M KCl 10 ml of 1M MgCl2 10 ml of 1M MgSO4 20 ml of 1M Glucose Distilled water up to 1L Filter-sterilized and stored at -20°C

3.5. Yeast Growth Media

The basic yeast media and supplements required for a two-hybrid screen were purchased from Clontech (CA, USA). These include YPD Medium (500 g), Minimal SD Base Medium (267 g), -Trp DO Supplement (10 g), -Leu DO Supplement (10 g), -Leu/-Trp DO Supplement (10 g), -His/-Leu/-Trp DO Supplement (10 g) and -Ade/-His/-Leu/-Trp DO Supplement (10 g). Additional media supplements include X-α-Gal (25 mg) as a stock solution of 20 mg/ml in dimethyl formamide, Adenine Sulfate (0.2 % stock solution) and L-Leucine.

For the preparation of rich YPDA media, 50 g YPD medium and 15 ml 0.2 % Adenine Sulfate were mixed with distilled water up to 1 L. pH of the solution was adjusted to 6.5 and then autoclaved.

For the preparation of Dropout (DO) media, 26.7 g Minimal SD Base was mixed with the appropriate DO Supplement (the amount as indicated in the manufacturer‟s recipe) and distilled water was added up to 1 L. pH of all Dropout Media was adjusted to 5.8 and then autoclaved. The solutions were stored at 4ºC in subdued light.

If agar plates were to be prepared, 20 g agar was included in the mixture prior to autoclaving. The plates were allowed to harden at room temperature and then stored in a plastic sleeve at 4ºC. In order to make X-α-Gal supplemented agar plates, X-α-Gal was diluted to 4 mg/ml in dimethyl formamide and spread 100 µl onto 10 cm plates or 200 µl onto 15 cm plates using a sterile glass rod.

3.6. Nucleic Acids

DNA molecular weight markers and deoxyribonucleotides were purchased from Fermentas (USA).

3.6.1. Plasmids

pEGFP-N2 (Clontech, CA, USA), pcDNA3 (Invitrogen, CA, USA) plasmids were commercially obtained. pGEMT Easy vector was commercially obtained from Promega, Wisconsin, USA. pcDNA3-S33Y-β-catenin mutant was kindly provided by Dr. Mehmet Öztürk, Bilkent University. LNCX-Wnt1, LNCX-Wnt3a and LNCX-Wnt5 plasmids were kindly provided by Dr. Xi He, Harvard Medical School. Control plasmids for the Matchmaker GAL-4 Yeast Two-Hybrid System, pGBKT7/p53 and pGADT7/T-antigen, were purchased from Clontech (CA, USA). The modified version of pcDNA3-HA vector was kindly provided by Dr. Nesrin Özören, Boğaziçi University. pBVI-NFkB-Luc (NFkB-luciferase plasmid) was kindly provided by Dr. Nesrin Özören, Boğaziçi University. pcDNA3-HA-NOD1 and pcDNA3-HA-NOD2 vectors were kindly provided by Dr. Nesrin Özören, Boğaziçi University.

3.6.2. Oligonucleotides

Primers used in polymerase chain reactions, sequencing and cloning were purchased from Harvard University MGH DNA Sequencing Core (Boston, USA) and Macrogen Inc. (Seoul, South Korea). Primers that were used in this study are tabulated in Table 3.10.

Table 3.10. Primers used throughout this study for cloning and diagnostic purposes.

Primer ID	**Sequence**	**Application**	**RE site**
BRI3_7F_cl	AAAGAATTCATGGACCACAAGCCGCT	Cloning	EcoRI
BRI3_8R_cl	AAAGTCGACTTAAGCGAAGGTGGCTCCA	Cloning	SalI
BRI3_9F_cl	AAAGCGGCCGCATGGACCACAAGCCGCT	Cloning	NotI
BRI3_10R_cl	AAATCTAGATTAAGCGAAGGTGGCTCCA	Cloning	XbaI
pACT2F	CTATTCGATGATGAAGATACCCCACCAAACC	Sequencing	-
pACT2R	GTGAACTTGCGGGGTTTTTCAGTATCTACGATT	Sequencing	-
pGADT7_seq_R	AGATGGTGCACGATGCACAG	Sequencing	-
briFmyc	AAATCTAGAATGGACCACAAGCCGCT	Cloning	XbaI
briRmyc	AAAGAATTCTTAAGCGAAGGTGGCTCCA	Cloning	EcoRI
bcr_gfp_R	AAAGGGCCCAGCGAAGGTGGCTCCACAG	Cloning	ApaI
IFITM_3F	AAAAAGCTTATGAATCACACTGTCCAAACC	Cloning	HindIII
IFITM_3R	AAAGGATCCTCCATAGGCCTGGAAGATCA	Cloning	BamHI
IFITM_4F	AAATCTAGAAATCACACTGTCCAAACCTTC	Cloning	XbaI
IFITM3_4R	AAAGAATTCCTATCCATAGGCCTGGAAGAT	Cloning	EcoRI
MGAT1_3F	AAATCTAGAATGCTGAAGAAGCAGTCTGCAG	Cloning	XbaI
MGAT1_4R	AAAGAATTCCTAATTCCAGCTAGGATCATAG	Cloning	EcoRI
MGAT_5F_cl	AAAAAGCTTATGCTGAAGAAGCAGTCTGCAG	Cloning	HindIII
MGAT_6R_cl	AAAGGATCCATTCCAGCTAGGATCATAGCC	Cloning	BamHI
BRI3_b_8R	AAAGTCGACTCAGGTACAGACTCTCAAAGG	Cloning	SalI
Bri3_b_9R	AAAGGGCCCGGTACAGACTCTCAAAGGAT	Cloning	ApaI
CTNNB1_7Fcl	GACTAGATCTATGGGTAAAGGCAATCCTGAGGAA	Cloning	BglII
CTNNB1_6Rcl	CCTCATCTAATGTCTCAGGG	Cloning	-
CTNNB1_10Fcl	AAAGGGCCCAGCGAAGGTGGCTCCACAG	Cloning	ApaI
CTNNB1_9Rcl	AAAGGATCCCAGGTCAGTATCAAACCAGGC	Cloning	BamHI
CTNNB1_11Fcl	AAAGGATCCATGGCTACTCAAGCTGATTTGAT	Cloning	BamHI
CTNNB1_12F	AAAGGATCCATGGAACCAGACAGAAAAGCG	Cloning	BamHI

Table 3.11. Primers used throughout this study for cloning and diagnostic purposes (cont.).

pGL3-RV3	CTAGCAAAATAGGCTGTCCC	Sequencing	-
pGL3-GL2	CTTTATGTTTTTGGCGTCTTCC	Sequencing	-
Traf2_HA_1F_cl	AAATCTAGAATGGCTGCAGCTAGCGTGAC	Cloning	XbaI
Traf2_HA_2R_cl	AAAGAATTCTTAGAGCCCTGTCAGGTCCA	Cloning	EcoRI
Traf2_3F_cl	AAAGAATTCATGGCTGCAGCTAGCGTGAC	Cloning	EcoRI
Traf2_4R_cl	AAAGGGCCCGAGCCCTGTCAGGTCCACAA	Cloning	ApaI
Traf6_HA_1F_cl	AAATCTAGAATGAGTCTGCTAAACTGTGA	Cloning	XbaI
Traf6_HA_2R_cl	AAAGAATTCCTATACCCCTGCATCAGTAC	Cloning	EcoRI
Traf6_3F_cl	AAAGAATTCATGAGTCTGCTAAACTGTGA	Cloning	EcoRI
Traf6_4R_cl	AAAGGGCCCTACCCCTGCATCAGTACTTC	Cloning	ApaI
BRI3_prmt_1F	TAAGCTAGCAGAGCTACAGTGCAGGTG	Cloning	NheI
BRI3_prmt_2R	TAAAAGCTTATAGGGTCATGACCTTTA	Cloning	HindIII
IFITM3_prmt_1F	TAAGCTAGCTAACTAGTGACTTCAAGT	Cloning	NheI
IFITM3_prmt_2R	TAAAAGCTTCTGCCAGGCCTGCGCTGA	Cloning	HindIII
MGAT1_prmt_1F	TAAGCTAGCCTTGTGACCGAGTCCTTC	Cloning	NheI
MGAT1_prmt_2R	TAAAAGCTTACCTACTCACCAGGTCCT	Cloning	HindIII

3.7. Antibodies

Table 3.12. Antibodies used throughout this study.

Antigen	Supplier	Host	MW (kDa)
HA	Sigma	Mouse	-
HA	Pierce	Rabbit	-
BRI3	Abcam	Rabbit	14
BRI3	Sigma	Rabbit	14
TNF-α	Cell Signaling	Rabbit	18

Table 3.13. Antibodies used throughout this study (cont.).

MGAT1	Abcam	Mouse	49
IFITM3	Cell Signaling	Rabbit	15
GFP	Santa Cruz	Rabbit	27
EpCAM	Abcam	Rabbit	40
NFkB-p65	Cell Signaling	Rabbit	65
p-NFkB-p65	Cell Signaling	Rabbit	65
IkB-α	Cell Signaling	Mouse	39
p-IkB-α	Cell Signaling	Rabbit	40
IKK-α	Cell Signaling	Mouse	85
IKK-β	Cell Signaling	Rabbit	87
p-IKK-α/β	Cell Signaling	Rabbit	85,87
TRAF2	Cell Signaling	Rabbit	53
TRAF6	Cell Signaling	Rabbit	60
NIK	Cell Signaling	Rabbit	125
B-catenin	BD Biosciences	Mouse	92
Non-phospho B-catenin	Cell Signaling	Rabbit	92
AKT	Cell Signaling	Rabbit	60
p-AKT (Thr308)	Cell Signaling	Rabbit	60
ERK1/2	Cell Signaling	Rabbit	42,44
p-ERK1/2	Cell Signaling	Rabbit	42,44
C-myc	BD Biosciences	Mouse	62
HSF2	BD Biosciences	Mouse	60
GAPDH	Santa Cruz	Rabbit	37
Anti-rabbit IgG (secondary)	Cell Signaling	Goat	-
Anti-mouse IgG (secondary)	Cell Signaling	Horse	-

3.8. Disposable Labware

Table 3.14. List of disposable labware used in this study.

Western Blotting Paper	Whatmann, UK
Centrifuge Tubes (15 ml, 50 ml)	TPP, Switzerland
Microfuge Tubes (1.5 ml, 2 ml)	Axygen, USA
PCR Tubes (0.2 ml)	Axygen, USA
Cryovial Tubes	Grenier Bio One, UK
Cell Culture Plates (10 cm, 6-well, 96-well)	TPP, Switzerland
Cell Scraper	TPP, Switzerland
Serological Pipettes (5 ml, 10 ml, 25 ml)	Capp, Denmark
Syringes (10 ml, 50 ml)	Set Medikal, Turkey
Insulin syringes (1 ml)	Set Medikal, Turkey
Pipette Tips (Filtered)	Capp, Denmark
Pipette Tips (Bulk)	Axygen, USA
96-well plates for qRT-PCR	Roche, Switzerland

3.9. General Equipment

Table 3.15. Equipment used in this study.

Agarose Gel Electrophoresis System	Mini-sub Cell GT, BioRad, USA
Autoclaves	MAC-601, Eyela, Japan ASB260T, Astell, UK
Balances	Electronic Balance VA 124, Gec Avery, UK DTBH 210, Sartorius, GERMANY
Carbon dioxide tank	2091, Habaş, TURKEY
Cell culture incubator	Hepa Class 100, Thermo, USA
Centrifuges	Centrifuge 5415R, Eppendorf, USA Allegra X22-R, Beckman, USA J2-21 Centrifuge, Beckman, USA J2-MC Centrifuge, Beckman, USA Mini Centrifuge 17307-05, Cole Parmer, USA
Cold room	Birikim Elektrik Soğutma, Turkey
Deep freezers	−20°C, 2021D, Arçelik, Turkey −70°C Freezer, Harris, UK −86°C ULT Freezer, ThermoForma, USA −152°C, MDF-1156, Sanyo,Japan
Documentation System	Gel Doc XR System, Bio-Doc, ITALY Stella, Raytest, Germany G:BOX Chemi XX6, Syngene, UK
Electrophoresis Equipments	Mini-Protean III Cell, Bio-Rad, USA
Flow Cytometer	FACSCalibur , Becton Dickinson, USA
Heat blocks	DRI-Block DB-2A, Techne, UK
Heating Magnetic Stirrer	M221 Elektro-mag, TURKEY Clifton Hotplate Magnetic Stirrer, HS31, UK

Table 3.15. Equipment used in this study (cont.).

Hemocytometer	Improved Neubauer, Weber Scientific Interna-tional Ltd. UK
Homogenizer	MagnaLyser
Hybridization Oven	Shake'n'Stack, Hybaid, UK
Ice Machine	Scotsman Inc., AF20, ITALY
Incubators	Hepa Class II Forma Series, Thermo, USA Weiss Gallenkamp, Plus Series, UK
Laboratory Bottles	Isolab, GERMANY
Laminar flow cabinet	Labcaire BH18, UK
Liquid Nitrogen Tank	Air Liquide, TR21, FRANCE
Luminometer	Fluoroskan Ascent FL, Thermo Electron, USA
Micropipettes	Finnpipette, Thermo, USA
Microplate Readers	680, Biorad, USA VersaMax, Molecular Devices, USA
Microscopes	Inverted Microscope, Axio Observer Z1, Zeiss, USA Light Microscope, CKX41, Olympus, JAPAN Confocal Microscope, DM 6000 CS, Leica, Germany
Microwave ovens	Philips Whirlpool, USA M1733N, Samsung, MALAYSIA
pH meter	WTW pH330i, GERMANY
Pipettor	Pipetus-akku, Hirscmann Labogerate, GERMANY
Power Supplies	Power Pac Universal, Biorad, USA EC135-90, Thermo Electron Corp,USA
Refrigerators	2082C, Arçelik, TURKEY 4030T, Arçelik, TURKEY

Table 3.16. Equipment used in this study (cont.).

Scales	Precisa XT4200C, Germany
Shakers	VIB Orbital Shaker, InterMed, DENMARK Lab-Line Universal Oscillating Shaker, USA Thermo EC, Forma Orbital Shaker 420, USA
Softwares	Quantity One, Bio-Rad, ITALY CellQuest Becton Dickinson, USA ImageJ, Image Analysis Software, NIH, USA XStella 1.0, Stella, GERMANY
Spectrophotometer	Agilent 8453, USA NanoDrop ND-1000, Thermo, USA
Speed Vacuum	Thermo EC, SPD111V, USA
Thermocyclers	GeneAmp PCR System 2700, Applied Biosystems, USA
Vacuum pump	KNF Neuberger, USA
Vortex	Vortexmixer VM20, Chiltern Scientific, UK
Water baths	TE-10A, Techne, UK
Water purification system	UTES, TURKEY

4. METHODS

4.1. Molecular Cloning

4.1.1. PCR Reaction

DNA fragments to be cloned into plasmid vectors were amplified using the Phusion High-Fidelity DNA Polymerase (NEB, USA). Primer design was done using NCBI Primer BLAST – Primer designing tool (http://www.ncbi.nlm.nih.gov/tools/primer-blast/). For cloning purposes, appropriate restriction endonuclease sites were attached at the 5' ends of the primers and "AAA" sequence is also added to the 5' ends as "spacers" for restriction enzyme binding. PCR reactions were carried out according to manufacturer's instructions. The protocol for Phusion polymerase is summarized in Table 4.1.

Table 4.1. PCR protocol using the Phusion High-Fidelity DNA Polymerase

Step #	Description	Temperature (°C)	Duration
1	Initial denaturation	98	30 s
2	Denaturation	98	10 s
3	Annealing	Primer specific Tm	10s
4	Elongation	72	15 s per 1 kb
5	Return to Step 2 (x30)	-	
6	Final Elongation	72	5 min

4.1.2. Restriction digestion of plasmids and PCR products

Restriction digestions of plasmid DNA or purified PCR products were carried out with suitable restriction enzymes at 37 ºC for 3-4 hours in an appropriate buffer containing 50 mM Tris-HCl (pH 8.0), 10 mM $MgCl_2$, and 100 mM NaCl. Restriction enzymes were purchased from Thermo Scientific (USA). One unit of enzyme was used for the digestion of 1µg of DNA. Inhibition of the restriction enzyme was performed at 80ºC for 20 min.

4.1.3. Agarose Gel Electrophoresis

DNA fragments were fractionated by horizontal electrophoresis using standard 1X TAE-based agarose gels (1 per cent to 2 per cent). Agarose powder was mixed with 1X TAE Buffer and allowed to boil in a microwave oven. After cooling for a couple of minutes, ethidium bromide was added to final concentration of 30 ng/ml and the solution was poured into the gel casting tray. Appropriate amounts of the DNA samples were mixed with 6X loading buffer to get 1X final concentration. Gene Ruler 1kb DNA ladder (Thermo Scientific, USA) was used as molecular weight marker. The solidified gels were run in 1X TAE buffer at varying voltage and time depending on the size the fragments. The gels were visualized under UV light and the images were documented with GelDoc imaging system (BioRad, USA).

4.1.4. PCR Purification and Agarose Gel Extraction

PCR products and restriction enzyme digested DNA fragments were purified with spin columns using the PCR purification kit (Qiagen, USA) according to manufacturer's instructions. For the restriction enzyme digested plasmid DNA, the sample was run on agarose gel and the DNA fragment of interest was cut from the gel using a razor blade under UV light. The DNA fragment in agarose gel was purified by using the Gel Extraction kit (Qiagen, USA), according to manufacturer's instructions.

4.1.5. Ligation of DNA molecules

Restriction enzyme digested vectors and inserts were ligated using T4 DNA Ligase (NEB, USA). The concentrations of vector and insert DNAs were determined by absorbance measurements at 260 nm and their purity was confirmed by agarose gel analysis. Ligations were performed in 10 µl of total reaction volume containing 50-100 ng of plasmid DNA and molar excess of insert DNA, approximately in 1:3 (vector : insert) ratio, in the presence of 1 unit of T4 DNA Ligase and 1X T4 Ligation Buffer at room temperature for 30 minutes. Inhibition of T4 DNA Ligase was performed by incubating the reaction tube at 70 ºC for 10 minutes.

4.1.6. Preparation of Chemically Competent Cells

5 ml LB medium containing streptomycin (25 µg/ml) was inoculated with E.coli strain DH5α and grown overnight at 37ºC with shaking at 200 rpm. After 16 hours, 25 ml LB was inoculated with 250 µl of the grown culture to make 1:100 dilution. Cells were grown in the shaker till OD 595 reached 0.4. Cells were harvested by centrifuging at 3000 rpm for 10 minutes at 4ºC. The pellet was resuspended in 12.5 ml of ice-cold sterile 50 mM $CaCl_2$ and incubated on ice for 30 min. Cells were centrifuged again (3000 rpm for 10 min at 4ºC) and the pellet was resuspended in 2.5 ml of ice-cold sterile 50 mM $CaCl_2$ containing 10% glycerol. The solution was aliquoted into Eppendorf tubes, 50-100 µl each. The aliquots were rapid-frozen in liquid nitrogen and stored at -80ºC until used.

4.1.7. Transformation of the Chemically Competent Cells

A vial (50-100 µl) of competent cells was thawed on ice for 10-15 min. 1 µl plasmid or 10 µl of the ligation product was added onto the competent cells and incubated on ice for 15-20 min. Next, the vial was placed in 42ºC heat block for 1 min and then immediately on ice for 2 min. 500 µl LB or SOC medium was added and the cells were incubated at 37ºC for 1 hour with shaking at 200 rpm. The cells were centrifuged for 2-3 min and resuspended in 100-150 µl LB medium and the suspension was spread onto LB plates containing the appropriate antibiotic. The plates were incubated overnight at 37ºC in inverted position.

4.1.8. Colony PCR

The following PCR reaction in a total volume of 25 µl was prepared. 1X Taq Polymerase Buffer, 2 mM $MgCl_2$, 0.25 mM dNTP mixture, 5 per cent DMSO, 0.4 µM of each primer, 0.05u/µl Taq DNA polymerase (Fermentas). As the template of PCR reaction, each of the transformed bacterial colonies were picked up from the LB Agar plates by using autoclaved tips and transferred to the corresponding PCR tubes. The PCR reaction was started with an initial denaturation step at 94ºC for 5 min. Cycling conditions of PCR were as following : denaturation step at 94ºC for 30 sec, annealing step at 55ºC for 30 sec

and elongation step at 72ºC for 30 sec or 1 min. After 28-32 cycles, the PCR reaction was ended with a final elongation step at 72ºC for 7 min.

4.1.9. Plasmid DNA Purification and Sequencing

Plasmid DNA purification from overnight grown bacterial cultures were performed using Qiagen QIAprep Spin Miniprep Kit and Roche High Pure Plasmid Isolation Kit for miniprep isolations, and Thermo Scientific Midiprep Kit and Roche Genopure Plasmid Midi Kit for midiprep isolations, according to the manufacturer's protocol. Only midipreps of plasmids were used for the transfection of cell lines. Quality and concentration of the isolated plasmids was checked by spectrophotometric measurements using a NanoDrop-1000 spectrophotometer with OD260/280 ratios of plasmid preparations being between 1.8 and 2.0. Sequencing of the plasmids was done at Macrogen Inc. (South Korea) using sequencing primers. The bacterial cells carrying the plasmids with the desired fragments were stocked by adding 10% glycerol into overnight bacterial culture and stored at -80ºC until used.

4.2. Cell Culture Experiments

4.2.1. Maintenance of Cells

HCC derived cell lines (Huh7, Hep3B, HepG2, Mahlavu), HCT116 (Human Colorectal carcinoma), HeLa (Human Cervical carcinoma) and HEK 293 FT (Human Embryonic Kidney) cell lines were grown in DMEM containing 10 per cent FBS (Gibco) and 1 per cent penicillin/streptomycin (Hyclone) in an incubator at 37ºC, with 5 per cent CO_2 and 95 per cent air. Media were kept at 4ºC and warmed to 37ºC in a water bath before use. Cells were routinely passaged before reaching ~90 per cent confluence. For this purpose, the growth medium was aspirated and the cells were washed once with 1X calcium and magnesium-free PBS. In order to remove the monolayer cells from the surface, the cells were treated with trypsin-EDTA solution (0.025 per cent trypsin, 0.5mM EDTA) and incubated at 37ºC for 5 minutes. 5 volumes of fresh medium were added to inactivate trypsin, the cell suspension was transferred to a 15 ml falcon tube and

centrifuged at 1600 rpm for 5 minutes. The supernatant was aspirated and cell pellet was suspended in 4 ml of fresh growth medium. The cells were transferred to sterile cell culture dishes containing growth medium in 1:5 ratio for standard passaging.

4.2.2. Cell Freezing

Mammalian cells were frozen as stocks until further usage. Freezing was applied to cells in 10 cm cell culture plates with ~90% confluency. The medium over the cells was aspirated and the cells were washed with 1X PBS. Then, trypsin was added onto the cells and incubated at 37ºC for 5 minutes. Fresh medium was added and the cell suspension was transferred into a 15 ml Falcon tube. Cells were pelletted by centrifugation at 1600 rpm for 4 minutes. Cell pellet was resuspended in 6-8 ml of fresh medium containing 10% DMSO. The cells suspension was distributed into 2 ml cryogenic vials and stored in isopropanol boxes at -80ºC for 1 day, then transferred to -150ºC for final storage.

4.2.3. Cell Thawing

The frozen cryogenic vials were thawed in a water bath at 37 °C and immediately mixed with 5 ml of cell culture medium and centrifuged at 1200 rpm for 4 min. Then, the cell pellet was resuspended in 10 ml of fresh growth medium and transferred to 10 cm culture dishes.

4.2.4. Transfection of Mammalian Cell Lines

Transfections were carried out using the Turbofect transfection reagent (Thermo Scientific Inc., USA) according to DNA: reagent ratios suggested by the manufacturer. Transfection complex was formed in pure DMEM without any FBS or antibiotics and added drop by drop over the attached cells on plate after incubation at room temperature for 15 minutes. Medium change was performed and fresh growth medium was added approximately 4 hours after transfection.

4.2.5. TNF-α treatment of HEK293-4KB-GFP cell lines

Lyophilized TNF-α (Santa Cruz, USA) is dissolved in 1X PBS (containing 10% Glycerol as cryopreservative) to a working concentration of 10 µg/ml, aliquoted and stored at -20°C. Any thawed aliquot was stored in refrigerator at 4°C for upto 4 weeks. The cells were incubated in the absence of serum the night before the treatment and during the treatment. On the day of experiment, the cells were washed with 1X PBS and treated with TNF-α with a final concentration of 20 ng/ml for time-course treatments. Reverse treatment was employed where all the cells at different time points were harvested at the same time (t=0 hr).

4.3. Yeast Two Hybrid Screening

Matchmaker GAL4-Yeast Two Hybrid System (Clontech) was used together with the pretransformed human liver cDNA library (Clontech). A fresh and large colony of the bait strain (AH109 [pGBKT7/Bri3]) was inoculated into 50 ml of SD/-Trp liquid medium and incubated at 30ºC with shaking (230-250 rpm) until the OD_{600} reaches 0.8. The cells were centrifuged at 1000 g for 5 min, and then resuspended in 5 ml of SD/-Trp. In a sterile 2 L flask, 1 ml aliquot of the library strain was combined with 5 ml bait strain. 45 ml of 2x YPDA liquid medium was added to the flask and incubated at 30ºC for 22 hr with slow shaking (50 rpm). After 22 hr, the cells were centrifuged. The 2L flask was rinsed twice with 50 ml 0.5x YPDA. The rinses were then combined and used to resuspend the pelleted cells. The cells were again centrifuged for 10 min and all pelleted cells were resuspended in 10 ml of 0.5x YPDA liquid medium. The mated culture was spread on SD/-Ade/-His/-Leu/-Trp plates (200 µl per 150 mm plate). The plates were incubated at 30ºC for 5-6 days.

4.4. SDS/PAGE and Western Blotting

4.4.1. Cell Lysis and Protein Extraction from HEK293FT Cell Line

Lysis of the cells and protein isolation was performed from cells either in 6-well plates or 10 cm plates. The adherent cells on the plates were washed once with 1X PBS. Then lysis buffer containing freshly added protease inhibitors, was added onto plates such as 100 µl for 6-well plate and 400 µl for 10 cm plate. Plates were placed onto ice and incubated for about 10 minutes. Cells were then scraped using cell scrapers, collected into 1.5 ml micro centrifuge tubes and incubated on ice for 15-20 min. Insulin syringes were used to homogenize the cells and get rid of genomic DNA. Cell lysates were centrifuged at 12000g for 10 minutes at 4°C. Supernatants obtained after centrifugation were transferred into fresh 1.5 ml micro centrifuge tubes. Protein lysates were stored at -20°C for short term storage or -80°C for long term.

4.4.2. Quantification of Protein Lysates

Protein quantification was performed by using BCA Protein Assay Kit (Thermo). BSA standards were prepared via serial dilution with 1X PBS to obtain different concentrations (125, 250, 500, 750, 1000, 1500, and 2000 µg/ml). Protein samples were prepared as 1/5 dilution in cell lysis buffer for the assay. All samples were prepared in triplicate. To prepare the BCA Working Reagent, 50 parts Reagent A was mixed with 1 part Reagent B. For each sample, 200 µl of BCA Working Reagent was prepared and added onto a 96 well plate. The plate was placed on ice. BSA standards and protein samples were added onto each well as 5 µl. The plate was then incubated at 37°C for 30 minutes and afterwards cooled at RT for 5 minutes. The absorbance of the samples was measured at 562 nm on the plate reader. Blank values were subtracted from the average value measured at 562 nm absorbance. To calculate the concentration of the samples, a standard curve was prepared by plotting blank corrected BSA measurements at 562 nm versus their corresponding concentrations in µg/ml. By using a standard curve, the concentration of each sample was calculated.

4.4.3. SDS/PAGE

SDS-PAGE gels were cast and run by using a Mini-Protean Tetra cell (BioRad). 10% separating gels (with 37.5:1, acrylamide: bis-acrylamide ratio) were cast first. In order to avoid any bubbles, distilled water was added on top of the separating gel until the end of polymerization reaction. Then, water was removed and a 5% stacking gel (with 37.5:1, acrylamide: bis-acrylamide ratio) was added on top of separating gel. The comb was inserted at the top and the polymerization of stacking gel was awaited.

Table 4.2. Reagents used to prepare SDS/PAGE gels (for 4 mini gels).

	Separating Gel	**Stacking Gel**
ddH_2O	12,6 ml	9,8 ml
1.5M Tris-Cl (pH:8.8)	7,87 ml	-
1M Tris-Cl (pH:6.8)	-	1,68 ml
Acrylamide:Bisacrylamide (30% / 0.8% w/v)	10,5 ml	1,8 ml
SDS (10% w/v)	315 µl	135 µl
APS (10% w/v)	207 µl	120 µl
TEMED	50 µl	30 µl

4.4.4. Western Blotting

Samples were mixed with 5X SDS-PAGE loading dye and denaturation of the proteins was achieved via boiling the samples at 95°C for 5 minutes. Prepared protein samples were loaded into wells generated in the stacking gel, after the removal of the comb. 30-50 µg protein was loaded to each well, depending on the efficiency of the

antibody that was used. 5 µl of pre-stained protein marker (Thermo) was used as the molecular weight standard. The gels were run with 1X running buffer at 80V until the BPB front entered the separating gel and then the voltage was increased up to 120V. Runs were stopped when the BPB front left the separating gel. After completion of the run, the glasses were removed from the gels, and the gels were equilibrated in 1X Transfer Buffer for 10-15 minutes. PVDF membrane was activated in methanol for 5 minutes and then transferred to ddH_2O. Gels were placed into transfer cassettes for the transfer of proteins onto the membrane. The proteins on the gel were transferred to PVDF membranes for 1 hour at 100V. The transfer process was carried out with 1X Transfer Buffer in the cold room using the Mini Trans-blot cell (BioRad). The system was supplied with an ice-block to prevent excess heating during the run. After the completion of the transfer, the membrane was removed from the cassette and it was blocked with 5% non-fat dry milk or 3% BSA in TBST for 1 hour at room temperature. After blocking, the membrane was washed with 1X TBST for 2 minutes. Primary antibody was prepared in 5% BSA in TBST and incubation with primary antibody was performed overnight at 4°C. After the incubation with primary antibody, the membrane was washed three times with TBST for 5-10 minutes each. Then, HRP-conjugated anti-rabbit or anti-mouse secondary antibody was prepared in 5% BSA in TBST at 1:5000 dilution. Incubation with secondary antibody was performed at room temperature for 2 hours. After the incubation, the membrane was washed three times with 1X TBST for 5-10 minutes each. For the visualization of the proteins, Super Signal West Femto Maximum Sensitivity Kit (Thermo) was used to develop the blots. The blots were analyzed by using chemiluminescence imaging system (Syngene, UK).

4.5. Total RNA Isolation

Total RNA isolation is performed with RNeasy RNA Isolation kit (Qiagen, USA). Adherent cells on cell culture dishes were washed with 1X PBS, trypsinized and centrifuged at 1600 rpm for 5 minutes. Cell pellets were dissolved in 600 µl Lysis Buffer and vortexed for 10 sec. Homogenization of the lysate was accomplished by passing through an RNase-free syringe several times. After addition of 360 µl Absolute EtOH, the sample was transferred to an RNA Purification Column and centrifuged for 1 min. at 12.000 g. The sample in the column was washed respectively with 700 µl Wash Buffer 1

and 600 µl Wash Buffer 2 and centrifuged for 1 min. at 12000 g between each wash. After last wash with 250 µl Wash Buffer 2 and centrifugation for 2 minutes at 12000 g, total RNA is eluted with 100 µl of nuclease-free water. Total RNA concentration is measured by nanodrop spectrophotometer and absence of DNA contamination is confirmed (OD 260/280 ratio>2). Total RNA integrity is checked by loading the samples on 1% denaturing agarose gel and confirming the presence of 18S and 28S ribosomal RNAs. Purified RNA samples were stored at -80ºC until use.

4.6. Reverse Transcription PCR (RT-PCR)

Total RNA is converted into cDNA by using Promega ImProm-II Reverse Transcription System. 1 µg total RNA was incubated with Oligo dT primers for 5 minutes at 70°C to achieve complete denaturation, followed by immediate cooling on ice for 5 minutes. The premix containing 6,25 mM $MgCl_2$, 1X ImProm-II reaction buffer, 0,5 mM PCR nucleotide mix, rRNasin Ribonuclease inhibitor and ImProm-II reverse transcriptase was prepared and distributed into the reaction mixes. The samples were first incubated for 5 min at 25°C to allow the annealing of primers, then for 1 hour at 42°C for the synthesis reaction to take place. Finally, reverse transcriptase was inactivated by incubating the reaction at 70°C for 5 minutes. After completion, each product was diluted by 1:5 with nuclease-free water.

4.7. Coimmunoprecipitation

HEK 293FT cells or HEK 293T cells were transfected with plasmids carrying the tagged versions of corresponding genes. Firstly, 1:1 suspension of protein G Agarose bead slurry was washed with ice-cold lysis buffer three times. Anti-HA antibody diluted in 1X PBS was incubated with 30 µl of Protein G Agarose beads for 4 hrs at room temperature by swinging head over tail. After the incubation, the antibody-bead complexes were washed 3 times with Co-IP Lysis Buffer at 4°C by spinning. 48 hours after transfection, adherent cells were washed with ice-cold 1X PBS and then lysed in ice-cold Co-IP Lysis Buffer supplemented with 1X Protease Inhibitor Cocktail and 1mM PMSF. The cells on

the plate were harvested using a cell scraper and transferred into an Eppendorf tube. Complete lysis was assured by pipetting the solution several times and incubating on ice for 30 mins. The cell lysate was centrifuged at 12.000 rpm for 15 mins at 4°C. 30-40 µl of input was obtained and the remaining supernatant was added onto the antibody-bead complex in Eppendorf tubes. The tubes were allowed to swing head-over-tail at 4ºC in cold room for overnight. Next day, the antibody-bead-protein complexes were washed 3 times with Co-IP Lysis Buffer and once with 1X PBS. Final supernatant was removed and the tubes were stored at -80ºC refrigerator until used in SDS-PAGE analysis.

4.8. Generation of Stable Cell Lines

Huh7 cells in 6-well plates were transfected separately with the following constructs: pIRES2-EGFP-BRI3, pIRES2-EGFP-MGAT1 and pIRES2-EGFP-GFP (as control construct). For optimization, the minimal concentration of antibiotic that efficiently kills all non-transfected cells between 4-6 days following the addition of antibiotic was identified. 24 hours after the transfection of Huh7 cell lines, antibiotic selection was initiated using Geneticin - G418 Sulfate - solution (Hyclone). From the 50 mg/ml stock solution, 1:100 dilution ratio was used in order to add into the growth medium of transfected cells. 500 µg/ml Geneticin was used as working solution for selection of stable cell lines. The growth medium was replaced with fresh medium supplemented with 500 µg/ml Geneticin every 2-3 days in order to prevent the antibiotic from losing its effect. The selection was carried on for 3-4 weeks, while the cells were passaged when confluency was reached. The cells were checked with the fluorescence microscope for the presence of GFP. 250 µg/ml Geneticin was used as working solution for the maintenance of stable cell lines.

4.9. PI Staining and FACS Analysis

Stably transfected Huh7 cells were allowed to grow on 6-cm plates for 2-3 days. At the day of experiment, the cells were trypsinized and centrifuged at 200 g for 5 mins. The growth medium was discarded and the cells were suspended in 5 ml of 1X PBS, then

centrifuged again at 200 g for 5 mins. Fixation of cells was performed by adding 5 ml of 70% EtOH drop by drop while vortexing at the same time in order to avoid clump formation. Then the cells were kept 30 minutes on ice. In order to remove EtOH, the cells were centrifuged at 300 g for 5 mins and then resuspended in 5 ml PBS. After a second round of centrifugation, the supernatant was decanted and 1 ml of Propidium iodide staining solution (20 µg/ml propidium iodide in 0.1% Triton X-100 + 200 µg/ml RNase at final concentration) was added and incubated for 20 minutes at 37ºC. The tubes were covered with aluminum foil to prevent direct light exposure. The cells were centrifuged at 200 g for 5 mins and resuspended in 750 µl of PBS for flow cytometric analysis.

4.10. Wound Healing Assay

Huh7 cells stably expressing the corresponding genes (BRI3, MGAT1 and GFP) were grown to full confluency on a 6-well cell culture plate. A wound is introduced by scratching the confluent monolayer cells using a plastic pipette tip (Time = 0). Plates were washed twice with 1X PBS in order to remove detached cells and the adherent cells were incubated with complete growth medium. The bottoms of the wells were marked to indicate where the initial pictures of the wound area were obtained. The closure of the wound was observed in the following 24, 48 and 72 hours by taking the images of the same areas at 10X magnification, and recorded using an Axio-vision inverted fluorescent microscope (Zeiss).

4.11. XTT Cell Proliferation Assay

XTT Cell Proliferation Assay Kit II (Roche, Switzerland) was used according to manufacturer's instructions. The stable Huh7 cells were seeded into 96-well cell culture plates at a concentration of 4 x 103 cells per well. The cells were incubated at 37°C incubator for 3 days. At the day of experiment, the XTT labeling reagent was mixed with electron-coupling reagent in a 50:1 ratio. 50 µl of XTT labeling mixture was added per well and the cells were incubated with this mixture for 2 hours at 37°C. The spectrophotometric absorbances of the samples at 475 nm were measured in a plate reader. A second measurement was performed at 650 nm as the reference wavelength.

4.12. Luciferase Reporter Assay

In order to determine any change in promoter activity, luciferase assay was performed according to Dual-Glo Luciferase Assay System (Promega) protocol. For the assay, cells were co-transfected with 1 μg of a pGL3-luciferase reporter plasmid including promoter of interest, 1 μg β-catenin, TCF4 or dNTCF4 expression plasmid and 100 ng of pGL3-SV40-Renilla (internal control) per well of a 12-well plate. Transfection is done by using Turbofect transfection reagent (Thermo Scientific) according to the manufacturer's instructions. About 48 hours post-transfection, cells were collected by trypsin, and then washed with 1X PBS twice. Pellet was completely resuspended in 100 μl 1X PBS and placed into 96-well plate. Then, 100 μl of Firefly luciferase substrate reagent added on to the lysates, and after 30 min incubation at room temperature (in the dark), measurements were taken 3 times using a fluorometer (Fluoroskan Ascent FL, Thermo Electron). Next, 100 μl of Renilla luciferase substrate reagent (Stop&Glo) that also quenches the Firefly luciferase luminescence was added and after 10 min incubation at room temperature (in the dark), measurements were taken 3 times. Luminescence reads were taken at 2 seconds of integration time. Firefly luciferase readings were normalized to Renilla luciferase readings and graphs were plotted in Microsoft Excel.

4.13. Lithium Treatment Assay

Huh7 cells were seeded into 10 cm culture dishes or 6-well plates based on the experiments. Following day, lithium chloride (LiCl) or sodium chloride (NaCl) was added to the medium of the cells to a final concentration of 25 mM. Reverse treatment was employed where all the cells treated at different time points (indicated at the results part) were harvested at the same time (t=0 hr). For protein isolation from the treated cell lines, cell lysis buffer with freshly added protease inhibitors was added on to the cells (100 μl for per well of 6-well plate and 400 μl for 10 cm plate) and the cells were subjected to protein extraction procedure.

4.14. Confocal Microscopy

Huh7 cells grown on 18 mm coverslips inside the 12-well culture plates were used for imaging with confocal microscopy. The cells were transfected with the plasmids expressing the fluorescent-tagged versions of our proteins in concern, by using the Turbofect transfection reagent (Thermo Scientific) according to the manufacturer's instructions. 48 hours after transfection, the growth medium was aspirated and the cells were washed with 1X PBS. 250-300 µl of ice-cold 4% paraformaldehyde was added on the cells in each well. The cells were incubated at room temperature for 20 min without shaking. Then, 4% paraformaldehyde was aspirated and the cells were washed with 1X PBS three times. 250 µl of DAPI solution (1 mg/ml) was added onto the cells. The cells were incubated with DAPI for 1-2 min, and then washed with 1X PBS three times. Using forceps, the coverslips inside the wells were placed onto the slides with 3 µl mounting medium. After drying for a few minutes, nail polish was applied to intersection areas around the coverslip. The preparations were stored in the refrigerator at 4°C until analyzed with the confocal microscope.

4.15. Quantitative Polymerase Chain Reaction

Real Time PCR was performed with gene specific primers using the Maxima SYBR Green/ROX qPCR kit (Thermo, USA) according to the manufacturer's protocol. The primers were chosen among the primers of MGH primer bank encompassing intron/exon junctions and blasted against the target genome. The reaction mixtures were distributed into the wells of 96-well qPCR plate and cDNAs were added last. The plate was covered with transparent foil and centrifuged at 2000 rpm for 2 min in order to collect the components to the bottom of the wells. PCR reaction was started with initial denaturation at 95°C for 10 min. Amplification cycle consists of three steps; a denaturation step at 95°C for 15 seconds, an annealing step at 60°C for 30 seconds and an elongation step at 72°C for 30 seconds. It was repeated for 40 cycles and finished by a melting curve step. For each gene, expression levels were normalized to GAPDH as control. Relative expression levels were calculated with the $2^{-\Delta\Delta Ct}$ method, comparing the expression level of the gene of interest between the test sample and control sample.

4.16. Human Cancer Cell Line Tumor Xenograft in NUDE/SCID mice

The growth medium over the full confluent cells in 10-cm cell culture plates was aspirated and the cells were washed twice with 1X PBS, then trypsin is added. The trypsinized cells were transferred into 15 ml Falcon tubes with growth medium and centrifuged at 1100 rpm for 5 minutes. The cells were resuspended in sterile PBS and centrifuged again. Cell pellet was resuspended in 150 µl PBS and kept on ice until injection. The cells in Eppendorf tubes were mixed and drawn into a syringe without a needle, then injected subcutaneously and bilaterally into the abdominal (flank) regions of 6-14 week old female NUDE or SCID mice. While right flanks of animals were injected with control cells, the left flanks of the same animals were injected with the cells overexpressing the genes of interest. Approximately 3-4 weeks later, tumor formations were started to be observed. The mice were sacrificed by using a carbon dioxide chamber, and the subcutaneous tumors were isolated, photographed and their weights were determined. The tumor samples were separately collected in 15 ml falcon tubes and stored at -80ºC for further analysis.

4.17. RNA Sequencing

Total RNA was isolated from the xenograft tumors with the purpose of RNA Sequencing. The concentration and purity of the isolated RNA was evaluated by nanodrop spectrophotometry. The integrity of RNA was checked on a denaturing formaldehyde agarose gel and each individual RNA sample was found to have distinct 28S and 18S ribosomal bands. Furthermore, the RNA preparations were analyzed by capillary electrophoresis using an Agilent Bioanalyzer 2100 prior to RNA Sequencing and their integrity was confirmed. Total RNA samples were processed with RNAstable kit (Biomatrica) to preserve RNA integrity during shipping at room temperature. 10 µg total RNA in nuclease free water was added into RNAstable tubes which contain RNAstable as a coating at the bottom. After mixing with RNAstable, the samples were dried by a freeze dryer Lyophilizer Machine (Biobase) for about 30 minutes. Tubes were kept at room temperature in sealed moisture barrier foil bags until shipping. The tubes were sent to GENEWIZ Genomics core at New Jersey, USA. Illumina HiSeq 2500 platform has been

used for sequencing. The samples were sequenced as single-end 50 bp reads. Bioinformatic analyses of the RNA-Seq raw data was done by Epigenetiks Genetik Biyoinformatik Yazılım A.Ş. (Istanbul, Turkey). Quantification of the mapped reads and determination of differentially expressed genes were performed by DESeq2 and Kallisto software.

5. RESULTS

The candidate transcriptional targets of the canonical Wnt/β-catenin pathway were determined previously in our laboratory by using genome wide microarray analyses and SAGE (Serial analysis of gene expression) techniques. BRI3 has been selected as being one of the most prominent targets of Wnt/β-catenin pathway, due to its transcriptional upregulation in hepatocellular carcinoma cells overexpressing the mutant and degradation-resistant form of β-catenin. This upregulation was further supported by experimental evidence coming from q-RTPCR analyses, chromatin immunoprecipitation assay (ChIP), luciferase reporter assay and treatment of cells with lithium chloride, which leads to the activation of Wnt/β-catenin pathway.

5.1. Identification of Interaction Partners of BRI3

Yeast Two Hybrid Assay was performed as a first step in order to determine the interaction partners of the BRI3 protein. For this purpose, pretransformed human liver cDNA library was used. Yeast mating has been performed between the MATa strain (AH109) transformed with the pGBKT7/Bri3 bait vector and the MATα strain (Y187) pretransformed with human liver cDNA library (Clontech, USA). The estimated number of independent clones screened by this mating was calculated to be 2.6×10^6. The mated culture was allowed to grow on SD/-Ade/-His/-Leu/-Trp agar plates, so that high stringency was used in order to detect the activation of the reporter genes ADE2 and HIS3. The positive clones obtained from yeast mating were re-streaked to single colonies on SD/-Ade/-His/-Leu/-Trp agar plates with X-α-Gal, in order to confirm the phenotype. As a result of two-hybrid interactions, in addition to ADE2 and HIS3 reporter genes, MEL1 which encodes the enzyme α-galactosidase will also be expressed. Yeast colonies that express Mel1 turn blue in the presence of the chromagenic substrate X-α-Gal. Therefore, those single blue colonies were analyzed primarily for being candidate positive colonies (Figure 5.1).

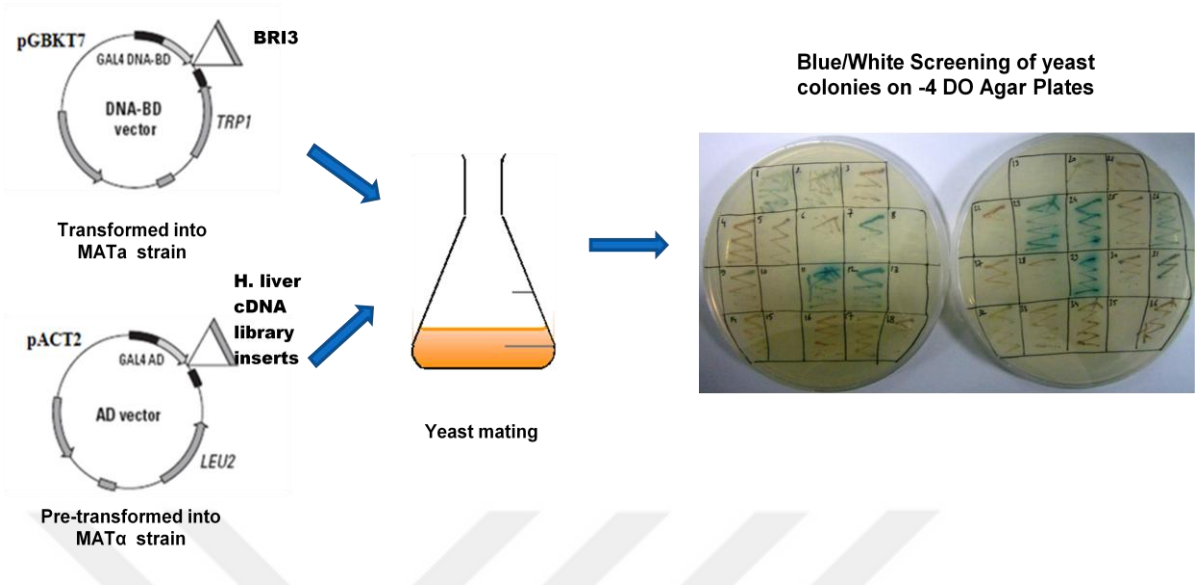

Figure 5.1. Yeast mating and subsequent screening of the resulting colonies on nutrient selective media.

The yeast colonies selected on the basis of blue/white screening were subjected to colony PCR analysis in order to identify the corresponding cDNA inserts. PCR products that corresponded to single and clear bands were sequenced and the identities of those cDNA clones were revealed by performing a BLAST search of the raw outputs over various databanks in order to find significant matches. Three candidate cDNA clones (IFITM3, IL-7R and MGAT1) were determined for further analysis. The vectors containing the cDNA insert of interest were isolated from the corresponding yeast colonies. Then, the bait vector together with the vector containing the candidate cDNA clone, were co-transformed into the yeast cells for confirmation. The transformed yeast cells were spread on nutrient selective media (SD/-Ade/-His/-Leu/-Trp) and tested for their ability to grow into colonies. As a result, co-transformation yielded colonies for two out of three selected cDNA clones (Figure 5.2). Thus, IFITM3 and MGAT1 were determined as candidate interacting partners for BRI3.

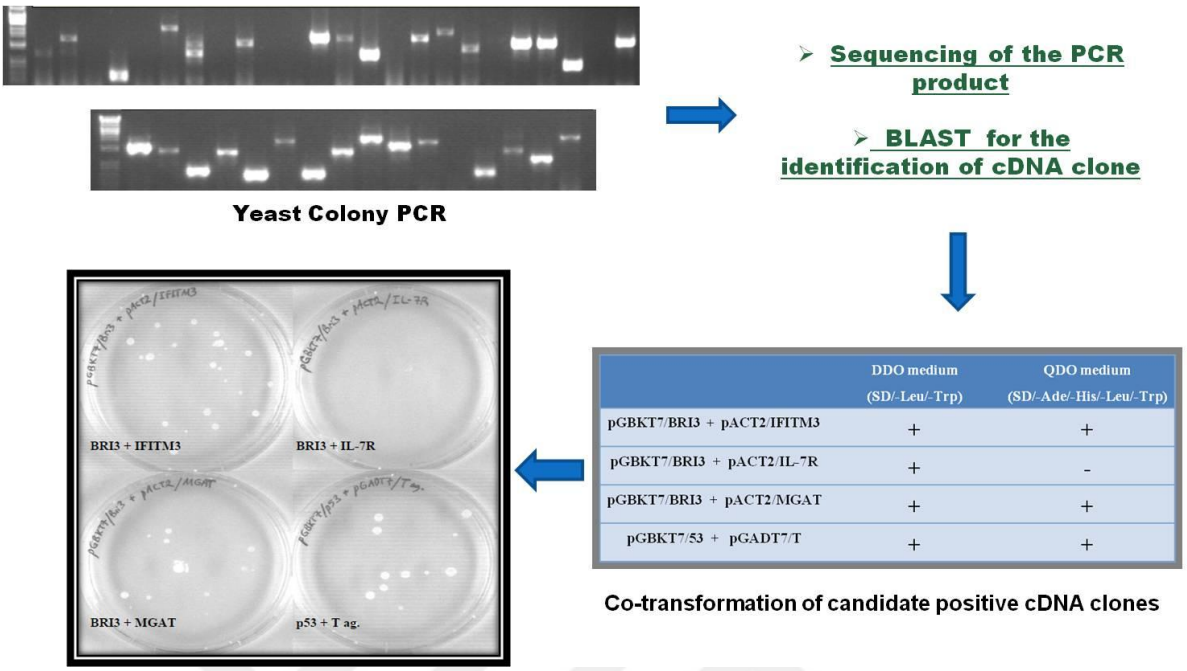

Figure 5.2. Identification of candidate cDNA clones by colony PCR, sequencing and confirmation by co-transformation into yeast cells.

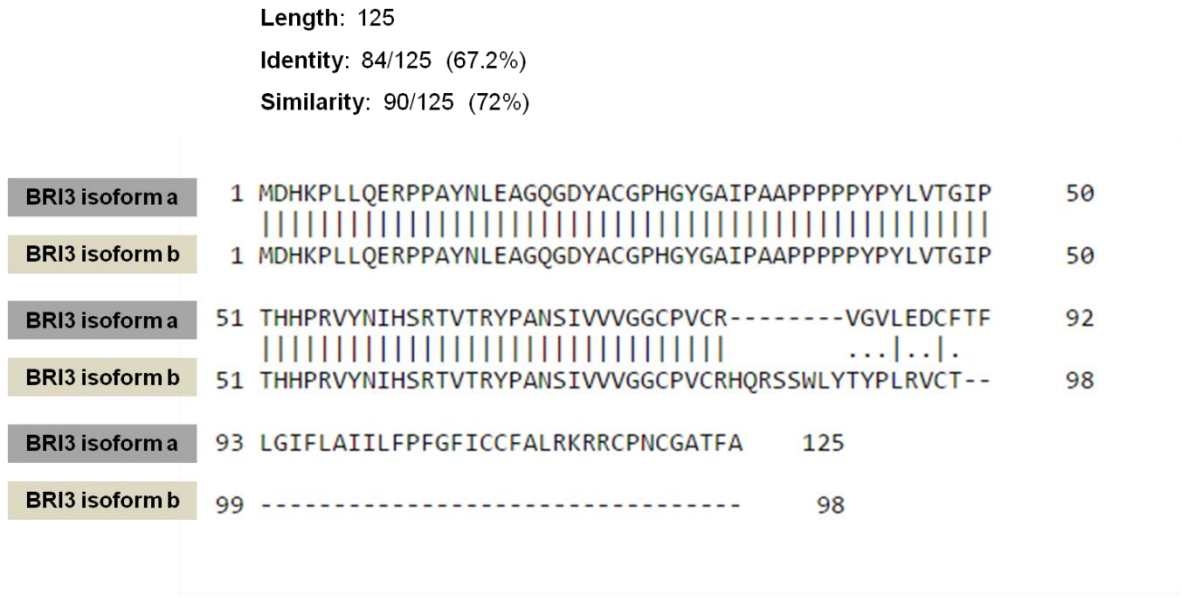

Figure 5.3. Alignment and comparison of the aminoacid sequences for the two isoforms of BRI3. Pairwise Sequence Alignment was performed by using EMBOSS Needle tool (Bleasby, 1999).

5.1.1. Co-Immunoprecipitation of BRI3 and its isoform with the candidate interaction partners

BRI3 protein has two isoforms. The a-isoform is 125 amino acids in length. On the other hand, the b-isoform of BRI3 is a 98 amino acid polypeptide sharing the same N-terminus but has a totally distinct C-terminus compared to the a-isoform (Figure 5.3).

Co-immunoprecipitation has been performed in order to test the interaction of the two BRI3 isoforms with the candidate proteins which were revealed as the result of yeast two-hybrid assay. For this purpose, the two isoforms of BRI3 are overexpressed in HEK-293T cells together with the candidate proteins IFITM3 and MGAT1, which were cloned into the pcDNA3-HA vector to express the HA-tag fusion constructs. Immunoprecipitation has been performed from HEK-293T lysates by using HA-antibody and immunoblotting was done with GFP-antibody and subsequently with BRI3-antibody in order to detect the GFP-fused versions of BRI3 isoforms. BRI3BP (BRI3 binding protein) was used as a positive control, since it is an already known interacting partner of BRI3 protein. Anti-Epcam antibody has been used as mock antibody for the control of immunoprecipitation.

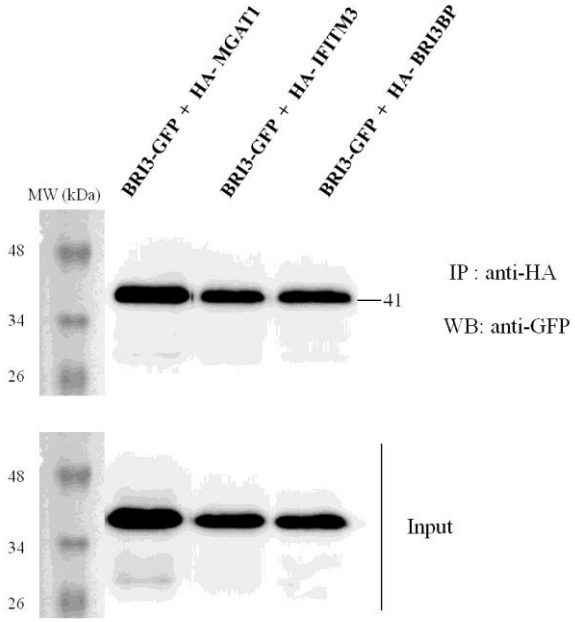

Figure 5.4. Western Blot of immunoprecipitated samples from HEK-293T cells transfected with the indicated constructs.

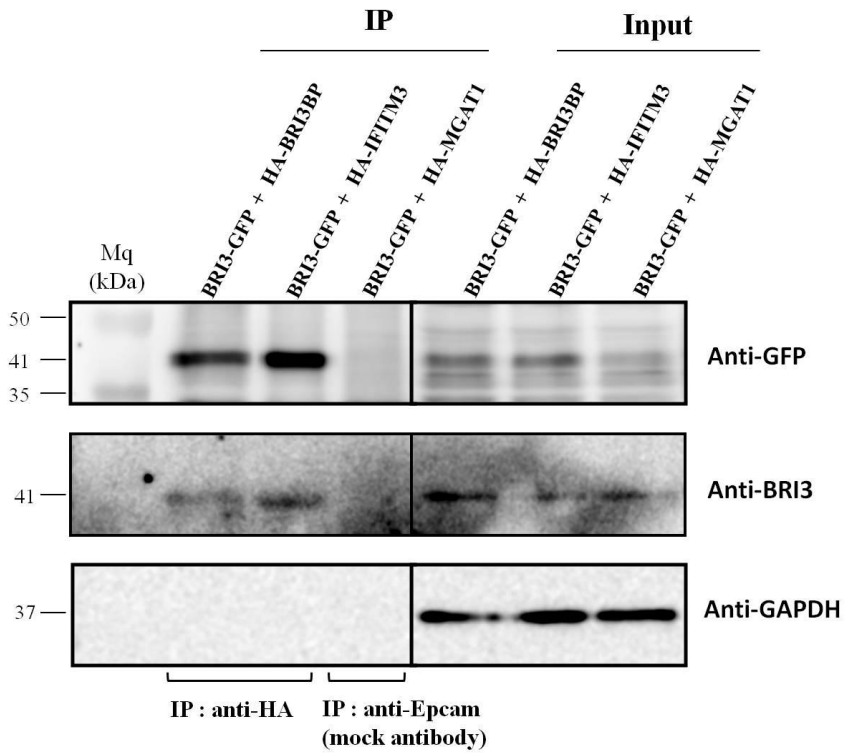

Figure 5.5. Coimmunoprecipitation of BRI3 a-isoform together with the candidate proteins from HEK-293T cells and immunoblotting with anti-GFP, anti-BRI3 and anti-GAPDH antibodies.

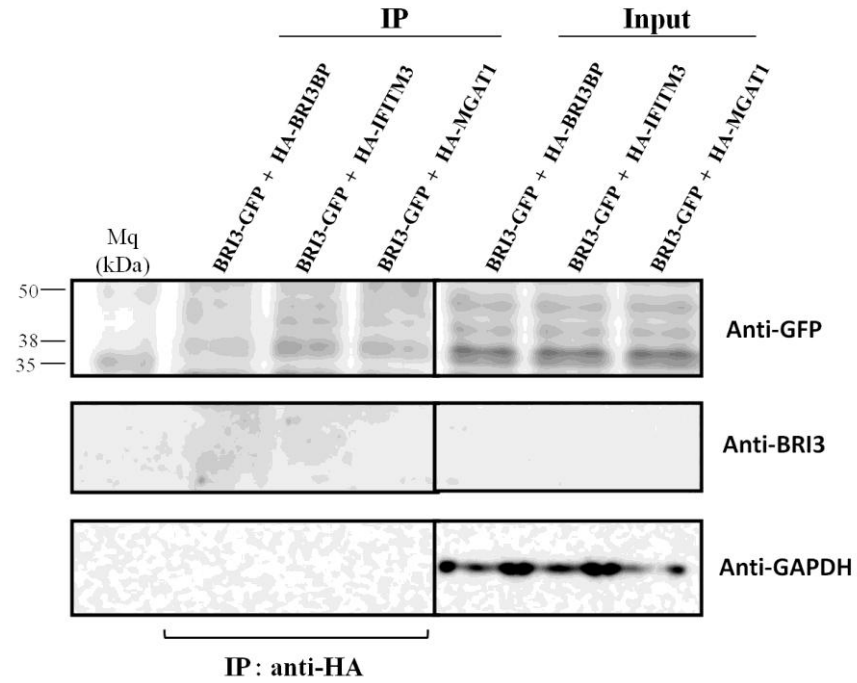

Figure 5.6. Coimmunoprecipitation of BRI3 b-isoform together with the candidate proteins from HEK-293T cells and immunoblotting with anti-GFP, anti-BRI3 and anti-GAPDH antibodies.

The results of coimmunoprecipitation experiments indicate that the a-isoform of BRI3 is able to interact both with the IFITM3 and MGAT1 proteins (Figure 5.4 and Figure 5.5), whereas the b-isoform of BRI3 does not show such an interaction (Figure 5.6).

5.1.2. Colocalization Assay in Huh7 cell lines

In order to visualize the possible interaction of BRI3 isoforms with the candidate proteins MGAT1 and IFITM3, colocalization assay has been performed in Huh7 Hepatocellular Carcinoma cell lines. For this purpose, GFP-tagged BRI3 isoforms were used together with dsRED-tagged MGAT1 and IFITM3. The fluorescent tagged proteins were expressed in Huh7 cells grown on 18 mm cover slips and 48 hours after transfection the cells were fixed and transferred onto glass slides in order to be imaged with confocal microscopy.

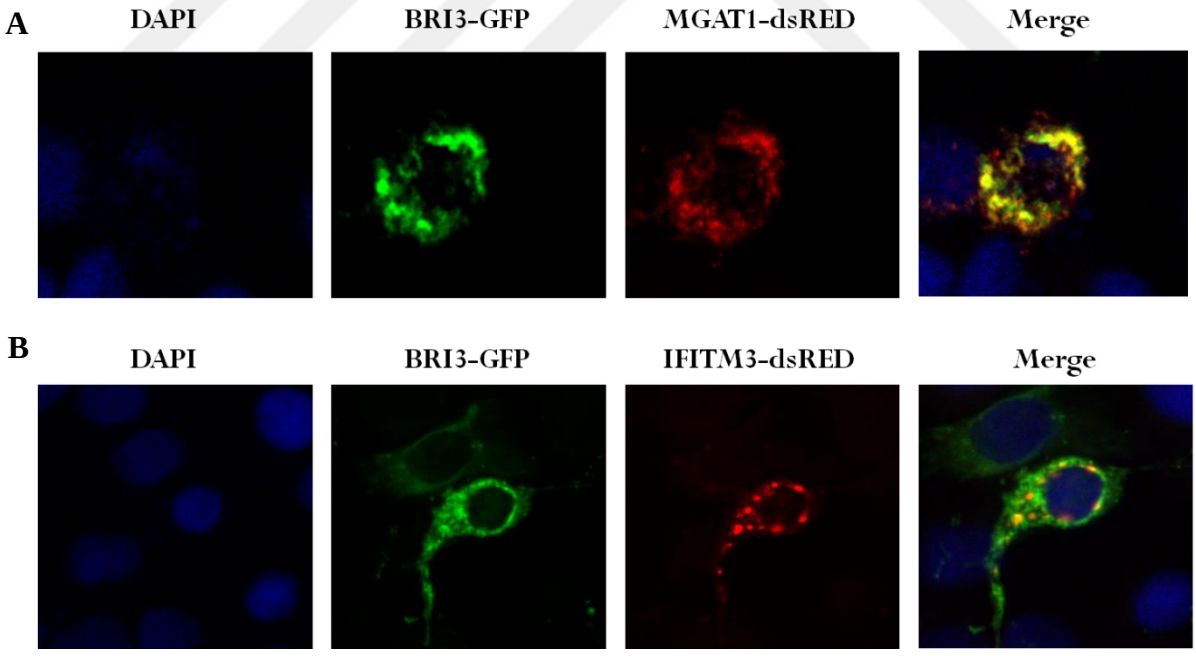

Figure 5.7. Colocalization Assay in Huh7 cells expressing GFP-tagged BRI3 (isoform a) together with either (A) MGAT1-dsRED or (B) IFITM3-dsRED.

As the result of colocalization assay, the a-isoform of BRI3 can be seen to colocalize with both MGAT1 and IFITM3, especially in the perinuclear area and possibly inside the organelles such as Golgi apparatus or ER (Figure 5.7). On the other hand, the b-isoform of BRI3 is mostly seen to be uniformly distributed throughout the cell, both in the cytoplasm and nucleus, and no specific colocalization was observed with MGAT1 or IFITM3 (Figure 5.8).

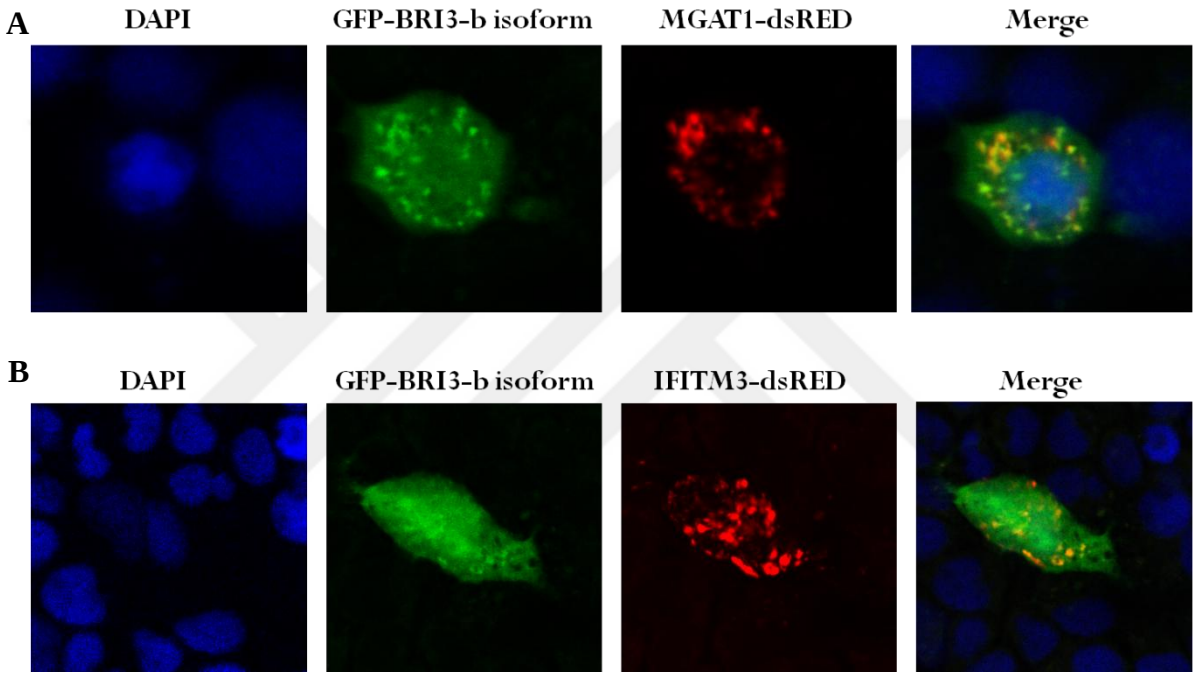

Figure 5.8. Colocalization Assay in Huh7 cells expressing GFP-tagged BRI3 (isoform b) together with either (A) MGAT1-dsRED or (B) IFITM3-dsRED.

5.2. MGAT1 and IFITM3 as potential targets of the Wnt/β-catenin pathway

MGAT1 gene has been included among the candidate Wnt/β-catenin target genes depending on the data obtained from SAGE and Microarray analyses that were previously performed in our laboratory. It is one of the genes that were shown to be upregulated in response to mutant β-catenin overexpression in Huh7 cell lines (Table 1.2). However, it has not been confirmed yet as a novel target by additional experiments.

On the other hand, with respect to previous studies, it was shown that IFITM family gene expression is significantly upregulated specifically in colorectal tumors and this might be regulated by Wnt/β-catenin signaling. IFITM1 gene has been determined as a potential target gene of the Wnt pathway during gastrulation in mouse embryos (Lickert *et al.*, 2005). Furthermore, IFITM family (IFITM1, IFITM2, and IFITM3) gene expression was found to be altered upon deregulation of the Wnt/β-catenin signaling in mouse and human intestinal epithelium (Andreu *et al.*, 2006).

Therefore, in this part of our study we aimed to test and confirm whether these two genes, MGAT1 and IFITM3, are transcriptional targets of Wnt/β-catenin pathway in hepatocellular carcinoma context.

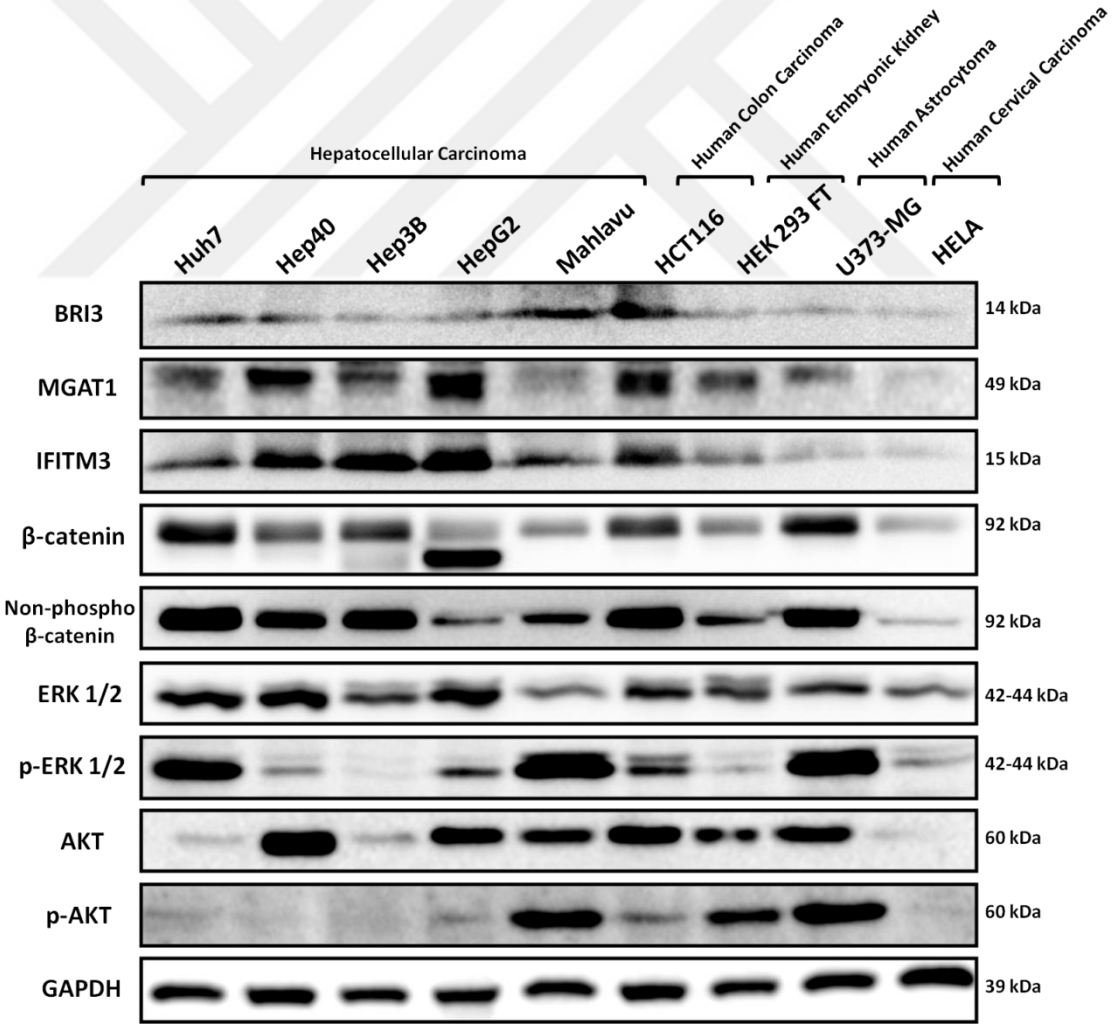

Figure 5.9. Basal expression levels of the indicated proteins for various cell lines.

Firstly, the basal protein levels of BRI3, MGAT1, and IFITM3 along with a few other key proteins of cell proliferation were determined in various cell lines (Figure 5.9). BRI3 is seen to be expressed in almost every cell line used, contrary to that implied by its name Brain protein I3. It is also observed that, the protein expression levels of MGAT1 and IFITM3 are higher in hepatocellular carcinoma cells (Hep40, Hep3B and HepG2) and colon carcinoma cells (HCT116), compared to the expression levels in other cell lines. This observation also contributed to our hypothesis that the two genes, MGAT1 and IFITM3, are indeed transcriptional target genes of Wnt/β-catenin signaling, since hepatocellular carcinoma and colon carcinoma are the two cancer types in which the deregulation of Wnt/β-catenin signaling is observed the most.

5.2.1. LiCl treatment leads to MGAT1 upregulation in Huh7 cells

LiCl is a widely used GSK-3β inhibitor, thus it results in the activation of Wnt/β-catenin signaling by interfering with the function of degradation complex and preventing β-catenin phosphorylation and degradation. Huh7 cells have been treated with LiCl and NaCl (as control) in time-dependent manner (0 hr, 24 hr and 48 hr). In 24-hour and 48-hour of LiCl treatment, both total β-catenin and non-phosphorylated (active) β-catenin protein levels are seen to be upregulated (Figure 5.10). C-myc and HSF2 are already known targets of β-catenin. C-myc protein is seen to be expressed at the 24 hr and 48 hr treatments with LiCl, whereas HSF2 protein is accumulated mostly at the 48 hr of LiCl treatment compared to other time points. With regard to the candidate targets, MGAT1 protein expression is seen to be upregulated at the 24 hr and 48 hr treatments with LiCl, which is in accordance with the increase in β-catenin expression. However, IFITM3 did not respond to LiCl treatment in neither of the time points and its protein expression levels were not found to be correlated with active β-catenin expression (Figure 5.10).

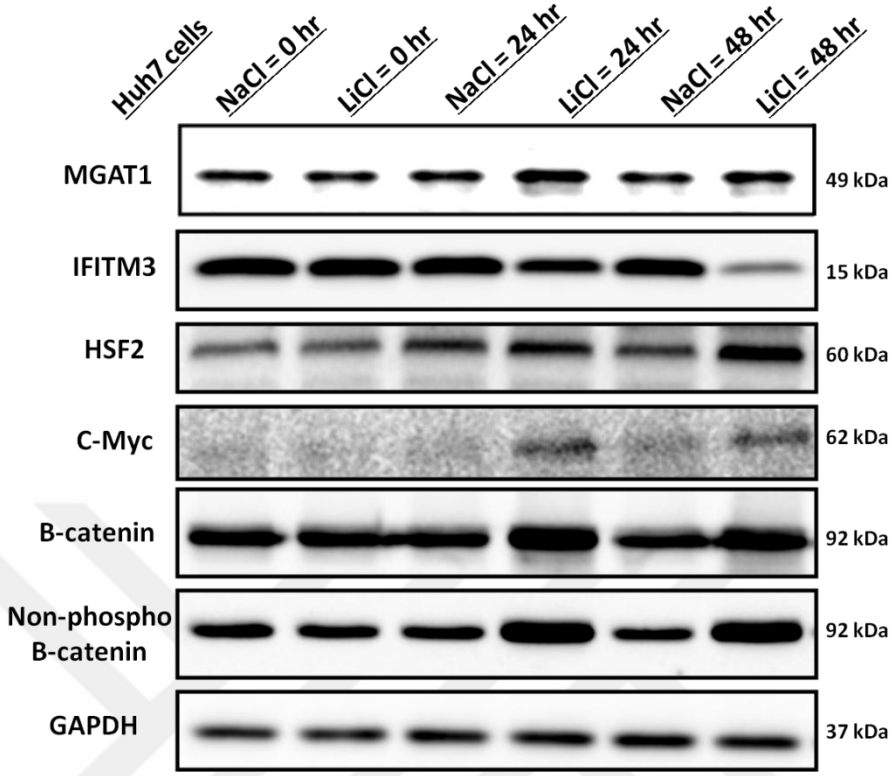

Figure 5.10. Western blotting for the expression levels of indicated proteins upon NaCl and LiCl treatment of Huh7 cells.

5.2.2. Analysis of MGAT1 and IFITM3 promoter activities

Luciferase Reporter Assays were carried out in order to analyze the promoter activities of MGAT1 and IFITM3 in response to Wnt/β-catenin pathway activation. For this purpose, approximately 1500 bp upstream of the transcription start site (TSS) of the two genes were amplified from genomic DNA by using specific primers with appropriate restriction enzyme sites. NheI (forward primer) and HindIII (reverse primer) were used for cloning the promoter regions of MGAT1 and IFITM3 into the luciferase reporter vector pGL3-basic. For positive control of luciferase activity, TOPFLASH vector which contains three copies of wild-type TCF4 binding sites. On the other hand, FOPFLASH vector has been used as negative control and it contains mutant TCF4 binding sites.

Degradation-resistant β-catenin mutant (S33Y-β-catenin) was used for the activation of Wnt/β-catenin signaling. Huh7 cells in 12-well plates were transfected with

pcDNA3-S33Y-β-catenin, pGL3-SV40-Renilla (as internal control) and one of the following luciferase reporter vectors - TOPFLASH, FOPFLASH, pGL3-MGAT1, pGL3-IFITM3 and pGL3-basic. The ratio of firefly luciferase to renilla luciferase was determined for each case and plotted as relative luciferase activity.

Overexpression of S33Y-β-catenin in Huh7 cells resulted in higher luciferase activity from MGAT1 promoter compared to the negative control vector FOPFLASH or the promoterless luciferase vector pGL3-basic. Luciferase reporter activity from positive control vector TOPFLASH was highest as expected. On the other hand, almost no detectable luciferase activity was observed from IFITM3 promoter (Figure 5.11).

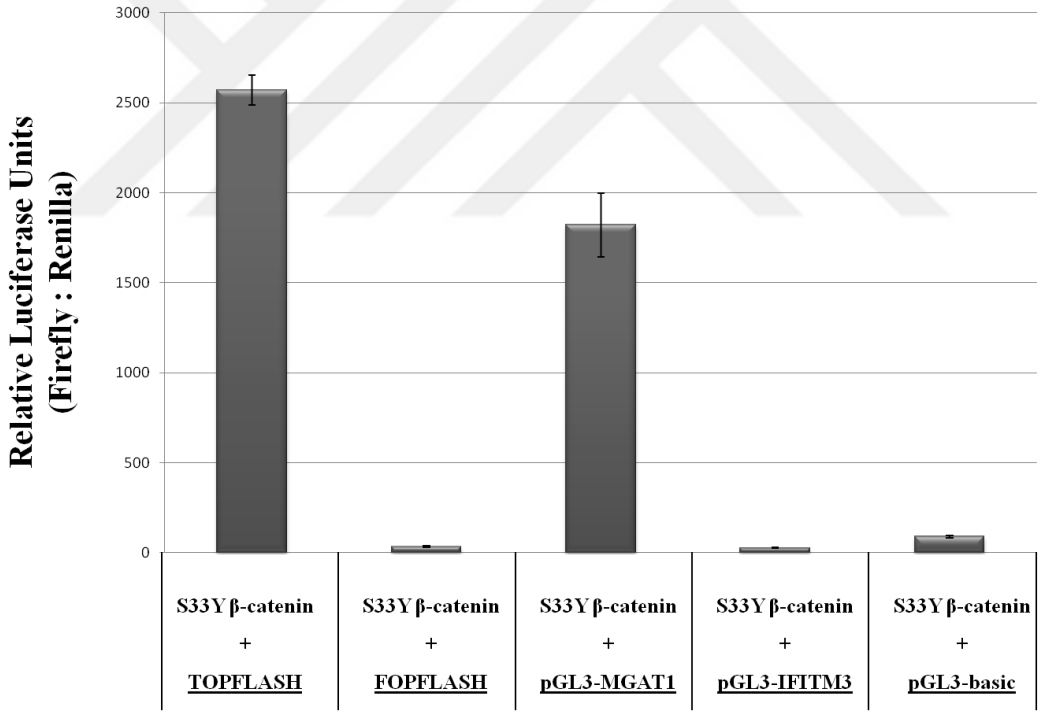

Figure 5.11. Luciferase reporter assay on Huh7 cells in the presence of S33Y-β-catenin overexpression. Error bars represent standard error. The graph indicates the results from three independent experiments.

Next, S33Y-β-catenin was overexpressed in Huh7 cells in combination with either wild-type transcription factor TCF4 or its dominant negative form (dN-TCF4). Relative

luciferase activities from MGAT1 and IFITM3 promoters were determined together with the activity from the promoterless pGL3-basic vector as the negative control.

Overexpression of S33Y-β-catenin together with TCF4 leads to a fold increase in MGAT1 promoter activity; however when dominant negative form of TCF4 (dN-TCF4) is overexpressed with S33Y-β-catenin, this activity is reduced nearly in half. Luciferase activity from IFITM3 promoter can only be hardly detected in response to overexpression of S33Y-β-catenin with either TCF4 or dN-TCF4 (Figure 5.12).

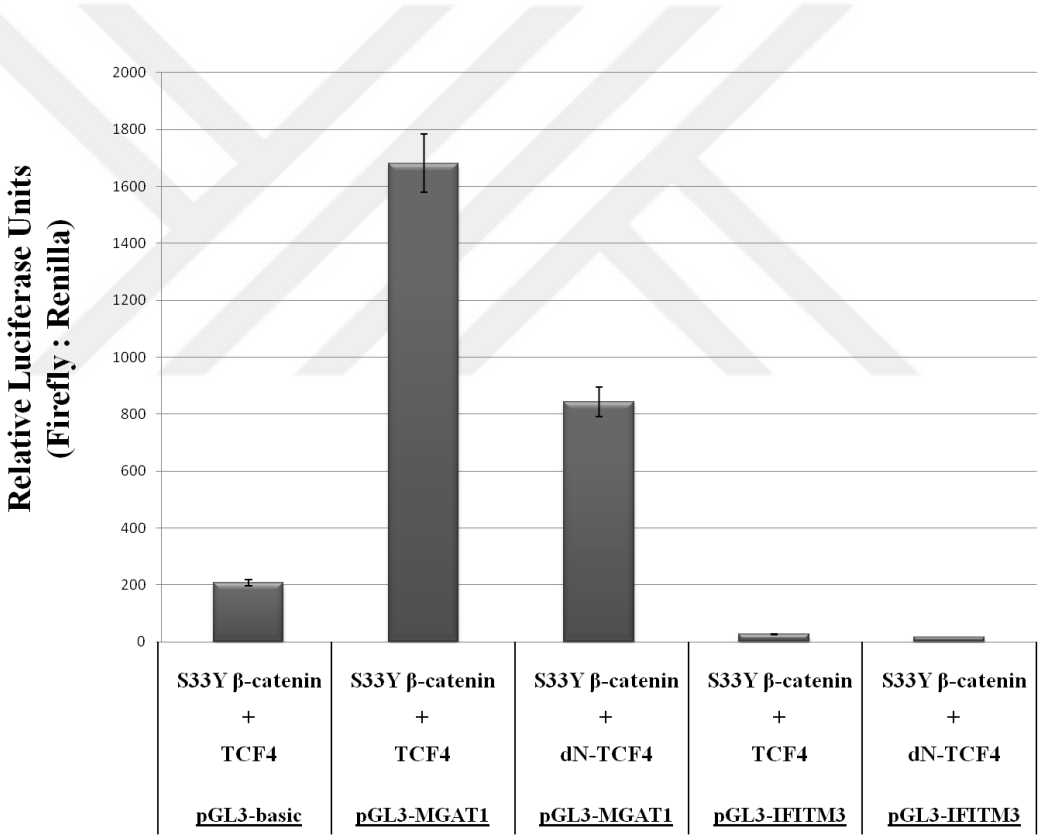

Figure 5.12. Luciferase reporter assay on Huh7 cells overexpressing S33Y-β-catenin in combination with either TCF4 or dN-TCF4. Error bars represent standard error. The graph indicates the results from two independent experiments.

Three different ligands of the canonical Wnt/β-catenin signaling pathway (Wnt1, Wnt3a and Wnt5) have been overexpressed in Huh7 cell lines by transfecting the cells with each of the pLNCX-Wnt1, pLNCX-Wnt3a and pLNCX-Wnt5 plasmids. Relative

luciferase activity from the MGAT1 promoter was determined in each case. Overexpression of Wnt1 led to the highest luciferase activity from MGAT1 promoter, whereas overexpression of Wnt3a and Wnt5 also caused considerable increase in luciferase activity compared to that with empty vector transfection (Figure 5.13).

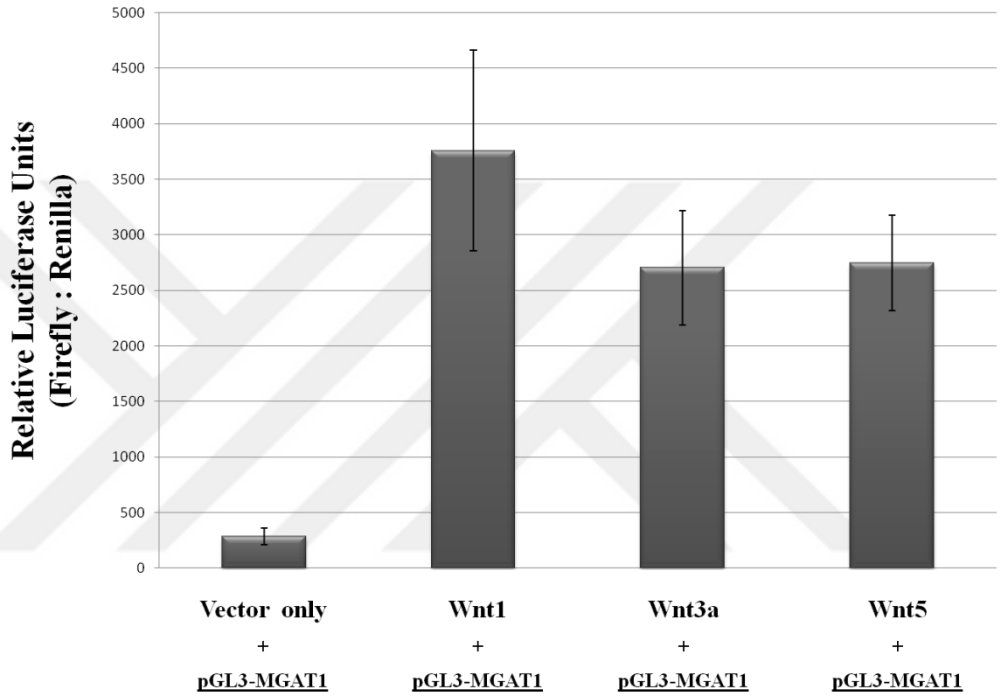

Figure 5.13. Luciferase reporter assay on Huh7 cells overexpressing S33Y-β-catenin in combination with either TCF4 or dN-TCF4. Error bars represent standard error. The graph indicates the results from two independent experiments.

5.2.3. Analysis of MGAT1 protein levels in response to β-catenin overexpression

Huh7 cells were transfected with the plasmids expressing either the wild-type β-catenin, S33Y-β-catenin or the combination of S33Y-β-catenin and TCF4. The protein levels of MGAT1 were determined by Western Blotting (Figure 5.14). HSF2 and c-Myc proteins were used as positive control, since they are already identified targets of the Wnt/β-catenin pathway. Non-phosphorylated β-catenin specifically recognizes β-catenin

only when Serine 45 residue of β-catenin is not phosphorylated and not targeted for degradation; therefore it indicates the active β-catenin levels. MGAT1 is seen to be accumulated most upon overexpression of S33Y-β-catenin and the combination of S33Y-β-catenin with TCF4. C-myc displays almost no protein expression in the cells transfected with the empty vector. However, upon overexpression of either wild-type β-catenin or S33Y-β-catenin leads to an increase in the protein levels of both C-myc and HSF2. Overall, MGAT1 protein levels are upregulated in correlation with β-catenin activation (Figure 5.14).

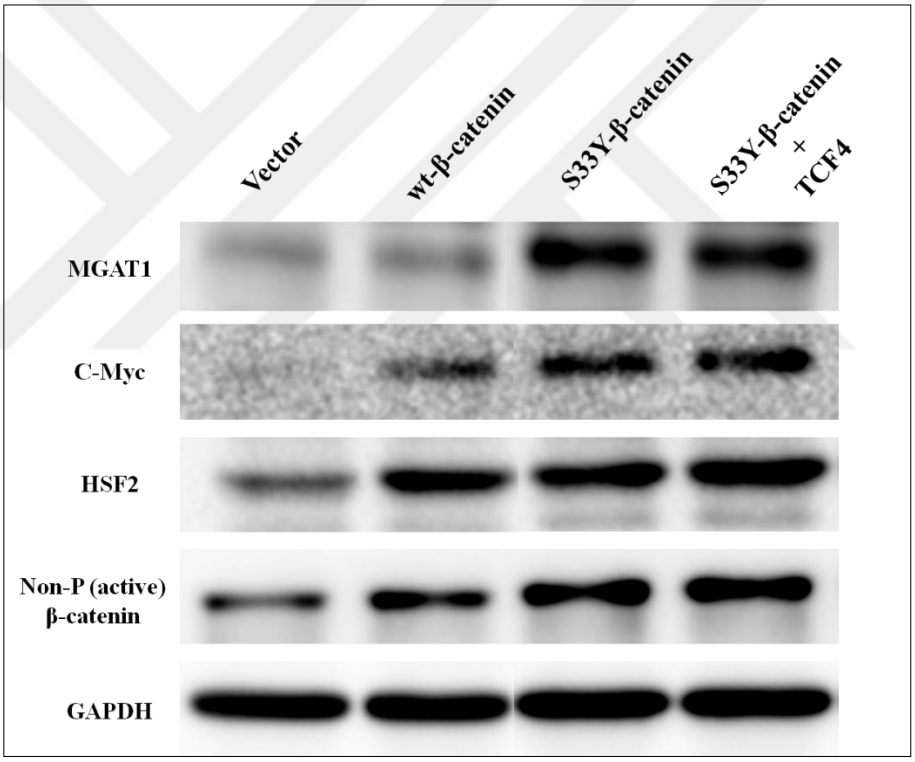

Figure 5.14. Overexpression of wild-type and mutant β-catenin in Huh7 cells and western blotting to detect the protein levels of the indicated proteins. GAPDH was used as loading control.

5.2.4. Determination of MGAT1 mRNA levels in the presence of Wnt agonists and GSK-3β inhibitor

In order to determine MGAT1 mRNA levels in response to Wnt/β-catenin pathway activation, Huh7 cells were treated with either Wnt agonist or GSK-3β inhibitor (TWS 119). Quantitative real-time PCR was performed to detect MGAT1 mRNA levels. AXIN2, being a widely known target of Wnt/β-catenin pathway, was used as positive control (Figure 5.15).

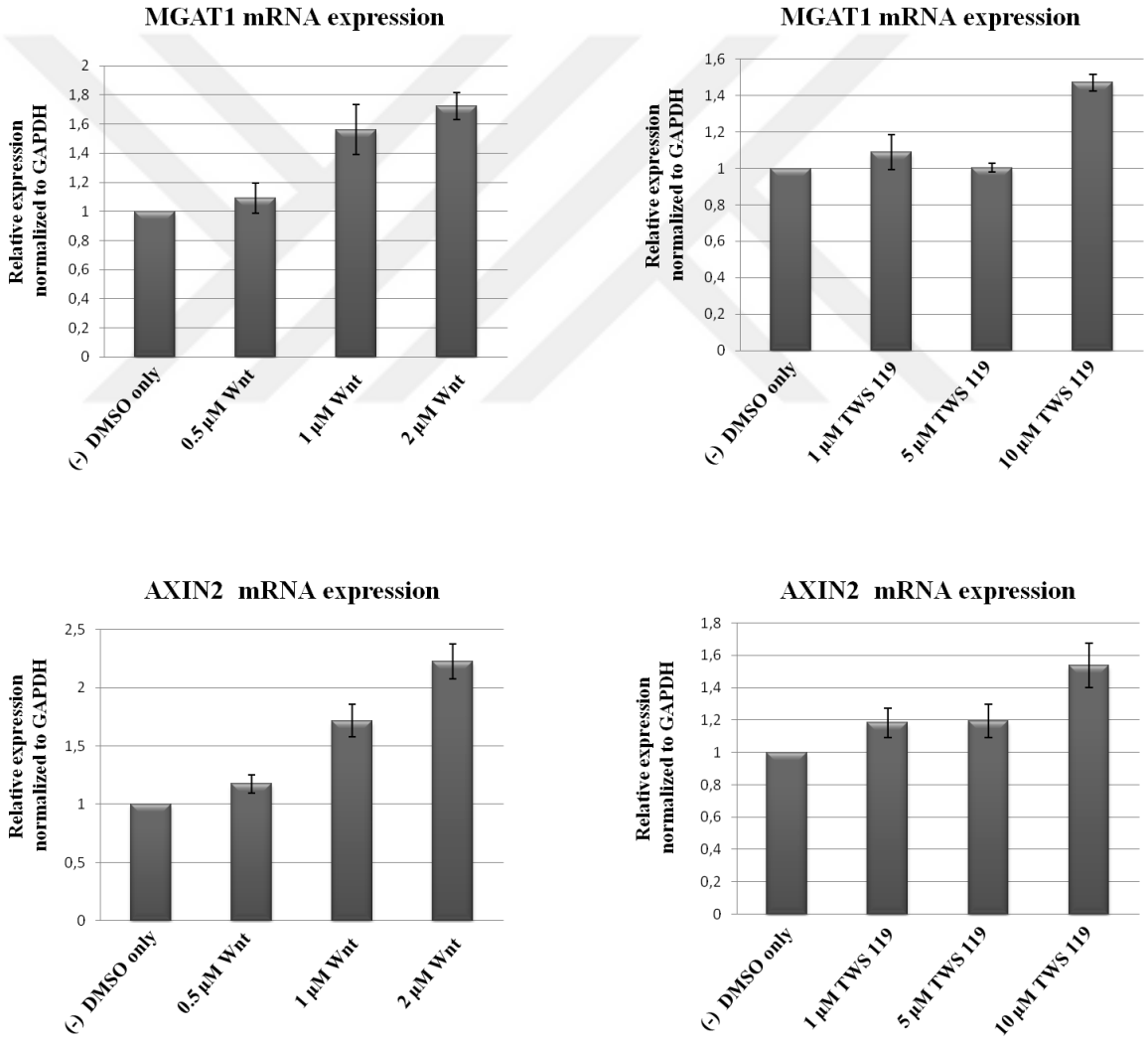

Figure 5.15. Quantitative real-time PCR analysis for the determination of MGAT1 mRNA levels in Huh7 cells treated with different concentrations of Wnt agonist and TWS 119 (GSK3β inhibitor). mRNA levels of AXIN2 was also determined as positive control. The graphs represent the results from two independent experiments.

The results of q-RTPCR indicate that MGAT1 mRNA levels increase gradually with increasing concentrations of Wnt agonist. AXIN2 mRNA is also seen to be upregulated by Wnt agonist treatment, as expected. TWS 119 is a synthetic chemical inhibitor of GSK3β and used commonly for the activation of Wnt/β-catenin signaling. MGAT1 mRNA levels display a marked increase only in the cells treated with 10 μM TWS 119 but not in other concentrations. AXIN2 mRNA is also upregulated most in response to the same concentration of TWS 119 (Figure 5.15).

5.3. BRI3 and the NFkB pathway

5.3.1. BRI3 might be involved in a complex with TRAF2/TRAF6 heterodimers

BRI3 has been previously shown to have a role in TNFα induced cell death (Zhao *et al.*, 2003) Furthermore, in another study, the binding partner of BRI3, which is named as BRI3BP (BRI3-binding protein), was found to have an interaction with TRAF6 (TNF receptor associated factor 6) (Bouwmeester *et al.* 2004). TRAF2 and TRAF6 are heterodimers and adaptor molecules for the signal transduction of TNFα from the plasma membrane to inside of the cell. Therefore, we wondered whether BRI3 might have an interaction with these adaptor molecules within the TNFα/NFkB signaling pathway. In order to check for this interaction, coimmunoprecipitation was performed from mammalian cell lines. Protein coding regions of TRAF2 and TRAF6 were cloned into pcDNA3-HA vector and were separately overexpressed in HEK293-FT cells together with the pEGFP-N2-BRI3 construct. Immunoprecipitation was performed with anti-HA antibody, and visualized on Western Blot using an anti-GFP antibody. Coimmunoprecipitation results indicate an interaction of BRI3 protein with TRAF2 and TRAF6. The known interaction of BRI3 with BRI3BP has been used as a positive control (Figure 5.16).

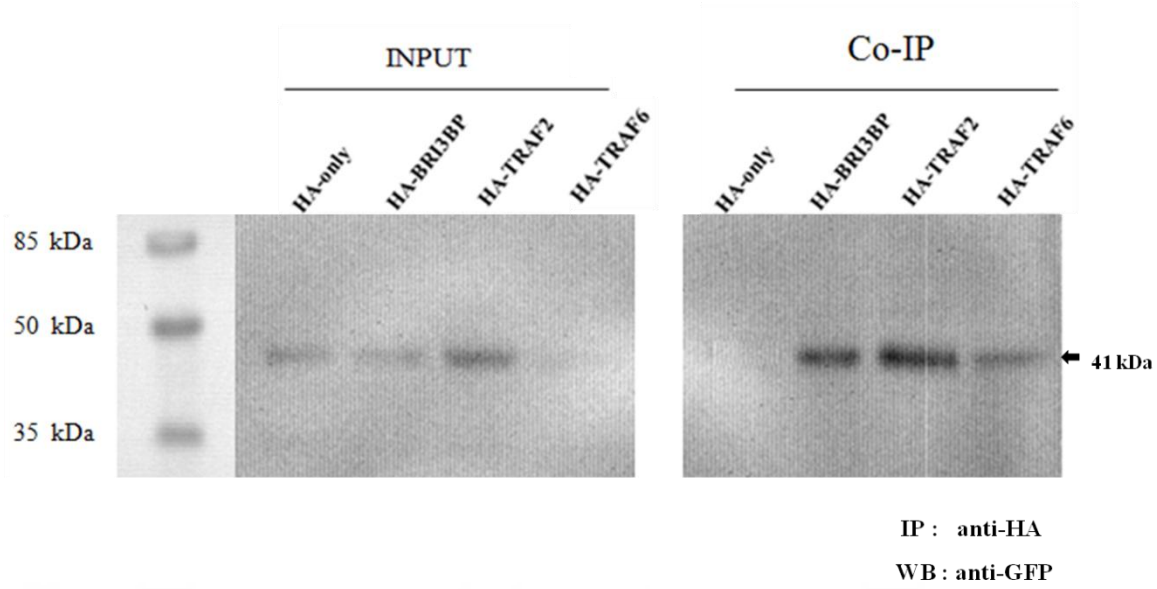

Figure 5.16. Coimmunoprecipitation from HEK293-FT cells transfected with the indicated constructs. The protein band corresponding to the fusion protein of BRI3-EGFP (41 kDa) is observed.

5.3.2. Analysis of NFkB promoter activity in response to BRI3 overexpression

In order to determine whether BRI3 has an effect on the promoter activity of NFkB, luciferase reporter assay has been performed. HEK293-FT cells in 12-well plate were transfected with either pcDNA3-NOD1, pcDNA3-myc-BRI3 or empty vector. NOD1 is an intracellular pattern recognition receptor and stimulation of NOD1 results in the activation of NFkB. Thus, NOD1 has been used as a positive control for NFkB promoter activity. pBVI-NFkB-Luc was used as the reporter plasmid containing multiple NFkB binding sites. Renilla luciferase activity has been determined by cotransfecting the cells with pGL3-SV40-Renilla vector as internal control. Relative luciferase activity was calculated as the ratio of firefly luciferase to renilla luciferase.

Promoter activity of NFkB appeared to be highest in NOD1 overexpressing cells, as expected. BRI3 expression led to a comparably high level of promoter activity, which is about half of the activity caused by NOD1. No significant luciferase activity was observed in empty vector transfection (Figure 5.17).

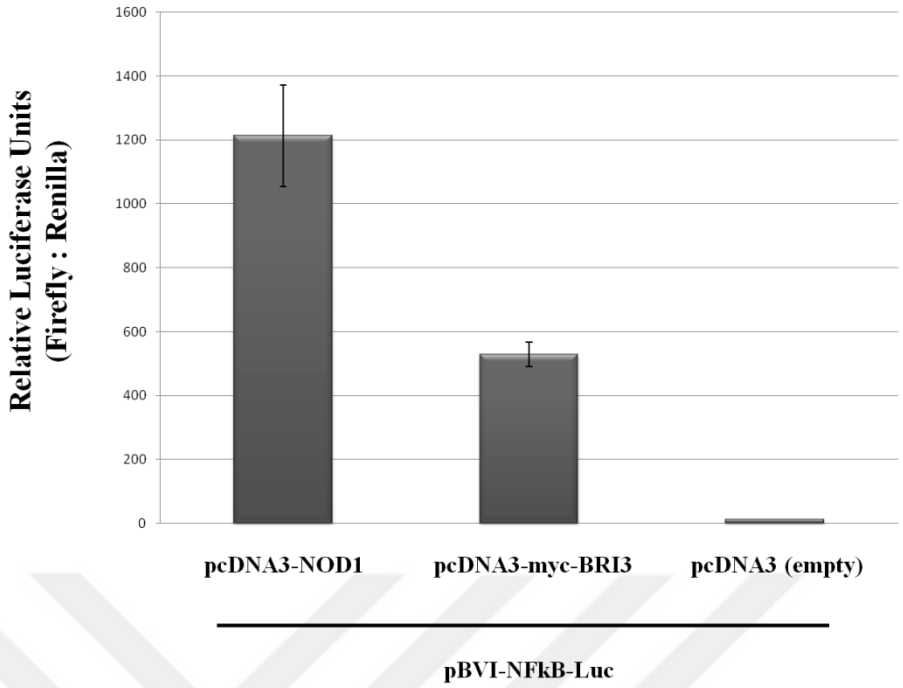

Figure 5.17. Luciferase reporter assay for the determination of NFkB promoter activity. Error bars represent standard error. The graph indicates the results from two independent experiments.

5.3.3. BRI3 protein expression correlates with TNFα levels

TNFα treatment of cells has been performed in order to activate NFkB signaling. The possible changes in protein levels of BRI3 and several other important molecules of NFkB pathway were determined by Western Blotting. Mammalian cell lines generally do not respond well to TNFα treatment, therefore HEK293 cells stably transfected with pTurboGFP-Fos-4KB (including a minimal Fos promoter with four tandem repeats of NFkB binding sites) were used. Time-course treatment of cells with TNFα (20 ng/ml) was performed between 0 hr to 8 hrs. BRI3 protein expression is seen to be highest around 4 hrs of treatment, where TNFα is also accumulated most inside the cell (Figure 5.18).

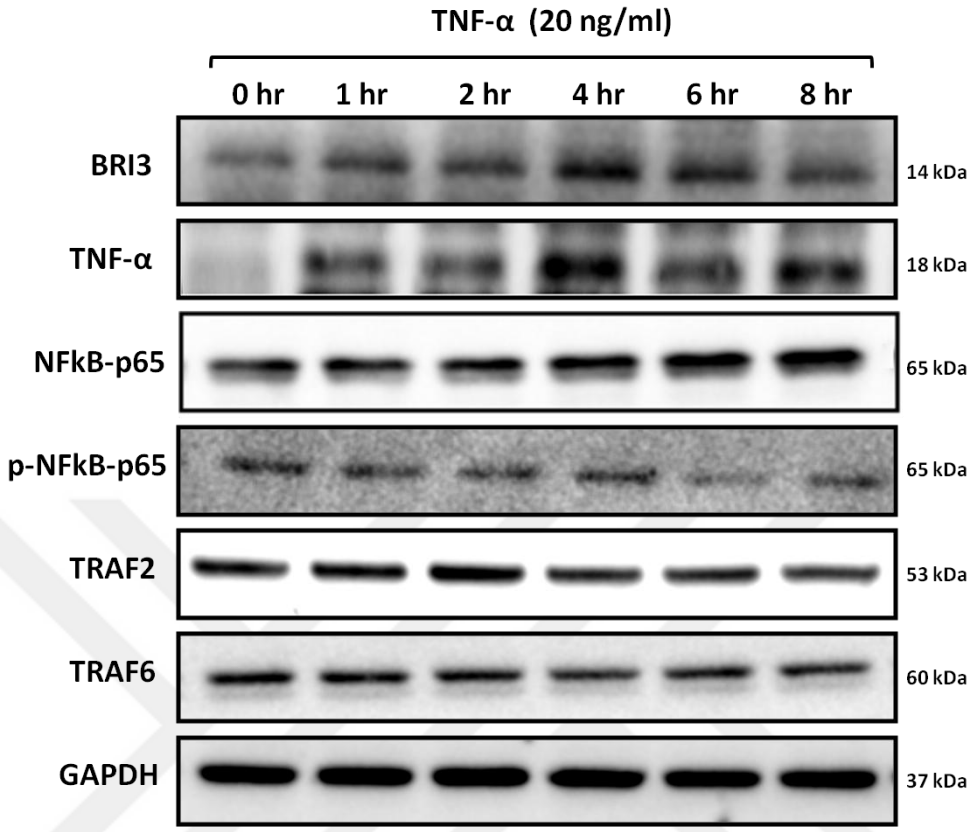

Figure 5.18. Time-course TNFα treatment of stable HEK293 cells and determination of the expression levels of indicated proteins by Western Blotting. GAPDH is used as loading control.

5.4. Assessing the tumorigenic potentials of BRI3 and MGAT1

In this part of our study, we focused on the possible effects of these two proteins, BRI3 and MGAT1, on cell survival and proliferation. As being novel transcriptional targets of the Wnt/β-catenin pathway, we aimed to determine whether they have tumorigenic potentials when overexpressed in cells.

5.4.1. Generation of stable cell lines overexpressing BRI3 and MGAT1

Stable expression of BRI3, MGAT1 and GFP (as negative control) genes in Huh7 (Hepatocellular Carcinoma) cells was established as a first step, in order to analyze the effects of these genes both in vitro and in vivo. The coding sequences of the corresponding genes were amplified by specific primers containing restriction enzyme sites suitable for cloning into pIRES2-EGFP. This construct provides the native expression of our genes due to the presence of IRES (Internal Ribosome Entry Site). Additionally, expression of GFP fluorescent protein enables us to visualize the transfection efficiency and the ongoing antibiotic selection process of the cells.

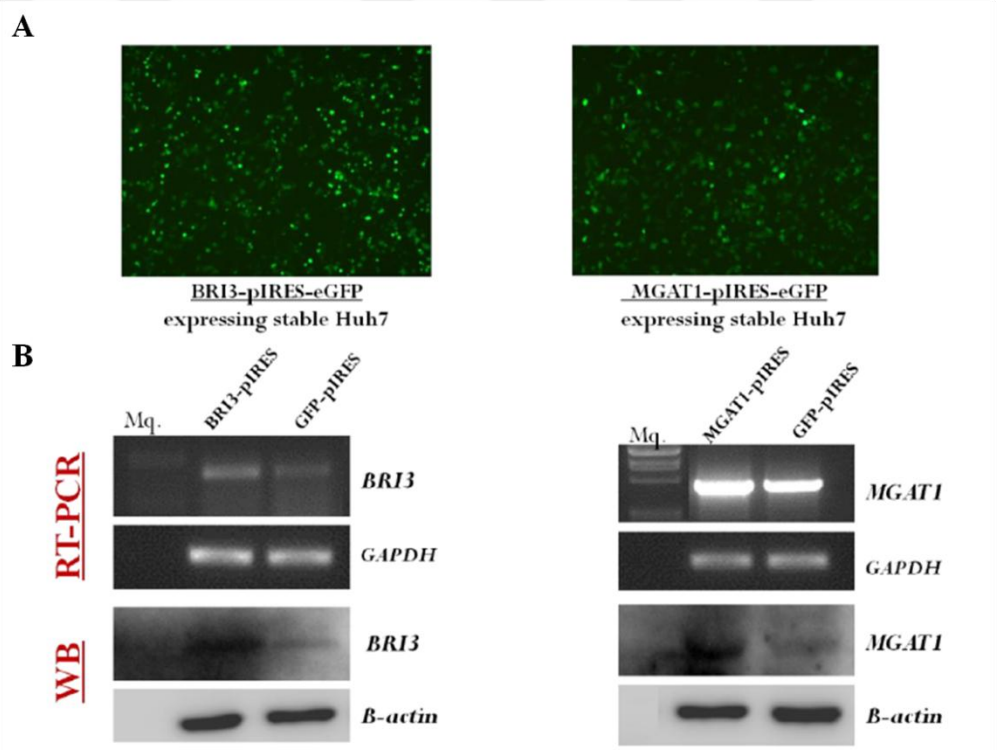

Figure 5.19. Stable Huh7 cells visualized by the fluorescent microscope (A) and determination of RNA and protein levels by RT-PCR and western blotting (B).

5.4.2. Comparison of migration and proliferation abilities of stable cell lines

Wound healing assay has been performed in order to determine whether there exists any difference in the cell migration capacities of the stable cells. BRI3, MGAT1 and GFP overexpressing Huh7 cells were used for this assay. After introducing a scratch over the confluent and adherent layer of cells in 6-well plates, the cells were visualized under the

microscope at different time points starting from 0 hr upto 72 hrs. The widths of the scratches indicated by yellow lines were quantified by Image J software (Figure 5.20A).

As a result of wound healing assay, differences between wound closure capacities of the stable cells were observed at the end of 72 hours. Distances across the wound were measured at each time point and difference between the initial and final values were computed as percent wound closure for each stable cell line. Overall, BRI3 and MGAT1 overexpressing stable Huh7 cells exhibited higher percentages of wound closure compared to those overexpressing GFP as the control (Figure 5.20B).

The stable cell lines were subjected to PI (Propidium iodide) staining and FACS analysis in order to examine the cell cycle characteristics of these cells and to determine any possible differences in cell viabilities. PI is a fluorescent molecule that is able to intercalate nucleic acids and it is commonly used in flow cytometry for cell cycle analyses. After ethanol fixation and PI staining procedures, the cell cycle profiles of the stable cells are analyzed by FACS machine. The analysis was configured to include only the GFP-positive cells as the total cell population. Then, histograms were plotted for each of the BRI3, MGAT1 and GFP overexpressing cell lines (Figure 5.21). The percentages of cells in each phase of the cell cycle are tabulated. The results did not indicate any significant difference between the percentages of S and G2/M phases of BRI3, MGAT1 and GFP stable cell lines (Table 5.1).

A

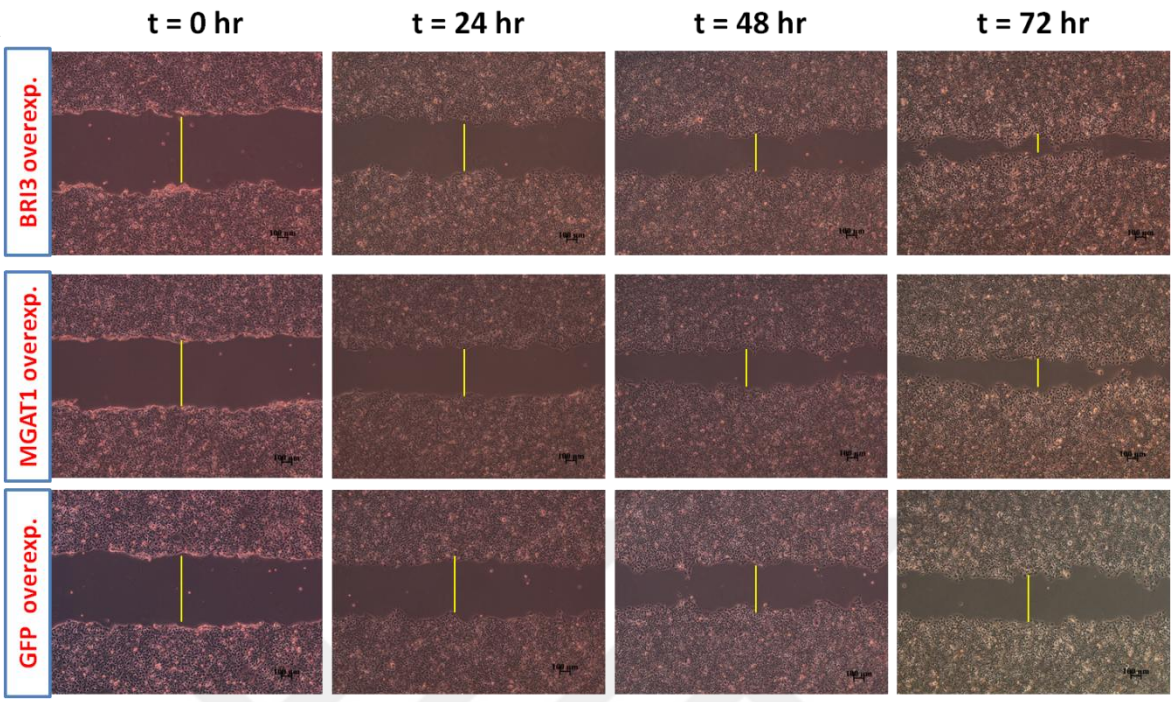

B

	t = 0 hr	t = 24 hr	t = 48 hr	t = 72 hr
BRI3/ Huh7 stable cells	724 µm	524 µm	372 µm	180 µm
MGAT1/Huh7 stable cells	688 µm	484 µm	344 µm	272 µm
GFP/Huh7 stable cells	696 µm	552 µm	464 µm	400 µm

C

Stable cells	Percent wound closure
BRI3/ Huh7	75,1 %
MGAT1/ Huh7	60,4 %
GFP/ Huh7	42,5 %

Figure 5.20. Wound healing assay for the stable cells overexpressing the indicated genes (A). The distances across the wound are measured by Image J and the differences are presented as percent wound closure (B and C). The images are representative of the results from two independent experiments.

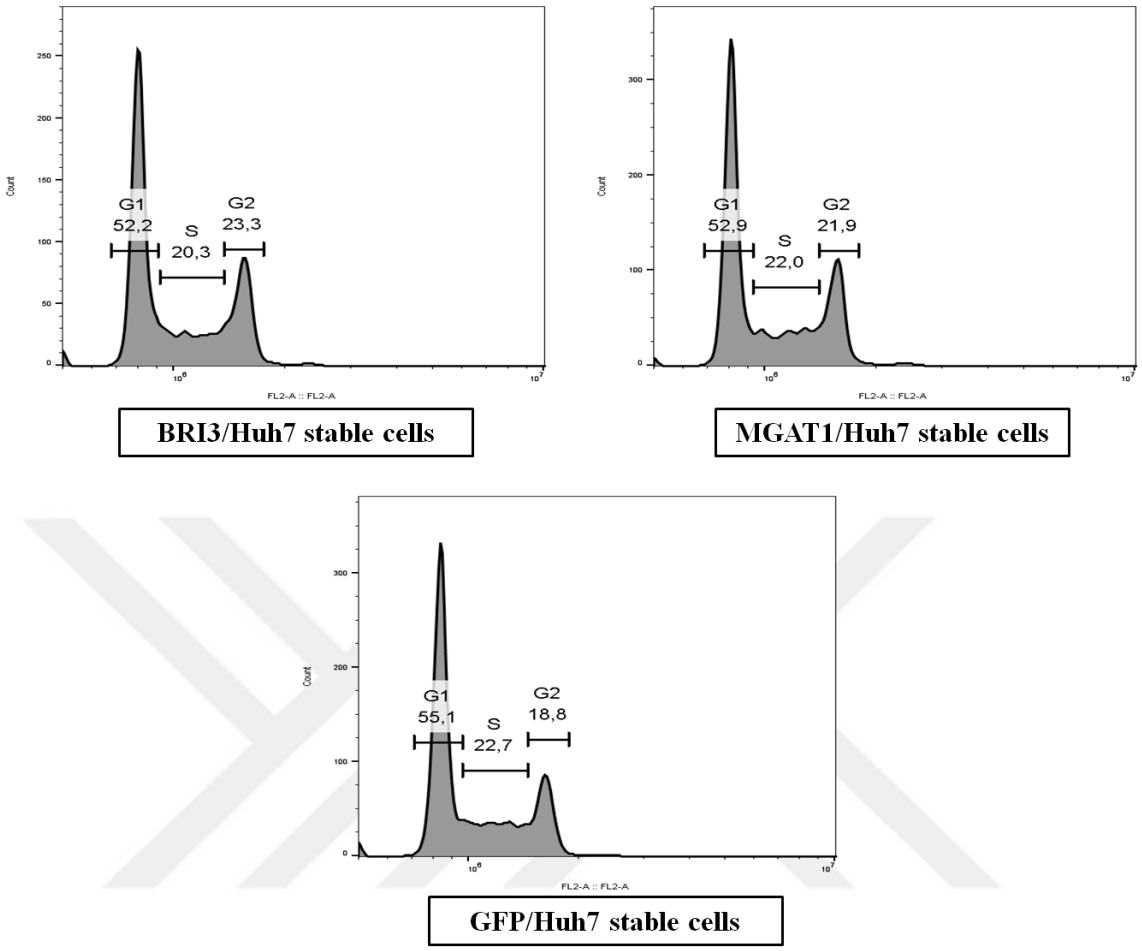

Figure 5.21. Cell cycle profiles of BRI3, MGAT1 and GFP overexpressing stable cells are demonstrated as histograms. The graphs are representative of two independent experiments.

Table 5.1. The percentage of cells in each phase of cell cycle shown in Figure 5.21.

Stable cells overexpressing	BRI3	MGAT1	GFP
G1 (%)	52.2	52.9	55.1
S (%)	20.3	22.0	22.7
G2/M (%)	23.3	21.9	18.8
S + G2/M (%)	**43.6**	**43.9**	**41.5**

In order to determine whether there is any difference in the cellular proliferation properties of the stable cell lines, XTT Assay has been performed. XTT Assay is a colorimetric assay for the spectrophotometric quantification of cell proliferation and is based on the cleavage of the tetrazolium salt XTT to produce a soluble formazan salt. The amount of formazan dye formed is directly correlated with the number of metabolically active cells in the culture.

The stable Huh7 cell lines overexpressing BRI3, MGAT1 and GFP (control) were grown at 96-well culture plates for three days under two different sets of serum starvation conditions (2% FBS and 5% FBS). At the end of three days, the cells were incubated with the XTT reagent for 3 hours at 37°C and the absorbance measurement for the cell culture plate was performed at 475 nm using an ELISA plate reader. Normalization was done by taking another set of measurements at the reference wavelength of 650 nm. As a result, the relative absorbance values were determined to be higher for BRI3 and MGAT1 overexpressing cells compared to those for GFP overexpressing cells in both of the serum starvation conditions (Figure 5.23).

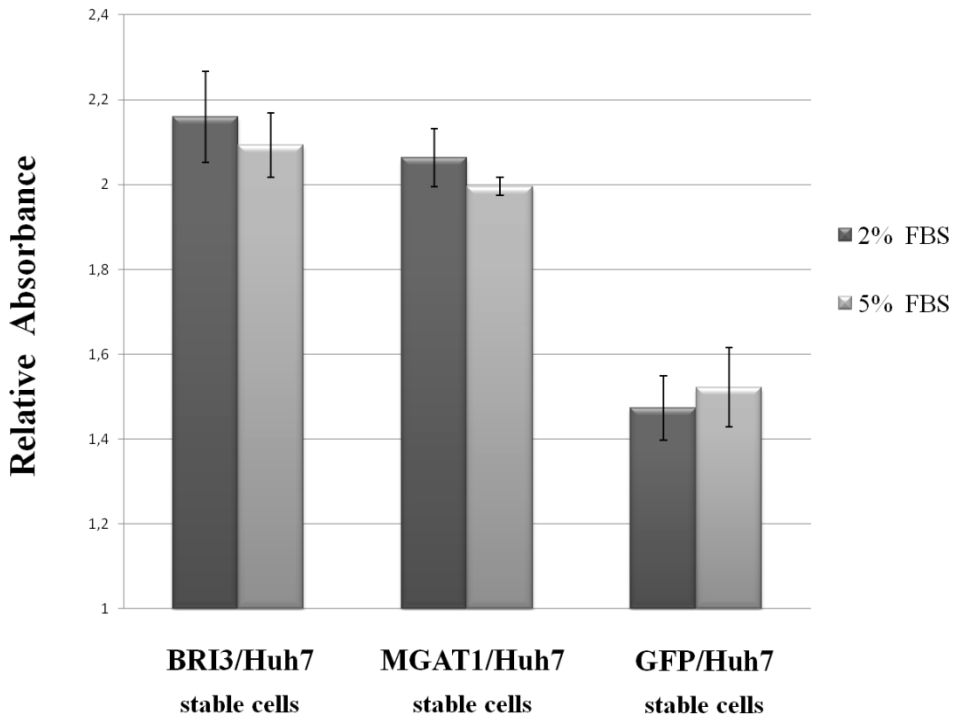

Figure 5.22. BRI3 and MGAT1 stable expression in Huh7 cells results in higher proliferation rate compared to GFP-expressing control stable cells.

5.4.3. In vivo analysis of tumorigenesis

Xenograft assays were carried out in NUDE and SCID mice, in order to test for the tumor forming abilities of the stable Huh7 cell lines in vivo. The mice were injected subcutaneously and bilaterally from their flank regions near the abdomen. BRI3 or MGAT1 overexpressing Huh7 cells were injected on the left flank of the mice, while GFP overexpressing Huh7 cells were injected on the right flank as the control (Figure 5.23 and Figure 5.24).

The mice were checked for tumor formation regularly. Approximately 3-4 weeks after the injection, differences between tumor sizes were observed. At that point, the mice were sacrificed and tumors were isolated (Figure 5.25). Differences between the tumors were determined by weighting (Table 5.2).

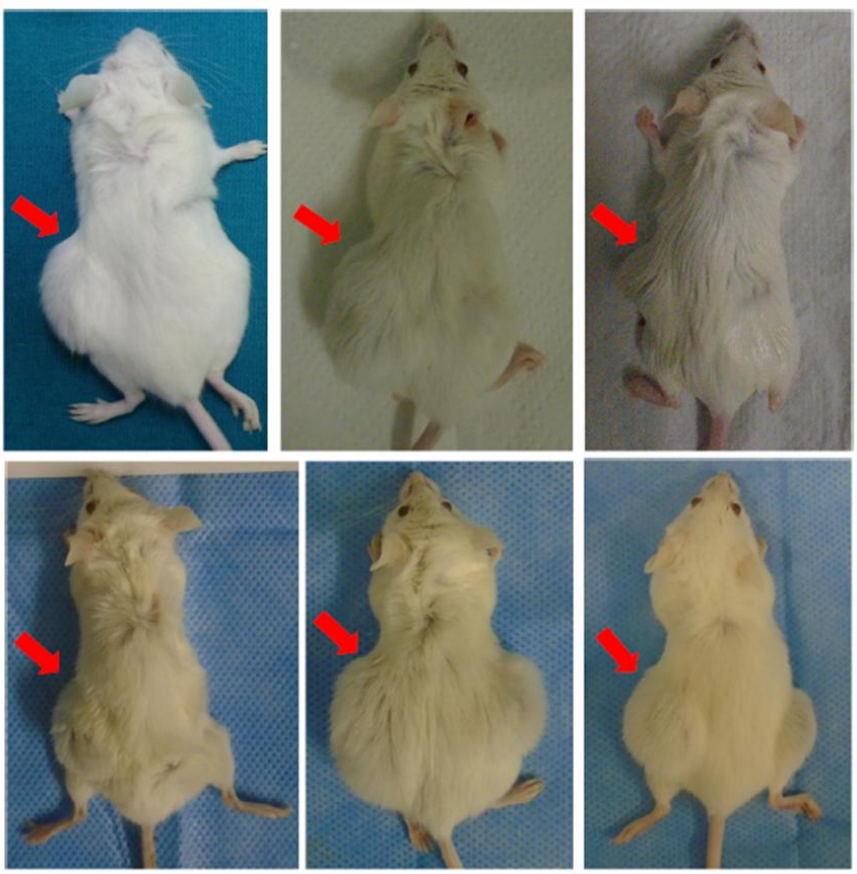

Figure 5.23. MGAT1 overexpressing stable cells are subcutaneously injected into the left flank region of each mouse (indicated by the red arrows). GFP overexpressing stable cells are injected into the right flank as control.



Figure 5.24. BRI3 overexpressing stable cells are subcutaneously injected into the left flank region of each mouse (indicated by the red arrows). GFP overexpressing stable cells are injected into the right flank as control.

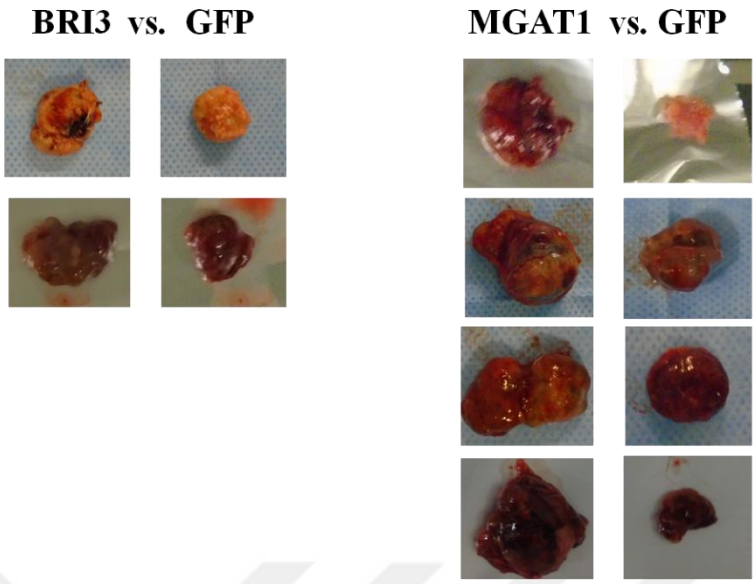

Figure 5.25. Representative tumor images were obtained for comparison. Mice were sacrificed after tumor formations become evident and the subcutaneous tumors were isolated for further analysis.

Table 5.2. Weights of the isolated tumors.

BRI3	GFP
2,66 gr	1,03 gr
2,06 gr	0,44 gr
1,41 gr	1,16 gr
1,65 gr	0,27 gr
1,24 gr	None

MGAT1	GFP
1,18 gr	0,04 gr
4,46 gr	2,26 gr
3,30 gr	1,19 gr
2,64 gr	0,17 gr
1,38 gr	None

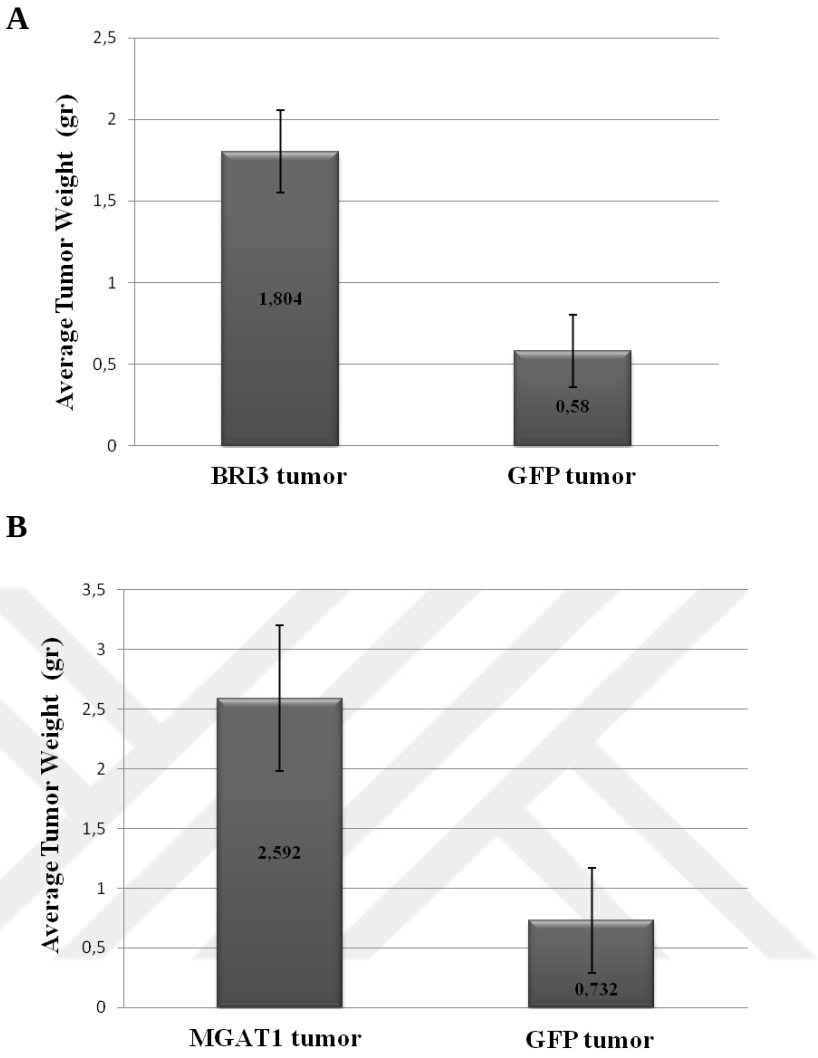

Figure 5.26. Average weights of tumors are plotted for (A) BRI3 vs GFP and (B) MGAT1 vs GFP tumors. n=5 for each graph. Error bars represent standard deviation.

5.5. Transcriptomic analysis via RNA Sequencing

The tumors derived from BRI3 or MGAT1 overexpressing cells together with the corresponding control tumors derived from the GFP overexpressing cells have been used for RNA Isolation and the RNA samples were subjected to RNA Sequencing (Figure 5.27). By this approach, it is able to cover the entire transcriptome and measure precisely the levels of transcripts expressed. The results and data obtained from RNA Sequencing technique were processed by using bioinformatics analyses in order to determine the differentially expressed genes and to reveal the enriched pathways which are specifically contributing to the tumorigenicity as observed in xenograft experiments.

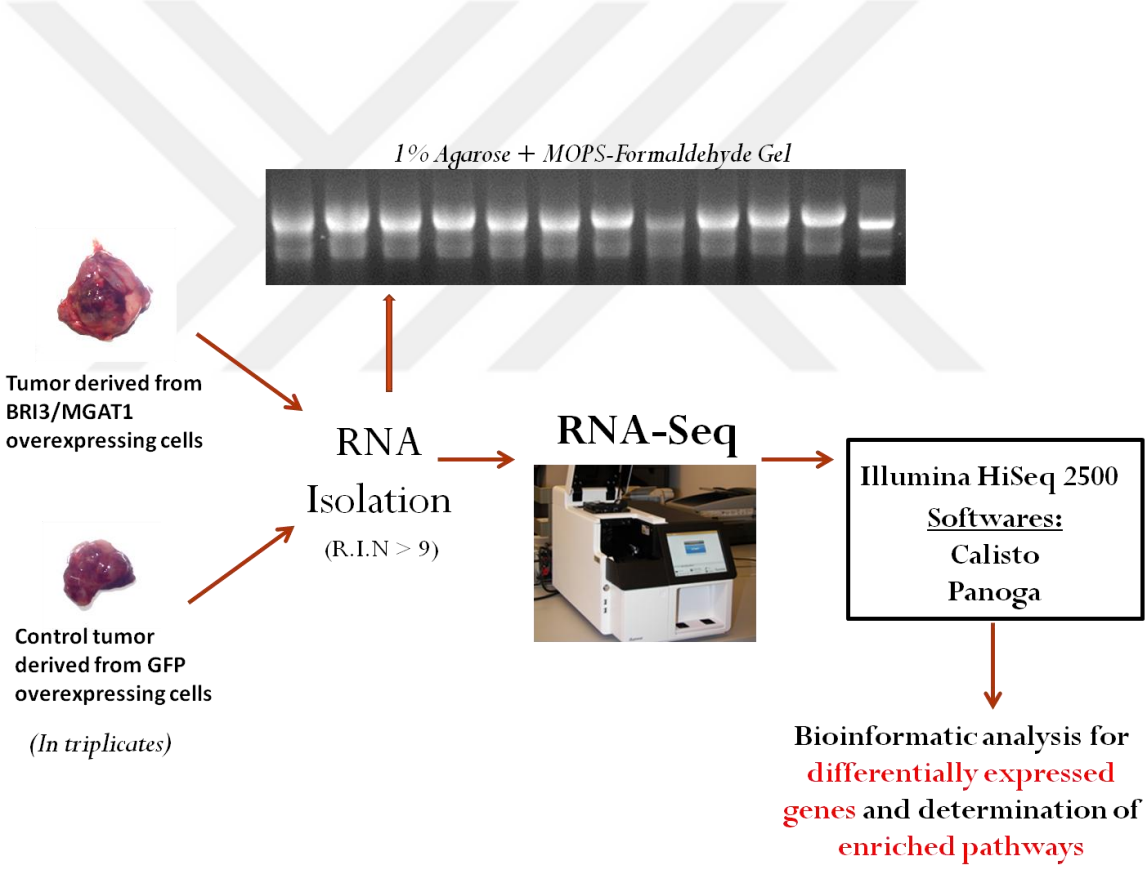

Figure 5.27. Overview of the strategy employed for RNA-Sequencing procedure. Three biological replicates were used for each of the two genes and their controls. RNA sequencing was initiated after confirmation of RNA integrity by spectrophotometry and agarose gel electrophoresis.

Table 5.3. Significantly upregulated genes in BRI3 overexpressing tumors in comparison with the GFP overexpressing tumors. Top 30 genes with highest fold changes are depicted in the list ($p<0.05$).

Gene	Description	Log_2 Fold Change
CSNK2B	Casein Kinase 2 Beta	2,028
HNRNPF	Heterogeneous Nuclear Ribonucleoprotein F	2,017
B3GAT1	Beta-1,3-Glucuronyltransferase 1	2,016
MAP7D1	MAP7 Domain Containing 1	1,996
GON4L	Gon-4 Like	2,001
FNBP4	Formin Binding Protein 4	1,916
PISD	Phosphatidylserine Decarboxylase	2,003
NIPAL3	NIPA Like Domain Containing 3	1,992
USP54	Ubiquitin Specific Peptidase 54	1,954
MYZAP	Myocardial Zonula Adherens Protein	1,993
AFP	Alpha Fetoprotein	1,928
IL17RD	Interleukin 17 Receptor D	1,942
UBAP2L	Ubiquitin Associated Protein 2 Like	1,965
TRAF3	TNF Receptor Associated Factor 3	1,881
COLEC11	Collectin Subfamily Member 11	1,955
SAMD8	Sterile Alpha Motif Domain Containing 8	1,932
PTDSS	Phosphatidylserine Synthase 1	1,945
ZCWPW2	Zinc Finger CW-Type And PWWP Domain Containing 2	1,930
IFNA	Interferon, Alpha	1,929
VSIR	V-Set Domain-Containing Immunoregulatory Receptor	1,813
ANKRD13D	Ankyrin Repeat Domain 13 Family Member D	1,890
EDA	Ectodysplasin A	1,878
COQ9	Coenzyme Q9	1,927
COMMD7	COMM Domain Containing 7	1,760
ANP32	Acidic Nuclear Phosphoprotein 32 Family Member A	1,845
CSPP1	Centrosome And Spindle Pole Associated Protein 1	1,909
TMEM39A	Transmembrane Protein 39A	1,903
MUL1	Mitochondrial E3 Ubiquitin Protein Ligase 1	1,901
SCARF1	Scavenger Receptor Class F Member 1	1,888
PRSS58	Protease, Serine 58	1,878

Table 5.4. Significantly downregulated genes in BRI3 overexpressing tumors in comparison with the GFP overexpressing tumors. Top 30 genes with highest fold changes are depicted in the list ($p<0.05$).

Gene	Description	Log_2 Fold Change
YAP1	Yes Associated Protein 1	-2,034
KCTD18	Potassium Channel Tetramerization Domain Containing 18	-1,922
ALDH3A2	Aldehyde Dehydrogenase 3 Family Member A2	-1,905
SGMS2	Sphingomyelin Synthase 2	-1,888
TMEM33	Transmembrane Protein 33	-1,705
LYPD6	LY6/PLAUR Domain Containing 6	-1,873
SUCLG1	Succinate-CoA Ligase Alpha Subunit	-1,807
C2	Complement Component 2	-1,611
TACR1	Tachykinin Receptor 1	-1,832
SRRT	Serrate, RNA Effector Molecule	-1,649
NUDT8	Nudix Hydrolase 8	-1,796
ZSCAN21	Zinc Finger And SCAN Domain Containing 21	-1,755
CHODL	Chondrolectin	-1,769
SNX25	Sorting Nexin 25	-1,766
RTKN2	Rhotekin 2	-1,786
RNF157	Ring Finger Protein 157	-1,782
NCL	Nucleolin	-1,755
PAN3	Poly(A) Specific Ribonuclease Subunit	-1,714
TRIO	Trio Rho Guanine Nucleotide Exchange Factor	-1,766
RBM25	RNA Binding Motif Protein 25	-1,756
HDAC10	Histone Deacetylase 10	-1,697
NWD1	NACHT And WD Repeat Domain Containing 1	-1,743
GBA2	Glucosylceramidase Beta 2	-1,727
SH2B2	SH2B Adaptor Protein 2	-1,567
ST8SIA3	ST8 Alpha-N-Acetyl-Neuraminide Alpha-2,8-Sialyltransferase 3	-1,737
FAM160A1	Family With Sequence Similarity 160 Member A1	-1,733
ZFP536	Zinc Finger Protein 536	-1,710
CHN2	Chimerin 2	-1,580
RAB7	RAB7A, Member RAS Oncogene Family	-1,625
FAM131A	Family With Sequence Similarity 131 Member A	-1,706

Table 5.5. Significantly upregulated genes in MGAT1 overexpressing tumors in comparison with the GFP overexpressing tumors. Top 30 genes with highest fold changes are depicted in the list ($p<0.05$).

Gene	Description	Log_2 Fold Change
TMEM38A	Transmembrane Protein 38A	2,569
NEB	Nebulin	2,521
SIGLEC1	Sialic Acid Binding Ig Like Lectin 1	2,397
PNPLA2	Patatin Like Phospholipase Domain Containing 2	2,538
OBSCN	Obscurin, Cytoskeletal Calmodulin And Titin-Interacting RhoGEF	2,533
DCN	Decorin	2,425
HSD17B10	Hydroxysteroid (17-Beta) Dehydrogenase 10	2,509
DPT	Dermatopontin	2,504
CFH	Complement Factor H	2,480
GPD1	Glycerol-3-Phosphate Dehydrogenase 1	2,459
ATP1A2	ATPase Na+/K+ Transporting Subunit Alpha 2	2,512
KLHL41	Kelch Like Family Member 41	2,463
CBR2	Carbonyl Reductase 2	2,374
EDNRB	Endothelin Receptor Type B	2,332
TACC1	Transforming Acidic Coiled-Coil Containing Protein 1	2,472
C4B	Complement Component 4B	2,014
MYBPC1	Myosin Binding Protein C	2,353
FCGRT	Fc Fragment Of IgG Receptor And Transporter	2,116
PYGM	Phosphorylase, Glycogen, Muscle	2,359
XIRP1	Xin Actin Binding Repeat Containing 1	2,394
FOLR2	Folate Receptor Beta	2,330
CSRP3	Cysteine And Glycine Rich Protein 3	2,415
FABP4	Fatty Acid Binding Protein 4	1,995
CSNK1D	Casein Kinase 1 Delta	2,401
ECM1	Extracellular Matrix Protein 1	2,191
MYOM1	Myomesin 1	2,310
HSPB6	Heat Shock Protein Family B Member 6	2,394
PTX3	Pentraxin 3	2,214
NRAP	Nebulin Related Anchoring Protein	2,334
LRG1	Leucine-Rich Alpha-2-Glycoprotein 1	2,186

Table 5.6. Significantly downregulated genes in MGAT1 overexpressing tumors in comparison with the GFP overexpressing tumors. Top 30 genes with highest fold changes are depicted in the list ($p<0.05$).

Gene	Description	Log_2 Fold Change
HSPA8	Heat Shock Protein Family A (Hsp70) Member 8	-2,287
RPL13	Ribosomal Protein L13	-2,271
EIF4G1	Eukaryotic Translation Initiation Factor 4 Gamma 1	-2,040
NOSIP	Nitric Oxide Synthase Interacting Protein	-2,287
ACTB	Actin, Beta	-2,214
MAP4K4	Mitogen-Activated Protein Kinase Kinase Kinase Kinase 4	-2,257
SEC63	SEC63 Homolog, Protein Translocation Regulator	-2,080
RPL18	Ribosomal Protein L18	-1,973
USO1	USO1 Vesicle Transport Factor	-2,178
PUM2	Pumilio RNA Binding Family Member 2	-2,222
BLOC1S1	Biogenesis Of Lysosomal Organelles Complex 1 Subunit 1	-2,214
MAPKAP1	Mitogen-Activated Protein Kinase Associated Protein 1	-2,056
ADAM17	ADAM Metallopeptidase Domain 17	-2,189
TNRC6C	Trinucleotide Repeat Containing 6C	-2,200
DAZAP1	DAZ Associated Protein 1	-2,136
CLK2	CDC Like Kinase 2	-2,182
ACIN1	Apoptotic Chromatin Condensation Inducer 1	-2,166
GPX3	Glutathione Peroxidase 3	-2,165
CRBN	Cereblon	-1,988
SIRPA	Signal Regulatory Protein Alpha	-2,116
TUBGCP4	Tubulin Gamma Complex Associated Protein 4	-2,100
PAPOLA	Poly(A) Polymerase Alpha	-1,955
RPL36	Ribosomal Protein L36	-1,746
UBE2D2A	Ubiquitin Conjugating Enzyme E2 D2	-1,813
HPN	Hepsin	-2,059
SBF1	SET Binding Factor 1	-2,068
RALGAPB	Ral GTPase Activating Protein Non-Catalytic Beta Subunit	-1,895
CELF1	CUGBP, Elav-Like Family Member 1	-1,814
RPS9	Ribosomal Protein S9	-1,704
MRPS24	Mitochondrial Ribosomal Protein S24	-1,987

We ranked significantly differentially expressed genes depending on their fold changes as determined by DESeq2 and Kallisto softwares. The genes with the highest fold change values that were differentially expressed in BRI3 overexpressing tumors compared to the GFP overexpressing tumors are indicated separately as upregulated genes (Table 5.3) and downregulated genes (Table 5.4). In total, 139 genes were determined to be significantly upregulated upon BRI3 overexpression, whereas 49 genes were downregulated.

On the other hand, the genes with the highest fold change values that were differentially expressed in MGAT1 overexpressing tumors compared to the GFP overexpressing tumors are shown separately as upregulated genes (Table 5.5) and downregulated genes (Table 5.6). Overall, 173 genes were determined to be significantly upregulated upon MGAT1 overexpression, whereas 45 genes were found to be downregulated when compared to the GFP overexpressing control samples.

5.5.1. Pathway enrichment analysis via PANOGA

With the goal of revealing the functionally important pathways associated with the differentially expressed genes, the web server PANOGA (Pathway and Network Oriented GWAS Analysis) was utilized (Bakir-Gungor *et al.*, 2014).

The enrichment analysis obtained by using the differentially expressed genes between BRI3 vs. GFP tumor samples demonstrate that “Regulation of autophagy”, “Mismatch repair” and “Citric acid cycle” are among the most affected pathways (Table 5.7).

On the other hand, the enrichment analysis for the differentially expressed genes between MGAT1 vs. GFP tumor samples indicates that “ECM-receptor interaction”, “Notch signaling pathway” and “Proteoglycans in cancer” are among the most affected pathways (Table 5.8).

Table 5.7. List of enriched pathways associated with the differentially expressed genes in BRI3 vs. GFP samples as determined by the PANOGA analysis software.

KEGG ID	KEGG Term	P Value
KEGG:04140	Regulation of autophagy	3,45E-09
KEGG:03430	Mismatch repair	3,26E-08
KEGG:00020	Citrate cycle (TCA cycle)	7,48E-08
KEGG:04320	Dorso-ventral axis formation	1,83E-07
KEGG:05020	Prion diseases	8,27E-07
KEGG:04960	Aldosterone-regulated sodium reabsorption	8,48E-07
KEGG:03440	Homologous recombination	3,33E-06
KEGG:05210	Colorectal cancer	3,50E-06
KEGG:05216	Thyroid cancer	3,26E-05

Table 5.8. List of enriched pathways associated with the differentially expressed genes in MGAT1 vs. GFP samples as determined by the PANOGA analysis software.

KEGG ID	KEGG Term	P Value
KEGG:04512	ECM-receptor interaction	2,17E-11
KEGG:04330	Notch signaling pathway	5,51E-11
KEGG:05205	Proteoglycans in cancer	1,74E-10
KEGG:04520	Adherens junction	9,72E-08
KEGG:00471	D-Glutamine and D-glutamate metabolism	5,32E-06
KEGG:05100	Bacterial invasion of epithelial cells	1,29E-05
KEGG:03450	Non-homologous end-joining	3,95E-05
KEGG:05120	Epithelial cell signaling in Helicobacter pylori infection	4,53E-05
KEGG:04920	Adipocytokine signaling pathway	5,49E-05

5.5.2. Gene Ontology Enrichment Analysis via GOrilla

In order to determine the enriched GO (Gene Ontology) terms in Biological Process domain (GO_BP), significantly differentially expressed genes were loaded into GOrilla (Gene ontology enrichment analysis and visualization tool) (Eden *et al.*, 2009).

Table 5.9. GO enrichment analysis (Biological Process) for the differentially expressed genes in BRI3 vs. GFP samples as determined by GOrilla analysis.

GO term	Description	P-value	FDR q-value	Enrichment
GO:0044237	cellular metabolic process	6,18E-05	8,06E-01	1,44
GO:0090153	regulation of sphingolipid biosynthetic process	9,54E-05	6,22E-01	30,75
GO:1905038	regulation of membrane lipid metabolic process	9,54E-05	4,15E-01	30,75
GO:0071704	organic substance metabolic process	1,17E-04	3,83E-01	1,39
GO:0044238	primary metabolic process	2,85E-04	7,44E-01	1,39
GO:0008152	metabolic process	3,49E-04	7,59E-01	1,34
GO:0044260	cellular macromolecule metabolic process	5,04E-04	9,39E-01	1,46
GO:0044087	regulation of cellular component biogenesis	5,57E-04	9,08E-01	2,55
GO:1901360	organic cyclic compound metabolic process	7,03E-04	1,00E+00	1,56
GO:0043170	macromolecule metabolic process	8,22E-04	1,00E+00	1,4
GO:0006686	sphingomyelin biosynthetic process	8,73E-04	1,00E+00	41
GO:1903897	regulation of PERK-mediated unfolded protein response	8,73E-04	9,49E-01	41
GO:0046292	formaldehyde metabolic process	8,73E-04	8,76E-01	41
GO:0009987	cellular process	9,55E-04	8,90E-01	1,22

Table 5.10. GO enrichment analysis (Biological Process) for the differentially expressed genes in MGAT1 vs. GFP samples as determined by GOrilla analysis.

GO term	Description	P-value	FDR q-value	Enrichment
GO:0042221	response to chemical	5,67E-12	7,51E-08	2,44
GO:0044699	single-organism process	4,30E-11	2,85E-07	1,38
GO:0010033	response to organic substance	5,09E-11	2,24E-07	2,6
GO:0030198	extracellular matrix organization	1,02E-10	3,36E-07	6,47
GO:0043062	extracellular structure organization	1,02E-10	2,69E-07	6,47
GO:0050896	response to stimulus	1,14E-10	2,51E-07	1,86
GO:0006936	muscle contraction	1,76E-10	3,33E-07	7,23
GO:0003012	muscle system process	5,49E-10	9,09E-07	6,26
GO:0044763	single-organism cellular process	9,61E-10	1,41E-06	1,44
GO:0032501	multicellular organismal process	2,08E-09	2,76E-06	2,12
GO:0051239	regulation of multicellular organismal process	5,75E-09	6,92E-06	2,16
GO:0006952	defense response	1,54E-08	1,70E-05	3,37
GO:0022617	extracellular matrix disassembly	2,33E-08	2,38E-05	12,88
GO:0048583	regulation of response to stimulus	3,78E-08	3,57E-05	1,83
GO:0048518	positive regulation of biological process	4,52E-08	3,99E-05	1,63
GO:1901700	response to oxygen-containing compound	4,92E-08	4,07E-05	2,62
GO:0006950	response to stress	1,25E-07	9,77E-05	1,94
GO:0006954	inflammatory response	1,35E-07	9,94E-05	4,68
GO:0044767	single-organism developmental process	1,36E-07	9,48E-05	1,72
GO:0003008	system process	2,16E-07	1,43E-04	2,83
GO:0009719	response to endogenous stimulus	2,25E-07	1,42E-04	2,76
GO:0008150	biological_process	3,84E-07	2,31E-04	1,09
GO:0009605	response to external stimulus	3,97E-07	2,28E-04	2,59

Table 5.10. GO enrichment analysis (Biological Process) for the differentially expressed genes in MGAT1 vs. GFP samples as determined by GOrilla analysis (cont.).

GO:0065009	regulation of molecular function	4,87E-07	2,69E-04	1,86
GO:0002576	platelet degranulation	7,18E-07	3,80E-04	7,59
GO:0048856	anatomical structure development	7,91E-07	4,03E-04	1,85
GO:0030049	muscle filament sliding	8,54E-07	4,18E-04	12,97
GO:0033275	actin-myosin filament sliding	8,54E-07	4,04E-04	12,97
GO:0051094	positive regulation of developmental process	8,83E-07	4,03E-04	2,59

GO enrichment analysis with the differentially expressed genes in BRI3 vs. GFP samples demonstrate that “cellular metabolic process”, “regulation of sphingolipid biosynthetic process”, “regulation of membrane lipid metabolic process” and “organic substance metabolic process” are the most over-represented biological processes (Table 5.9).

On the other hand, differentially expressed genes of MGAT1 vs. GFP samples were found to have enriched GO terms as the followings: “response to chemical”, “single-organism process”, “response to organic substance”, “extracellular matrix organization” and “extracellular structure organization” (Table 5.10).

5.5.3. Candidate Gene Selection for Further Analysis

In order to verify the differential expression as detected by RNA-Sequencing, quantitative real-time PCR will be performed. For this purpose, three genes are selected from each analysis in the first place. YAP1, CSNK2B and ABL1 are selected from the differentially expressed genes in BRI3 vs. GFP analysis. EDNRB, ADAM17 and HSPA8 are the genes selected from MGAT1 vs. GFP analysis (Table 5.11). These genes are chosen on the basis of having the highest fold change values and their relevance with respect to carcinogenesis.

Table 5.11. List of candidate genes selected for further verification.

	Gene	Description	Log_2FC
BRI3 vs. GFP	YAP1	Yes Associated Protein 1	-2,034
	CSNK2B	Casein Kinase 2 Beta	2,028
	AFP	Alpha Fetoprotein	1,928
MGAT1 vs. GFP	EDNRB	Endothelin Receptor Type B	2,332
	ADAM17	ADAM Metallopeptidase Domain 17	-2,189
	HSPA8	Heat Shock Protein Family A (Hsp70) Member 8	-2,287

6. DISCUSSION

The canonical Wnt/β-catenin signaling pathway is a highly conserved pathway and it is involved in various differentiation events during embryonic development, such as axis formation, cellular proliferation, differentiation and morphogenesis. β-catenin is considered to be the key molecule in this pathway. In addition to its functions in vertebrate early development, Wnt/β-catenin pathway has the potential to initiate tumor formation when aberrantly activated. Those characteristics of the Wnt/β-catenin signaling pathway makes the pathway itself and its targets important subjects in cancer research fields, since genes regulated by this pathway are potential drug and gene therapy targets. Therefore, in order to identify novel transcriptional targets of the Wnt/β-catenin pathway, SAGE and microarray screens were carried out in our laboratory. As the result of analyses, a number of genes were determined to be either upregulated or downregulated significantly by means of mimicking the active status of the Wnt/β-catenin pathway.

BRI3 was determined to be one of the novel transcriptional targets of the Wnt/β-catenin signaling pathway. It has been selected from the SAGE screen results due to the fact that overexpression of the degradation-resistant β-catenin mutant (S33Y-β-catenin) resulted in significant upregulation of BRI3. Supporting data was obtained from lithium treatment of Huh7 cell lines, luciferase reporter assay, overexpression of Wnt ligands and chromatin immunoprecipitation (ChIP) assay by using the anti-β-catenin antibody (Kavak *et al.*, 2010).

BRI3 has been poorly characterized with respect to the previous literature. Its function and action mechanism were largely unknown. Therefore, we aimed to provide clues about functional relevance of BRI3 with respect to the Wnt/β-catenin pathway. As a first step in our study, we sought to discover novel interaction partners of BRI3 protein in order to shed light on the exact action mechanism of BRI3. Yeast two-hybrid assay was employed for this purpose. We screened a human liver cDNA library by using BRI3 protein as bait.

For the yeast-two hybrid assay, either yeast mating or yeast cotransformation can be employed to enable the expression of bait and prey vectors. Prey vectors have been commercially obtained as human liver cDNA library pretransformed into the yeast strain MATα. Therefore, in our studies yeast mating was preferred instead of transformation. Furthermore, yeast mating is advantageous over yeast transformation due to being more practical and a relatively high efficiency procedure (Soellick and Uhrig, 2001). As a result of two-hybrid library screening by yeast mating, colonies were selected on high stringency growth media (-4 Dropout media lacking Ade/His/Leu/Trp aminoacids) (Figure 5.1). Identification of the candidate interaction partners corresponding to the positive colonies was performed by means of yeast colony PCR and sequencing (Figure 5.2). We were able to identify MGAT1 (Mannosyl α-1,3-glycoprotein β-1,4-N-acetylglucosaminyl transferase) and IFITM3 (Interferon induced transmembrane protein 3) as candidate positive interactors, which was also confirmed by cotransformation into yeast cells. On the other hand, the third possible candidate protein IL-7R was eliminated as a result of yeast cotransformation due to lack of colony growth on -4 DO selective media (Figure 5.2).

The finding of MGAT1 as an interacting partner of BRI3 appeared to be promising in the sense that MGAT1 was also one of the genes that exhibit differential expression levels in response to β-catenin activation and it was included among the candidate target genes of Wnt/β-catenin signaling with respect to the SAGE analysis performed previously in our laboratory. Nevertheless, initially it was not focused in the first place for further characterization. MGAT1 is known to code for an enzyme essential for the synthesis of hybrid and complex N-glycans, but not associated with carcinogenesis yet.

According to previous literature, IFITM3 has been identified as a new molecular marker in human colorectal tumors and it has been stated that IFITM3 gene expression is controlled by the Wnt/β-catenin signaling in mouse and human intestinal epithelium (Andreu *et al.*, 2006). Furthermore, the results of a more recent study indicate elevated IFITM3 expression in colon cancer cells compared to normal colon cells. The data obtained from this study suggest that IFITM3 plays an important role in early colon cancer development (Fan *et al.*, 2008).

BRI3, as being the first gene selected among the candidate target genes of the Wnt/β-catenin pathway, has two isoforms due to an alternative splicing event. The longer isoform of BRI3 (isoform-a) codes for a protein of 125 aa in length, whereas the shorter one (isoform-b) has 98 aa. Alignment of the aminoacid sequences of the two BRI3 isoforms suggest that the N-terminals are the same, however BRI3 isoform-a has a distinct C-terminus compared to BRI3 isoform-b (Figure 5.3).

In order to test for the interaction of these BRI3 isoforms with the candidate binding partners obtained from yeast-two hybrid assay, coimmunoprecipitation was performed. Initial experiments were done with using only the longer BRI3 isoform and positive interaction of BRI3 was determined with both MGAT1 and IFITM3 proteins (Figure 5.4). BRI3BP was also cloned and used as a positive control since it is the only known protein interactor of BRI3 with respect to previous literature. Further coimmunoprecipitation experiments showed the interaction of BRI3 isoform-a with the candidate proteins MGAT1 and IFITM3, however the shorter isoform of BRI3 failed to interact with these two proteins (Figure 5.5 and Figure 5.6). For the second set of coimmunoprecipitation experiments, anti-EpCam antibody was used as mock antibody as the negative control for immunoprecipitation. We also used anti-BRI3 antibody to detect the BRI3-GFP fusion protein in immunoprecipitated samples. However, in the case of BRI3 isoform-b, we could not detect any band corresponding to isoform-b even for the input samples in western blotting, possibly due to the lack of the antibody to recognize this shorter BRI3 isoform (Figure 5.6).

Colocalization assay has been performed in Huh7 cell lines by expressing the fluorescent protein fused versions of our proteins in order to visualize any possible interaction inside the cells. For this purpose, the GFP-tagged fusion proteins of either BRI3 isoform-a or isoform-b were expressed in Huh7 cells together with either MGAT1-dsRED or IFITM3-dsRED. The results indicate an intense colocalization of BRI3 with MGAT1, especially in the perinuclear area of Huh7 cells, which might be inside an organelle such as Golgi apparatus or ER (Figure 5.7A). In fact, a previous study has been carried out in order to determine the subcellular localization of BRI3 (Wu *et al.*, 2003). The results obtained from this study suggested that BRI3-GFP fusion protein localizes in the lysosomes within the cell and the function of BRI3 may be related to lysosomes. Colocalization was also

observed between the fluorescent-tagged proteins of BRI3 and IFITM3, however to a lesser extent (Figure 5.7B). On the other hand, expression of BRI3 isoform-b together with the candidate binding proteins MGAT1 and IFITM3 did not result in a specific colocalization inside the cells. BRI3 isoform-b rather appeared to be distributed almost uniformly throughout the cells, including both the cytosol and nucleus (Figure 5.8). This observation prompts us to hypothesize that BRI3 protein might have a specific localization signal sequence in its C-terminus which is not present in the shorter isoform-b.

Various carcinoma cell lines (mostly hepatocellular carcinoma) and normal cell lines were used for western blotting in order to observe the basal protein expression levels of our proteins in concern, together with a number of key proteins important in cell proliferation (Figure 5.9). BRI3 protein expression has been detected in every cell line we used, contrary to that implied by its name Brain protein I3. On the other hand, MGAT1 and IFITM3 proteins were detected mostly in hepatocellular carcinoma and colon carcinoma cell lines. This observation also contributed to our hypothesis that MGAT1 and IFITM3 can be novel transcriptional targets of the Wnt/β-catenin pathway, since hepatocellular carcinoma and colon carcinoma are the two types of carcinoma which displays the highest Wnt/β-catenin pathway activation. This can also be seen from the protein expression levels of non-phospho (active) β-catenin, which is higher in hepatocellular carcionoma and colon carcinoma cell lines (Figure 5.9). Among the hepatocellular carcinoma cell lines, HepG2 cells endogenously express an N-terminal deleted form of β-catenin which is constitutively active, therefore total β-catenin protein appears to be at lower molecular weight, and it is not recognized by the non-phospho (active) β-catenin antibody. Human astrocytoma cell lines U373-MG, have endogenously high wild-type β-catenin levels, whereas HeLa (human cervical cancer) cells are Wnt inactive (Figure 5.9).

In order to determine the expression levels of MGAT1 and IFITM3 in response to lithium treatment, western blotting has been performed from NaCl (control) and LiCl treated Huh7 cell lines. LiCl treatment is a commonly used method to mimic the active status of the Wnt/β-catenin pathway, since lithium is known for its GSK-3β inhibiting activity (Rubinfeld *et al.*, 1996; Levy *et al.*, 2002). Artificial inhibition of GSK-3β results in the malfunctioning of the degradation complex and subsequent stabilization of β-catenin. The results of western blotting indicates an upregulation of MGAT1 protein levels

in response to LiCl treatment at 24 and 48 hours, which is in correlation with the increase in active β-catenin levels (Figure 5.10). However IFITM3 did not exhibit such a correlation, thus did not respond to LiCl treatment in Huh7 cells. HSF2 and C-myc were previously identified targets of Wnt/β-catenin pathway, and both of these proteins increase in response to 24 and 48 hours of LiCl treatment.

Luciferase assay is a widely employed method for studying promoter function. So, in order to test for the promoter activities of our candidate target genes, we cloned the 5'-end upstream regions of MGAT1 (784 bp) and IFITM3 (1539 bp) genes into the promoterless luciferase vector pGL3-basic. Promoter activity of MGAT1 was found to be increased upon transient expression of the degradation-resistant β-catenin mutant (S33Y-β-catenin), whereas IFITM3 did not display any promoter activity in the same conditions (Figure 5.11). Furthermore, expression of S33Y-β-catenin and TCF4 in combination resulted in a significant increase in MGAT1 promoter activity compared to that from the promoterless pGL3-basic vector. However, coexpression of a dominant-negative TCF4 (dNTCF4) and S33Y-β-catenin in Huh7 cells, diminished the promoter activity-stimulating effect of S33Y-β-catenin, since dNTCF4, which competes with the wild-type TCF4 for the TBEs (TCF4 binding elements), lacks β-catenin binding region and cannot be activated. Coexpression of S33Y-β-catenin either with TCF4 or dNTCF4 did not result in any comparable luciferase activity from the IFITM3 promoter (Figure 5.12). Finally, several canonical Wnt ligands have been expressed in Huh7 cells in order to detect the activity of MGAT1 promoter in response. For all the ligands expressed, MGAT1 promoter exhibited a marked increase compared to the expression of empty vector as the negative control (Figure 5.13).

Overexpression of either S33Y-β-catenin by itself or in combination with TCF4 also caused an increase in the protein levels of MGAT1 (Figure 5.14). This increase was not detected in the expression of wild-type β-catenin or empty vector. As expected, the known target proteins HSF2 and C-myc also displayed high expression levels upon expression of S33Y-β-catenin or coexpression of S33Y-β-catenin and TCF4. Protein levels of MGAT1 seem to be correlated with the levels of active β-catenin in Huh7 cells. Furthermore, in order to detect the mRNA levels of MGAT1, q-RTPCR was performed. Huh7 cells were treated with Wnt agonist or synthetic GSK-3β inhibitor (TWS 119) in

varying concentrations, in order to mimic pathway activation. MGAT1 mRNA levels were determined to augment gradually upon increasing concentrations of Wnt agonist treatment. However, only the highest concentration of TWS 119 resulted in a marked increase in MGAT1 mRNA. AXIN2, which is one of the best known targets of Wnt/β-catenin pathway, has been used as positive control (Figure 5.15).

Our previous studies indicated BRI3 to be a novel transcriptional target of Wnt/β-catenin pathway (Kavak *et al.*, 2010). With respect to literature findings, BRI3 was shown to be involved in TNFα-mediated cell death pathway (Zhao et al, 2003). Consistent with these findings, our coimmunoprecipitation experiments show that BRI3 might be involved in a complex with TRAF2 and TRAF6 (Figure 5.16). These two proteins are important adapter molecules in the signal transduction of NFkB pathway. They can act either separately or in the form of heterodimers through the pathway. However, the exact function of BRI3 with respect to the NFkB pathway or the importance of this interaction could not yet be clarified. In our studies, luciferase assay was also performed in order to determine NFkB promoter activity in response to BRI3 overexpression. NOD1, which is an already known activator of NFkB signaling, was used as positive control and resulted in an elevated luciferase activity from NFkB promoter. Overexpression of BRI3 also led to comparably high levels of NFkB promoter activity (Figure 5.17). We also sought to determine BRI3 protein levels in the stable HEK293-4KB-GFP cells subjected to TNF-α treatment for various time intervals. TNF-α levels can be seen to maximize around 4 hours of treatment, which also coincides with the protein levels of BRI3 (Figure 5.18). Thus, we can hypothesize that BRI3 might have a function in the signal transduction of TNF-α/NFkB pathway, and overexpression of BRI3 results in NFkB activation.

In our study with BRI3 and MGAT1, the two novel targets of Wnt/β-catenin pathway, we wanted to extend our research with in vivo studies. Therefore, stable Huh7 cell lines overexpressing BRI3 and MGAT1 were generated. Huh7 cells were chosen as the most common cell line being used in our laboratory within the context of hepatocellular carcinoma. Besides, as being a cancer cell line, they are also suitable to be used in xenograft experiments due to their inherent ability to adhere and proliferate when injected subcutaneously into mice. The coding sequences of these two genes were cloned into the vector pIRES2-EGFP, since it provides the native expression of our genes due to the

presence of IRES (Internal Ribosome Entry Site) and GFP fluorescent protein expression enables us to visualize the transfection efficiency and the ongoing antibiotic selection process of successfully overexpressing cells. A second GFP was also cloned to generate pIRES2-EGFP-GFP in order to express GFP in place of our genes and used as a negative control vector. Before proceeding with the in vivo analysis, a series of cell migration and proliferation assays were performed to assess the proliferative potentials of the stable cell lines in vitro. The results of wound healing assay suggests that BRI3 and MGAT1 overexpressing stable cells were more effective in closing the wound compared to GFP overexpressing cells, which gives us a hint about their higher migration and proliferation abilities (Figure 5.20). Furthermore, the stable cell lines were subjected to PI staining and FACS analysis in order to determine whether there is any difference between their cell cycle profiles, especially the percentage of cells in S and G2 phases of the cell cycle. Nevertheless, no significant difference was observed between any of the three stable cell lines (Figure 5.21 and Table 5.1). The stable cell lines were analyzed by XTT cell proliferation assay to test for proliferation related to metabolic activities of the cells. At normal growth conditions (10% FBS) there appeared to be no significant difference between the absorbance values of the stable cell lines (data not shown). However, under serum starvation conditions (2% and 5% FBS), BRI3 and MGAT1 overexpressing cells displayed higher proliferation rate compared to GFP overexpressing cells (Figure 5.22).

After these in vitro analyses, the stable cell lines were subsequently used for xenograft assays in order to assess their *in vivo* tumorigenesis abilities. Initial experiments were performed in NUDE mice and optimizations were done for the injection region, amount to be injected and number of cells used in the injection. However, we later switched to using SCID mice, since they are deficient in both T and B cells, so it is easier to develop tumors in SCID mice in a relatively shorter period of time. The injections were made subcutaneously and bilaterally such that the left flank regions of mice were injected with either BRI3 or MGAT1 overexpressing cells, whereas the right flank regions were injected with control cells (GFP overexpressing Huh7 cells). Thus, *in vivo* xenograft experiments demonstrated that, both the BRI3 and MGAT1 overexpressing cells were able to generate larger tumors when compared to GFP overexpressing cells (Figure 5.23 and Figure 5.24). Tumor formations were evident 3-4 weeks after the injections. The tumors were then isolated from both flanks of the mice and their weights were determined for

comparison (Figure 5.25 and Table 5.2). Averages of weights for each case were computed and plotted (Figure 5.26). As a result, BRI3 and MGAT1 overexpressing cells were found to induce bigger tumor formations compared to their GFP overexpressing counterparts.

Next, we employed RNA Sequencing method in order to determine the differentially expressed genes and identify the enriched pathways by comparing the transcriptomic profiles of these tumors. By means of RNA-Seq, a snapshot of transcript levels at a given time and condition is determined. Furthermore, with this technique, novel transcript discovery or transcript quantification can be accurately accomplished. Compared to the microarray technology, which has been the traditional method for transcriptome profiling until recently, RNA-Seq enables us to obtain digital sequencing read counts rather than fluorescence intensity values. This technique is also advantageous in the sense that it is not restricted to predesigned probes as in microarrays; therefore there is no requirement for prior knowledge about the transcriptome of interest. Thus, novel transcripts or isoforms can be detected.

The total RNA extracted from isolated tumors was first analyzed by spectrophotometry and denaturing agarose gel electrophoresis in order to confirm its integrity. RNAstable kit has been used to assure that the RNA samples remain intact during shipping at room temperature. RNA Sequencing followed by bioinformatic analyses determined the significantly differentially expressed genes in both BRI3 overexpressing tumors and MGAT1 overexpressing tumors compared to GFP overexpressing tumors as controls.

Upregulated and downregulated genes in BRI3 overexpressing samples were determined separately (Table 5.3 and Table 5.4). Among the genes, several potential targets which have important roles in carcinogenesis were able to be specified. YAP1 and AFP are included in the Hippo signaling pathway. YAP1 is a downstream nuclear effector of Hippo signaling and it is known to play a role in the development and progression of multiple cancers as a transcriptional regulator of this pathway. YAP1 gene is frequently amplified in several human cancers including liver, breast, prostate and esophageal cancer (Harvey and Tapon, 2007). However, in some cancers YAP1 can also play a role as a tumor suppressor (Bertini *et al.*, 2009). CSNK2B is another differentially expressed gene,

which encodes for a ubiquitous protein kinase which regulates metabolic pathways, signal transduction, transcription and replication. It is also frequently upregulated in various human cancers, although the exact mechanism of CSNK2B activation in cancer remains unknown. Nevertheless, it affects several cell signaling pathways including TNF-α/NFkB, PI3K and Wnt Signaling Pathways. TRAF3 is also among the differentially expressed genes and it functions in the NFkB signaling, but unlike the other TRAF proteins, TRAF3 negatively regulates the pathway. These findings strengthen our hypothesis that BRI3 might have an important role in TNFα/NFkB signaling pathway. However, the drastic changes in the levels of YAP1 and AFP suggest that BRI3 may have an effect on Hippo/YAP signaling pathway.

The differentially expressed genes obtained from the comparison of MGAT1 overexpressing tumors with GFP overexpressing tumors were indicated separately as upregulated and downregulated ones (Figure 5.5 and Figure 5.6). Among these genes, emphasis will be given primarily to EDNRB, HSPA8 and ADAM17. EDNRB gene codes for Endothelin Receptor Type B which is associated with pathways such as GPCR signaling, calcium signaling and pathways in cancer. EDNRB is upregulated with MGAT1 overexpression. ADAM17 belongs to the disintegrin and metalloprotease family of proteins which contribute to the regulation of cell-cell and cell-matrix interactions that are critical determinants of malignancy. It has the potential to regulate extracellular matrix remodeling and cell migration. Furthermore, expression of some ADAM proteins was found to be increased in malignant cell populations, including pancreatic and hepatocellular carcinoma cells (Tannapfel *et al.*, 2003). HSPA8 is a member of the Heat Shock Protein Family A, and it is the most downregulated gene upon MGAT1 overexpression. Among the pathways associated with HSPA8 are apoptosis pathway and MAPK signaling pathway, thus this gene is also worth focusing on for further analysis.

In order to understand which pathways and biological processes are enriched among the differentially expressed genes, PANOGA pathway analysis and GOrilla gene ontology enrichment analysis were performed. Comparison of transcriptomic profiles of BRI3 vs. GFP samples yielded “regulation of autophagy” as the most significant pathway affected. “Colorectal cancer” and “thyroid cancer” are also among the significantly overrepresented KEGG pathways, which are relevant to our study as well. The genes

associated with these pathways include the followings: ATG5, ATG7 for the regulation of autophagy; TGFBR1, MAPK3, CTNNB1, APC and AKT1 for colorectal cancer; MAPK3 and KRAS for thyroid cancer.

With regard to the enriched pathways upon MGAT1 overexpressing, ECM-receptor interaction was found to be the most overrepresented pathway. Notch signaling pathway, proteoglycans in cancer and adherens junction are also among the significantly enriched pathways. MGAT1 is one of the proteins functioning in the process of N-glycan synthesis, which play important roles in cell-cell and cell-matrix interactions essential for the development of multicellular organisms (Schachter, 2011). Considering this role of MGAT1, "proteoglycans in cancer" come out to be the most relevant pathway within our context. Proteoglycans are the key regulators of cell-matrix dynamics and there are numerous studies showing that the abnormal or erroneous expression of proteoglycans can lead to various types of carcinoma. Furthermore, gene ontology enrichment by GOrilla suggest that "extracellular matrix organization", "extracellular structure organization" and "extracellular matrix disassembly" are among the most overrepresented biological processes.

When we look at the overall picture, BRI3 and MGAT1 were determined as interaction partners at the beginning of our study. *In vivo* xenograft experiments and analysis of the transcriptomic profiles of tumors suggest that both of them are able to initiate tumorigenesis when overexpressed and their associated pathways are mostly related to carcinogenesis. However, their interaction in the protein level does not seem to be essential for the induction of tumorigenesis. In other words, both BRI3 and MGAT1 are able to induce tumorigenesis separately and independently from each other. This can also be understood from the fact that, the transcriptomic analyses reveal different pathways for each one and there is no common gene that is differentially expressed among these two profiles.

REFERENCES

Aberle, H., A. Bauer, J. Stappert, A. Kispert and R. Kemler, 1997, "beta-catenin is a target for the ubiquitin-proteasome pathway", *The EMBO Journal*, Vol. 16, No. 13, pp. 3797-3804.

Adhikari A., M. Xu and Z. J. Chen, 2007, "Ubiquitin-mediated activation of TAK1 and IKK", *Oncogene*. Vol. 26, No. 22, pp. 3214-26.

Ahmed I. and D. N. Lobo, 2009, "Malignant tumours of the liver", *Surgery*, Volume 27, No. 1, pp. 30–37.

Anastas J. N. and R. T. Moon, 2013, "WNT signalling pathways as therapeutic targets in cancer", *Nature Reviews Cancer*, Vol. 13, No. 1, pp. 11-26.

Andreu, P., S. Colnot, C. Godard, P. Laurent-Puig, D. Lamarque, A. Kahn, C. Perret and B. Romagnolo, 2006, "Identification of the *IFITM* Family as a new molecular marker in human colorectal tumors", *Cancer Research*, Vol. 66, No. 4, pp. 1949-1956.

Bakir-Gungor, B., E. Egemen and O. U. Sezerman, 2014, "PANOGA: a web server for identification of SNP-targeted pathways from genome-wide association study data", *Bioinformatics*, Vol. 30, No. 9, pp. 1287-1289.

Barker, N. and H. Clevers, 2006, "Mining the Wnt pathway for cancer therapeutics", *Nature Reviews Drug Discovery*, Vol. 5, No. 12, pp. 997-1014.

Bax, B. and H. Jhoti, 1995, "Protein-protein interactions: Putting the pieces together", *Current Biology*, Vol. 5, pp. 1119-1121.

Baxter, T. G., R. C. Kuo and O. J. Jupp, 1999, "Tumor necrosis factor mediates both apoptotic cell death and cell proliferation in a human hematopoietic cell line

dependent on mitotic activity and receptor subtype expression", *Journal of Biological Chemistry*, Vol. 274, No. 14, pp. 9539-9545.

Behrens, J., B. A. Jerchow, M. Wurtele, J. Grimm, C. Asbrand, R. Wirtz, M. Kuhl, D. Wedlich and W. Birchmeier, 1998, "Functional interaction of an axin homolog, conductin, with beta-catenin, APC, and GSK3beta", *Science*, Vol. 280, pp. 596-599.

Behrens, J., J. P. von Kries, M. Kuhl, L. Bruhn, D. Wedlich, R. Grosschedl and W. Birchmeier, 1996, "Functional interaction of beta-catenin with the transcription factor LEF-1", *Nature*, Vol. 382, pp. 638-642.

Beyaert R., B. Vanhaesebroeck, P. Suffys, F. Van Roy and W. Fiers, 1989, "Lithium chloride potentiates tumor necrosis factor-mediated cytotoxicity in vitro and in vivo", *Proceedings of the National Academy of Sciences of the United States of America*, Vol. 86, No. 23, pp. 9494-9498.

Bienz, M., 2002, "The subcellular destinations of APC proteins", *Nature Reviews Molecular Cell Biology*, Vol. 3, No. 5, pp. 328-338.

Bleasby, A., 1999, *EMBOSS Needle Tool*, http://www.ebi.ac.uk/Tools/psa/emboss_needle, accessed at April 2016.

Bosch F. X., Ribes J., Borràs J., 1999, "Epidemiology of primary liver cancer", *Seminars in Liver Disease*, Vol. 19, No. 3, pp. 271-85.

Bouwmeester T., Bauch A., Ruffner H., Angrand P.O., Bergamini G., Croughton K., Cruciat C., Eberhard D., Gagneur J., Ghidelli S., Hopf C., Huhse B., Mangano R., Michon A.M., Schirle M., Schlegl J., Schwab M., Stein M.A., Bauer A., Casari G., Drewes G., Gavin A.C., Jackson D.B., Joberty G., Neubauer G., Rick J., Kuster B., Superti-Furga G., 2004, "A physical and functional map of the human TNF-alpha/NF-kappa B signal transduction pathway", *Nature Cell Biology*, Vol. 6, No. 2, pp. 97-105.

Cadigan, K. M. and R. Nusse, 1997, "Wnt signaling: a common theme in animal development", *Genes & Development*, Vol.11, pp. 24-32.

Cadoret A., Ovejero C., Saadi-Kheddouci S., Souil E., Fabre M., Romagnolo B., Kahn A., Perret C., 2001, "Hepatomegaly in transgenic mice expressing an oncogenic form of beta-catenin", *Cancer Research,* Vol. 61, No. 8, pp. 3245-9.

Cavallo R.A., R. T. Cox, M. M. Moline, J. Roose, G. A. Polevoy, H. Clevers, M. Peifer and A. Bejsovec, 1998, "Drosophila Tcf and Groucho interact to repress Wingless signalling activity", *Nature*, Vol. 395, No. 6702, pp. 604-608.

Chuang S.C., C. La Vecchia and P. Boffetta, 2009, "Liver cancer: descriptive epidemiology and risk factors other than HBV and HCV infection", *Cancer Letters*, Vol. 286, No. 1, pp. 9-14.

Clevers, H. and R. Nusse, 2012, "Wnt/β-catenin signaling and disease", *Cell*, Vol. 149, No. 6, pp. 1192-1205.

Cohen, P., 1989, "The structure and regulation of protein phosphatases", *Annual Reviews in Biochemistry*, Vol. 58, pp. 453-508.

Croce, C. M., 2008, "Oncogenes and cancer", *The New England Journal of Medicine,* Vol. 358, No. 5, pp. 502-511.

Eden E., R. Navon, I. Steinfeld, D. Lipson and Z. Yakhini, 2009, "GOrilla: a tool for discovery and visualization of enriched GO terms in ranked gene lists", *BMC Bioinformatics,* Vol. 10, No. 48, pp. 1-7.

Escárcega, R. O., S. Fuentes-Alexandro, M. García-Carrasco, A. Gatica, and A. Zamora, 2007, "The transcription factor nuclear factor-kappa B and cancer", *Clinical Oncology*, Vol. 19, No. 2, pp. 154-161.

Daniels, D. L. and W. I. Weis, 2005, "Beta-catenin directly displaces Groucho/TLE repressors from Tcf/Lef in Wnt-mediated transcription activation", *Nature Structural & Molecular Biology*, Vol. 12, No.4, pp. 364-371.

De Ferrari, G. V. and R. T. Moon, 2006, "The ups and downs of Wnt signaling in prevalent neurological disorders", *Oncogene*, Vol. 25, pp. 7545-7553.

De Oliveria L.J., A. D'Oliveira, R. C. Melo, E. C. De Souza, C. A. Costa Silva and R. Paraná, 2009, "Association between hepatitis C and hepatocellular carcinoma", *Journal of Global Infectious Diseases*, Vol. 1, No. 1, pp. 33-37.

Deng J., Stephanie A. M., Hong-Ying W., Weiya X., Yong W., Binhua P. Z., Yan L., Du Q., Zhang X., Cardinal J., Cao Z., Guo Z., Shao L., Geller D.A., 2009, "Wnt/beta-catenin signaling regulates cytokine-induced human inducible nitric oxide synthase expression by inhibiting nuclear factor-kappaB activation in cancer cells", *Cancer Research*, Vol. 69, No. 9, pp. 3764-71.

Dhanasekaran, R., A. Limaye and R. Cabrera, 2012, "Hepatocellular carcinoma: current trends in worldwide epidemiology, risk factors, diagnosis, and therapeutics", *Hepatic Medicine*, Vol. 8, No. 4, pp. 19-37.

Fagotto, F., E. Jho, L. Zeng, T. Kurth, T. Joos, C. Kaufmann and F. Costantini, 1999, "Domains of axin involved in protein-protein interactions, Wnt pathway inhibition, and intracellular localization", *Journal of Cell Biology*, Vol. 145, No. 4, pp. 741-756.

Fan, J., Z. Peng, C. Zhou, G. Qiu, H. Tang, Y. Sun, X. Wang, Q. Li, X. Le and K. Xie, 2008, "Gene-expression profiling in Chinese patients with colon cancer by coupling experimental and bioinformatic genomewide gene-expression analyses: identification and validation of IFITM3 as a biomarker of early colon carcinogenesis", *Cancer*, Vol. 113, No. 2, pp. 266-275.

Fang, M., J. Li, T. Blauwkamp, C. Bhambhani, N. Campbell and K. M. Cadigan, 2006, "C-terminal-binding protein directly activates and represses Wnt transcriptional targets in Drosophila", *The EMBO Journal*, Vol. 25, No. 12, pp. 2735-2745.

Fields, S. and O. Song, 1989, "A novel genetic system to detect protein-protein interactions", *Nature*, Vol. 340, pp. 245-246.

Franke, T. F., S. I. Yang, T. O. Chan, K. Datta, A. Kazlauskas, D. K. Morrison, D. R. Kaplan and P. N. Tsichlis, 1995, "The protein kinase encoded by the Akt proto-oncogene is a target of the PDGF-activated phosphatidylinositol 3-kinase", *Cell*, Vol. 81, No. 5, pp. 727-736.

Freland, L. and J. M. Beaulieu, 2012, "Inhibition of GSK3 by Lithium, from Single Molecules to Signaling Networks", *Frontiers in Molecular Neuroscience*, Vol. 5, pp. 1-4.

Giles R. H., J. H. Van Es and H. Clevers, 2003, "Caught up in a Wnt storm: Wnt signaling in cancer", *Biochimica et Biophysica Acta*, Vol. 1653, No. 1, pp. 1-24.

Gilmore, T. D., 2006, "Introduction to NF-kappaB: players, pathways, perspectives", *Oncogene*, Vol. 25, No. 51, pp. 6680-6684.

Gong, Y., J. Wu, H. Qiang, B. Liu, Z. Chi, T. Chen, B. Yin, X. Peng and J. Yuan, 2008, "BRI3 associates with SCG10 and attenuates NGF-induced neurite outgrowth in PC12 cells", *BMB Reports*, Vol. 41, pp. 287-293.

Gould, T. D., N. A. Gray and H. K. Manji, 2003, "Effects of a Glycogen Synthase Kinase-3 Inhibitor, Lithium, in Adenomatous Polyposis coli Mutant Mice", *Pharmacological Research*, Vol. 48, pp. 49−53.

Greenbaum, L. E., 2004, "Cell cycle regulation and hepatocarcinogenesis", *Cancer Biology & Therapy*, Vol. 3, No. 12, pp. 1200-1207.

Huber, A. H., W. J. Nelson and W. I. Weis, 1997, "Three-dimensional structure of the armadillo repeat region of beta-catenin", *Cell*, Vol. 90, No.5, pp. 871-882.

Idriss, H. T. and J. H. Naismith, 2000, "TNF α and TNF Receptor Superfamily: Structure-Function Relationships", *Microscopy Research and Technique*, Vol. 50, pp. 184-195.

Ikeda S., S. Kishida, H. Yamamoto, H. Murai, S. Koyama and A. Kikuchi, 1998, "Axin, a negative regulator of the Wnt signaling pathway, forms a complex with GSK-3beta and beta-catenin and promotes GSK-3beta-dependent phosphorylation of beta-catenin", *The EMBO Journal*, Vol. 17, No. 5, pp. 1371-1384.

Ikeda, S., M. Kishida, Y. Matsuura, H. Usui and A. Kikuchi, 2000, "GSK-3beta-dependent phosphorylation of adenomatous polyposis coli gene product can be modulated by beta-catenin and protein phosphatase 2A complexed with Axin", *Oncogene*, Vol. 19, No. 4, pp. 537-545.

Jeng Y.M., Wu M.Z., Mao T.L., Chang M.H., Hsu H.C., 2000, "Somatic mutations of beta-catenin play a crucial role in the tumorigenesis of sporadic hepatoblastoma", *Cancer Letters*, Vol. 152, No.1, pp. 45-51.

Joung, J., E. Ramm and C. Pabo, 2000, "A bacterial two-hybrid selection system for studying protein-DNA and protein-protein interactions", *Proceedings of the National Academy of Sciences of the United States of America*, Vol. 97, No. 13, pp. 7382-7387.

Kavak E., Najafov A., Ozturk N., Seker T., Cavusoglu K., Aslan T., Duru A.D., Saygili T., Hoxhaj G., Hiz M.C., Unal D.O., Birgül-Iyison N., Ozturk M., Koman A., 2010, "Analysis of the Wnt/B-catenin/TCF4 pathway using SAGE, genome-wide microarray and promoter analysis: Identification of BRI3 and HSF2 as novel targets", *Cellular Signalling*, Vol. 22, No. 10, pp. 1523-35.

Kavak, E., 2009, *Defining novel cancer genes, SAGE tags and co-regulated regions of the human genome evolving from the search and identification of novel WNT/TCF/Beta-catenin targets*, Ph.D. Thesis, Boğaziçi University.

Kikuchi, A., 2000, "Regulation of β-catenin Signaling in the Wnt Pathway", *Biochemical and Biophysical Research Communications*, Vol. 268, No. 2, pp. 243-248.

Kim, K., K. M. Pang, M. Evans and E. D. Hay, 2000, "Overexpression of Beta-catenin induces apoptosis independent of its transactivation function with LEF-1 or the involvement of major G1 cell cycle regulators", *Molecular Biology of the Cell*, Vol. 11, pp. 3509-3523.

Kimelman, D. and W. Xu, 2006, "β-catenin destruction complex: insights and questions from a structural perspective", *Oncogene*, Vol. 25, pp. 7482-7491.

Kishida, S., H. Yamamoto, S. Ikeda, M. Kishida, I. Sakamoto, S. Koyama and A. Kikuchi, 1998, "Axin, a negative regulator of the Wnt signaling pathway, directly interacts with Adenomatous Polyposis Coli and regulates the stabilization of beta-catenin", *Journal of Biological Chemistry*, Vol. 273, pp. 10823-10826.

Kolligs F. T., G. Bommer and B. Göke, 2002, "Wnt/beta-catenin/Tcf signaling: a critical pathway in gastrointestinal tumorigenesis", *Digestion*, Vol. 66, No. 3, pp. 131-144.

Komiya Y. and R. Habas, 2008, "Wnt signal transduction pathways", *Organogenesis*, Vol. 4, No. 2, pp. 68-75.

Korinek, V., N. Barker, P. J. Morin, D. van Wichen, R. de Weger, K. W. Kinzler, B. Vogelstien and H. Clevers, 1997, "Constitutive transcriptional activation by a beta-catenin-Tcf complex in $APC^{-/-}$ colon carcinoma", *Science*, Vol. 275, pp. 1784-1787.

Lee H.C., M. Kim and J. R. Wands, 2006, "Wnt/Frizzled signaling in hepatocellular carcinoma", *Frontiers in Bioscience,* Vol. 11, pp. 1901-1915.

Li J., C. Sutter, D. S. Parker, T. Blauwkamp, M. Fang and K. M. Cadigan, 2007, "CBP/p300 are bimodal regulators of Wnt signaling", *The EMBO Journal,* Vol. 26, No. 9, pp. 2284-2294.

Li L., H. Yuan, C. D. Weaver, J. Mao, G.H. Farr, D. J. Sussman, J. Jonkers, D. Kimelman and D. Wu, 1999, "Axin and Frat1 interact with dvl and GSK, bridging Dvl to GSK in Wnt-mediated regulation of LEF-1", *The EMBO Journal*, Vol. 18, No. 15, pp. 4233-4240.

Lickert H., B. Cox, C. Wehrle, M. M. Taketo, R. Kemler and J. Rossant, 2005, "Dissecting Wnt/beta-catenin signaling during gastrulation using RNA interference in mouse embryos", *Development,* Vol. 132, No. 11, pp. 2599-2609.

Liu J., Liao Y., Ma K., Wang Y., Zhang G., Yang R., Deng J., 2013, "PI3K is required for the physical interaction and functional inhibition of NF-κB by β-catenin in colorectal cancer cells", *Biochemical and Biophysical Research Communications,* Vol. 434, No. 4, pp. 760-6.

Lizhu, L., Y. Hong, Y. Mingyao, T. Jiong, Z. Wei, Z. Shouyuan and L. Changben, 2002, "Cloning of murine BRI3 gene and study on its function for inducing cell death", *Chinese Science Bulletin,* Vol. 47, No. 5, pp. 376-379.

Llovet J.M., Burroughs A, Bruix J., 2003, "Hepatocellular carcinoma", *Lancet,* Vol. 362, No. 9399, pp. 1907-17.

Llovet J.M., S. Ricci, V. Mazzaferro, P. Hilgard and E. Gane, 2008, "Sorafenib in advanced hepatocellular carcinoma", *The New England Journal of Medicine,* Vol. 359, No. 4, pp. 378-390.

Logan, C. Y. and R. Nusse, 2004, “The Wnt signaling pathway in development and disease”, *Annual Review of Cell and Developmental Biology*, Vol. 20, pp. 781-810.

Lustig, B. and J. Behrens, 2003, “The Wnt signaling pathway and its role in tumor development”, *Journal of Cancer Research and Clinical Oncology*, Vol. 129, No. 4, pp. 199-221.

MacDonald, B. T., K. Tamai and X. He, 2009, “Wnt/beta-catenin signaling: components, mechanisms, and diseases”, *Developmental Cell*, Vol. 17, No. 1, pp. 9-26.

Malaterre, J., R. G. Ramsay and T. Mantamadiotis, 2007, "Wnt-Frizzled signalling and the many paths to neural development and adult brain homeostasis”, *Frontiers in Biosciences*, Vol. 12, pp. 492-506.

Mao, J., J. Wang, B. Liu, W. Pan, G. H. Farr, C. Flynn, H. Yuan, S. Takada, D. Kimelman, L. Li and D. Wu, 2001, “Low-density lipoprotein receptor-related protein-5 binds to Axin and regulates the canonical Wnt signaling pathway”, *Molecular Cell Biology*, Vol.7, No. 4, pp. 801-809.

Masui, O., Ueda Y., Tsumura A., Koyanagi M., Hijikata M., Shimotohno K., 2002, “RelA suppresses the Wnt/beta-catenin pathway without exerting trans-acting transcriptional ability”, *International Journal of Molecular Medicine*, Vol.9, No. 5, pp. 489-93.

Morin, P. J., A. B. Sparks, V. Korinek, N. Barker, H. Clevers, B. Vogelstein and K. W. Kinzler, 1997, "Activation of beta-catenin-Tcf signaling in colon cancer by mutations in beta-catenin or APC”, *Science*, Vol. 275, pp. 1787-1790.

Nakamura, T., F. Hamada, T. Ishidate, K. Anai, K. Kawahara, K. Toyoshima and T. Akiyama, 1998, “Axin, an inhibitor of the Wnt signaling pathway, interacts with beta-catenin, GSK-3beta and APC and reduces the beta-catenin level”, *Genes to Cells*, Vol. 3, No. 6, pp. 395-403.

Nejak-Bowen K., Kikuchi A., Monga S.P., 2013, "Beta-catenin-NF-κB interactions in murine hepatocytes: a complex to die for", *Hepatology,* Vol. 57, No. 2, pp. 763-74.

Nusse R., 2005, "Wnt signaling in disease and in development", *Cell Research,* Vol. 15, No. 1, pp. 28-32.

Nusse, R. and H. E. Varmus, 1992, "Wnt genes", *Cell,* Vol. 69, No. 7, pp. 1073-1087.

Obed A., T. Tsui, A. Schnitzbauer, M. Obed, H. J. Schlitt, H. Becker and T. Lorf (2008), "Liver transplantation as curative approach for advanced hepatocellular carcinoma: is it justified", *Langenbeck's Archives of Surgery,* Vol. 393, No. 2, pp. 141-147.

Peifer, M. and P. Polakis, 2000, "Wnt signaling in oncogenesis and embryogenesis--a look outside the nucleus", *Science,* Vol. 287, No. 5458, pp. 1606-1609.

Pittois, K., W. Deleersnijder and J. Merregaert, 1998, "cDNA sequence analysis, chromosomal assignment and expression pattern of the gene coding for integral membrane protein 2B", *Gene,* Vol. 217, pp. 14-19.

Polakis P., 1999, "The oncogenic activation of beta-catenin", *Current Opinion in Genetics & Development,* Vol. 9, No. 1, pp. 15-21.

Polakis, P., 2000, "Wnt signaling and cancer", *Genes and Development,* Vol. 14, No. 15, pp. 1837-1851.

Polakis, P., 2007, "The many ways of Wnt in cancer", *Current Opinion in Genetics and Development,* Vol. 17, No. 1, pp. 45-51.

Reya T. and H. Clevers, 2005, "Wnt signalling in stem cells and cancer", *Nature,* Vol. 434, No. 7035, pp. 843-850.

Rubinfeld, B., B. Souza, I. Albert, O. Müller, S. H. Chamberlain, F. R. Masiarz, S. Munemitsu and P. Polakis, 1993, "Association of the APC gene product with beta-catenin", *Science*, Vol. 262, No. 5140, pp. 1731-1734.

Rubinfeld, B., I. Albert, E. Porfiri, C. Fiol, S. Munemitsu and P. Polakis, 1996, "Binding of GSK3beta to the APC-beta-catenin complex and regulation of complex assembly", *Science*, Vol. 272, No. 5264, pp. 1023-1026.

Rubinfeld, B., P. Robbins, M. El-Gamil, I. Albert, E. Porfiri and P. Polakis, 1997, "Stabilization of beta-catenin by genetic defects in melanoma cell line", *Science*, Vol. 275, pp. 1790-1792.

Satoh, S., Y. Daigo, Y. Furukawa, T. Kato, N. Miwa, T. Nishiwaki, T. Kawasoe, H. Ishiguro, M. Fujita, T. Tokino, Y. Sasaki, S. Imaoka, M. Murata, T. Shimano, Y. Yamaoka and Y. Nakamura, 2000, "AXIN1 mutations in hepatocellular carcinomas, and growth suppression in cancer cells by virus-mediated transfer of AXIN1", *Nature Genetics*, Vol. 24, No. 3, pp. 245-250.

Shiaw-Yih L. and H. Mien-Chie, 2002, "B-catenin interacts with and inhibits NF-kB in human colon and breast cancer", *Cancer Cell*, Vol. 2, pp. 323-34.

Soellick, T. R. and J. F. Uhrig, 2001, "Development of an optimized interaction-mating protocol for large-scale yeast two-hybrid analyses", *Genome Biology*, Vol. 2, No. 12, pp. 1-7.

Stier, S., G. Totzke, E. Grunewald, T. Neuhaus, S. Fronhoffs, A. Sachinidis, H. Vetter, K. Schulze-Osthoff and Y. Ko, 2000, "Identification of syntenin and other TNF-inducible genes in human umbilical arterial endothelial cells by suppression subtractive hybridization", *FEBS Letters*, Vol. 467, No. 3, pp. 299-304.

Sun, J., Hobert M.E., Duan Y., Rao A.S., He T.C., Chang E.B., Madara J.L., 2005, "Crosstalk between NF-kappaB and beta-catenin pathways in bacterial-colonized

intestinal epithelial cells", *American Journal of Physiology: Gastrointestinal and Liver Physiology*, Vol. 289, No. 1, pp. 129-37.

Sun, V.C. and L. Sarna, 2008, "Symptom management in hepatocellular carcinoma", *Clinical Journal of Oncology Nursing*, Vol. 12, No. 5, pp. 759-66.

Takeichi, M., 1991, "Cadherin cell adhesion receptors as a morphogenetic regulator", *Science*, Vol.251, No. 5000, pp. 1451-1455.

Tamai, K., X. Zeng, C. Liu, X. Zhang, Y. Harada, Z. Chang and X. He, 2004, "A mechanism for Wnt coreceptor activation", *Molecular Cell Biology*, Vol. 13, No. 1, pp. 149-156.

Tannapfel, A. and C. Wittekind, 2002, "Genes involved in hepatocellular carcinoma: deregulation in cell cycling and apoptosis", *Virchows Archiv*, Vol. 440, No. 4, pp. 345-352.

Thomas, G. M., S. Frame, M. Goedert, I. Nathke, P. Polakis and P. Cohen, 1999, "A GSK3-binding peptide from FRAT1 selectively inhibits the GSK3-catalysed phosphorylation of axin and beta-catenin", *FEBS Letters*, Vol. 458, No. 2, pp. 247-251.

Thorgeirsson S. S. and J. W. Grisham, 2002, "Molecular pathogenesis of human hepatocellular carcinoma", *Nature Genetics*, Vol. 31, No. 4, pp. 339-346.

Tien L. T., M. Ito, M. Nakao, D. Niino, M. Serik, M. Nakashima, C. Y. Wen, H. Yatsuhashi and H. Ishibashi, 2005, "Expression of beta-catenin in hepatocellular carcinoma", *World Journal of Gastroenterology*, Vol. 28, No. 11, pp. 2398-2401.

van de Wetering, M., E. Sancho and C. Verweij, 2002, "The beta-catenin/TCF-4 complex imposes a crypt progenitor phenotype on colorectal cancer cells", *Cell*, Vol. 111, pp. 241-250.

van de Wetering, M., R. Cavallo, D. Dooijes, M. van Beest, J. van Es, J. Loureiro, A. Ypma, D. Hursh, T. Jones, A. Bejsovec, M. Peifer, M. Mortin and H. Clevers, 1997, "Armadillo coactivates transcription driven by the product of the Drosophila segment polarity gene dTCF", *Cell*, Vol. 88, No. 6, pp. 789-799.

Wickham, L., S. Benjannet, E. Marcinkiewicz, M. Chretien and N. G. Seidah, 2005, "β-Amyloid protein converting enzyme 1 and brain-specific type II membrane protein BRI3: binding partners processed by furin", *Journal of Neurochemistry*, pp. 93-102.

Willert, K. and R. Nusse, 1998, "β-catenin: a key mediator of Wnt signaling", *Current Opinion in Genetics and Development,* Vol. 8, pp. 95-102.

Wodarz, A. and R. Nusse, 1998, "Mechanisms of Wnt signaling in development", *Annual Review of Cell and Developmental Biology*, No. 14, pp. 59-88.

Wu, H., G. Liu, C. Li and S. Zhao, 2003, "Bri3, a novel gene, participates in tumor necrosis factor-alpha-induced cell death", *Biochemical and Biophysical Research Communications*, Vol. 14, No. 311, pp. 518-24.

Yamamoto, H., S. Kishida, M. Kishida, S. Ikeda, S. Takada and A. Kikuchi, 1999, "Phosphorylation of axin, a Wnt signal negative regulator, by glycogen synthase kinase-3beta regulates its stability", *Journal of Biological Chemistry*, Vol. 274, No. 16, pp. 10681-10684.

Yamazaki T., N. Sasaki, M. Nishi, D. Yamazaki, A. Ikeda, Y. Okuno, S. Komazaki and H. Takeshima, 2007, "Augmentation of drug-induced cell death by ER protein BRI3BP", *Biochemical and Biophysical Research Communications*, Vol. 362, pp. 971-975.

Ye, Q., K. Singh, J. D. Blonde and Z. Jia, 2004, "Crystallization and preliminary X-ray analysis of the GST-fused human Bri3 N-terminal domain", *Structural Biology and Crystallization Communications*, Vol. 61, pp. 62-64.

Zhou, W., G. Q. Wang, J. Xiao, H. Yu, L. Z. Lin, Q. Zhao, S. Y. Zhao and C. B. Li, 2000, "Isolation of TNF-α related genes expressing in the endothelial cells by suppression subtractive hybridization", *High Technology Letters*, Vol. 10, pp. 9-11.

Zhu A.X., 2006, "Systemic therapy of advanced hepatocellular carcinoma: how hopeful should we be", *Oncologist*, Vol. 11, No. 7, pp. 790-800.

APPENDIX A: PLASMID MAPS

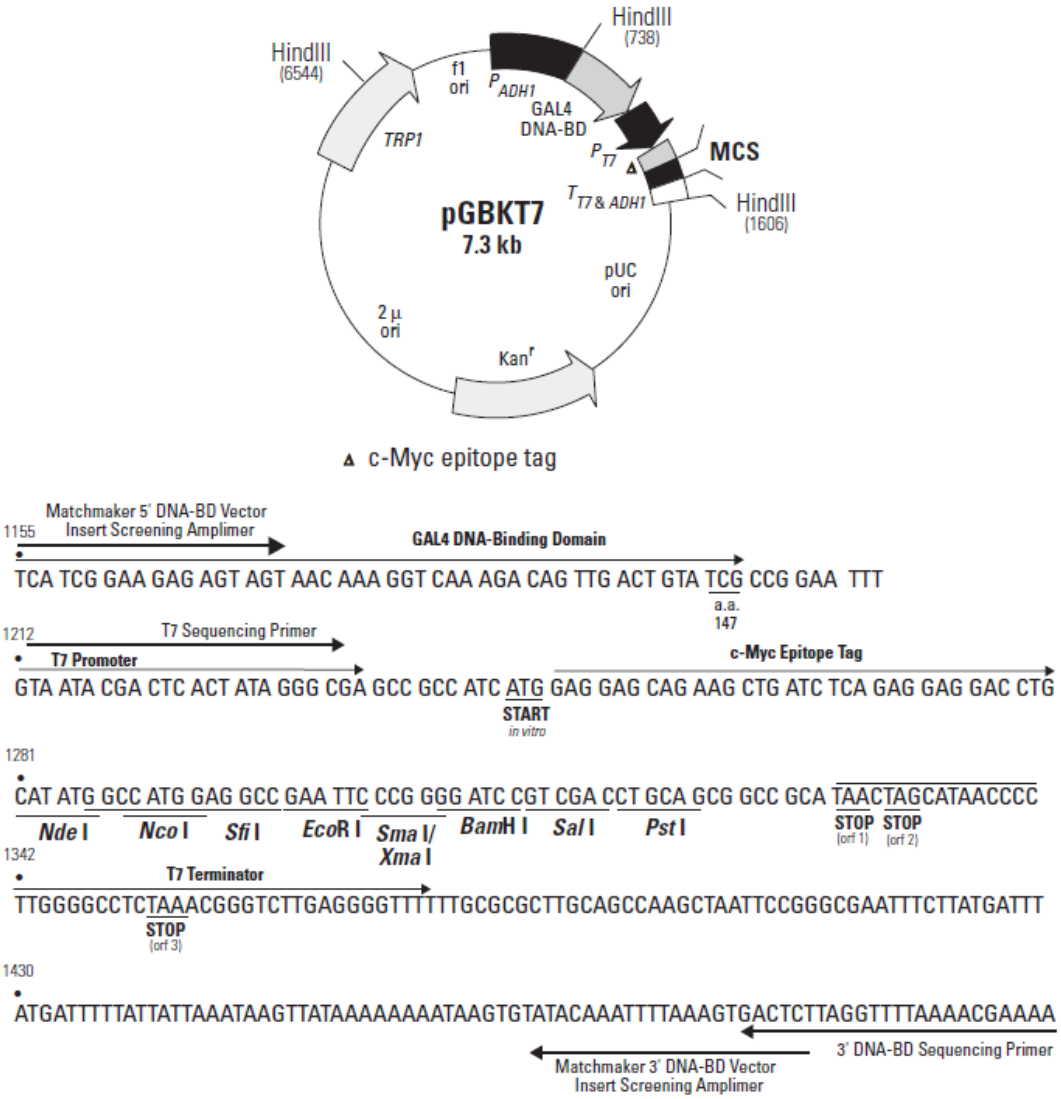

Figure A.1. Restriction map and Multiple Cloning Site (MCS) of pGBKT7 vector which is used in Yeast-two Hybrid screening for the cloning and expression of the bait protein.

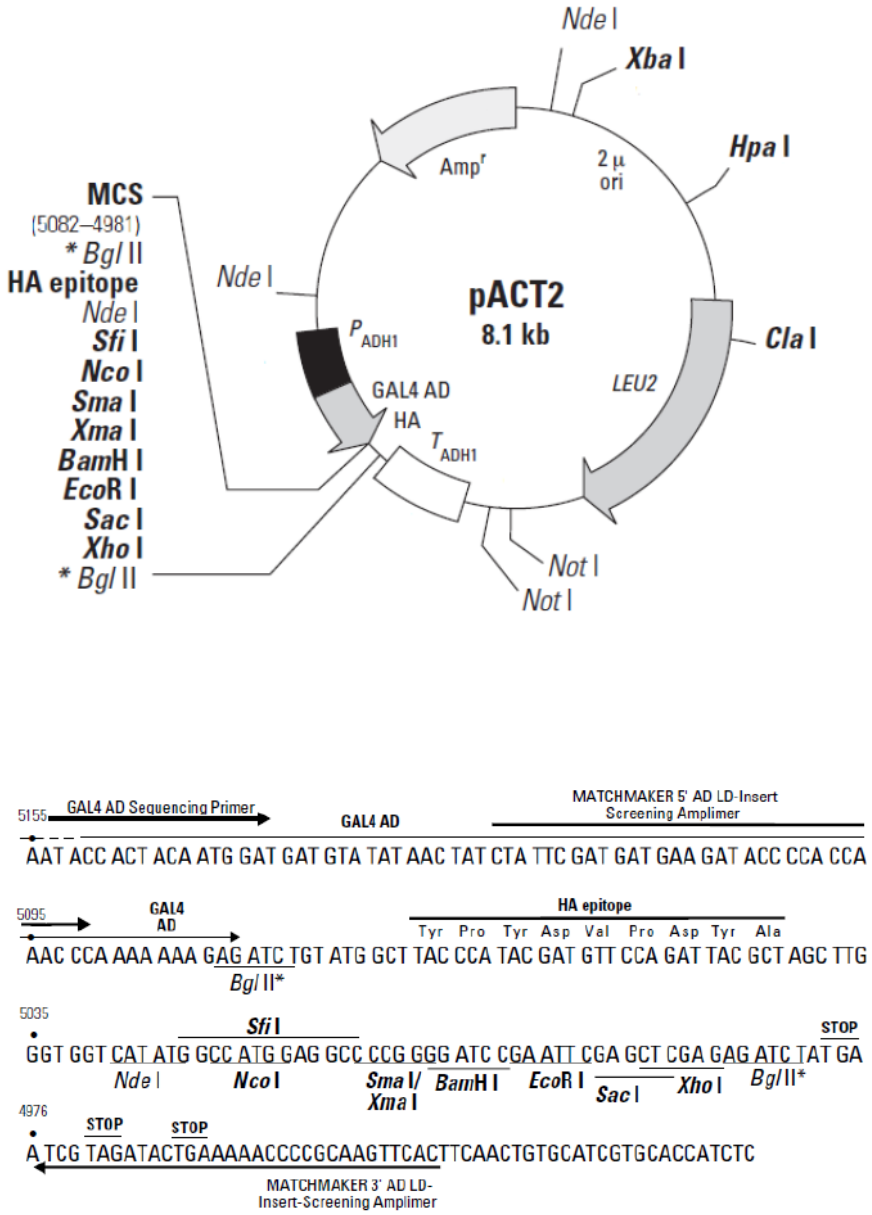

Figure A.2. Restriction map and Multiple Cloning Site (MCS) of pACT2 vector which is used in Yeast-two Hybrid screening for the expression of cDNA library proteins.

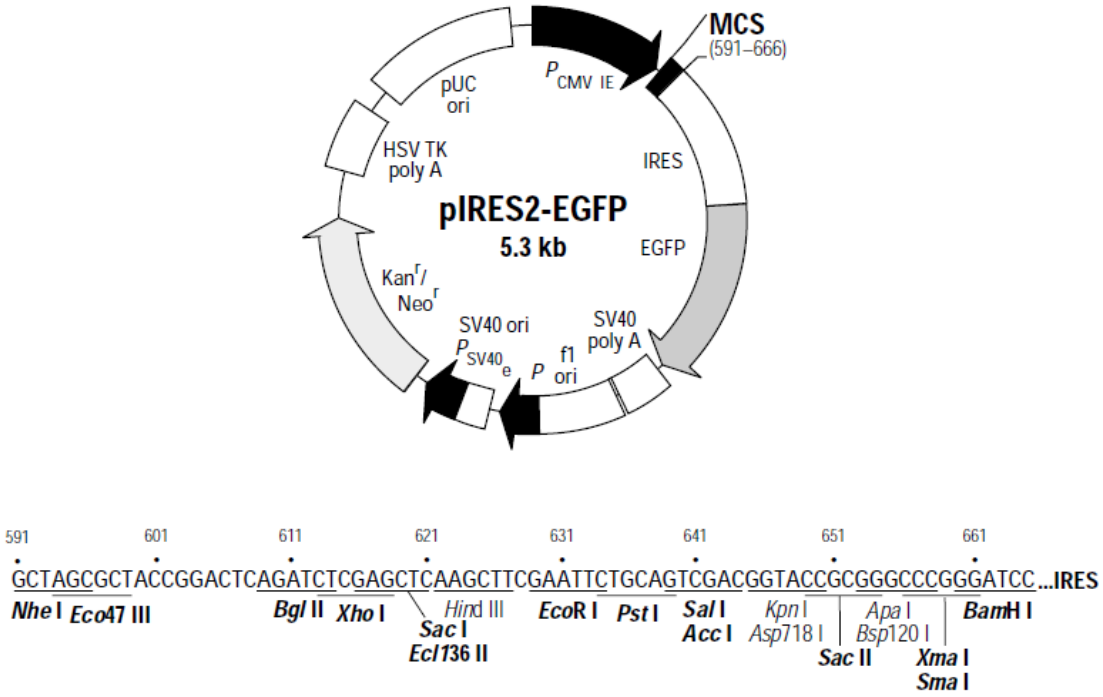

Figure A.3. Restriction map and Multiple Cloning Site (MCS) of pIRES2-EGFP vector which is used for the cloning and stable expression of the genes in mammalian cells.

APPENDIX B: QUANTITATIVE REAL-TIME PCR ANALYSIS OF MGAT1 AND BRI3 IN ISOLATED TUMOR SAMPLES

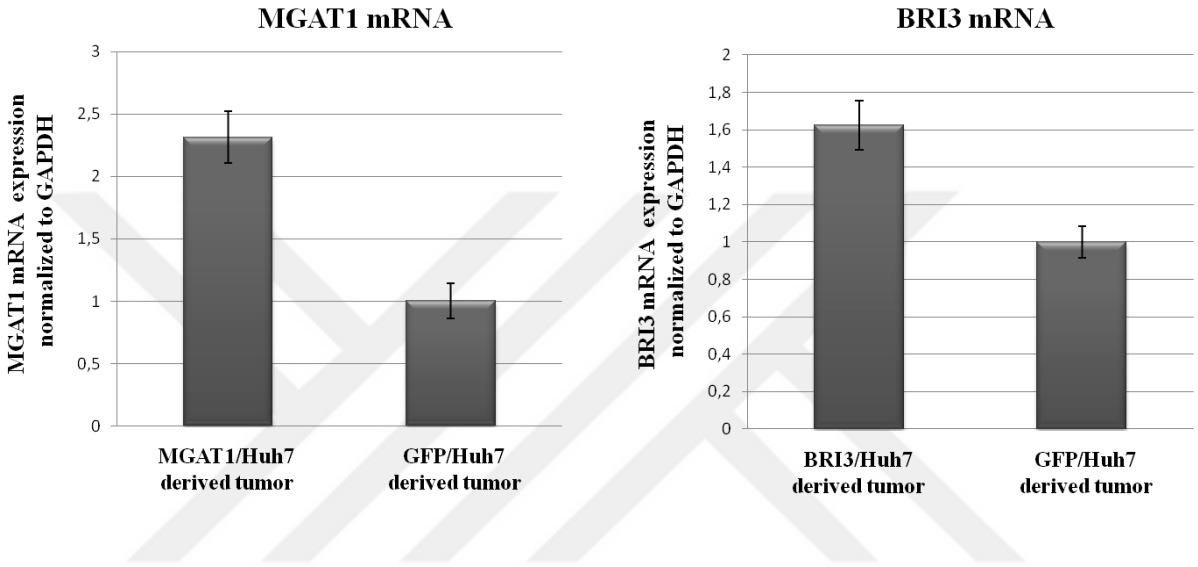

Figure B.1. Determination of MGAT1 and BRI3 mRNA levels in isolated tumors samples. Error bars represent standard error. Expression levels of MGAT1 and BRI3 were normalized to GAPDH as the control.

APPENDIX C: COUNT NUMBERS OF MGAT1 AND BRI3 IN TUMOR SAMPLES AS DETECTED BY RNA SEQUENCING

Table C.1. RNA-Seq count numbers of MGAT1 in three pairs of biological replicates.

	Count numbers of MGAT1		
MGAT1-replicate 1	199,64	42,40	**GFP-replicate 1**
MGAT1-replicate 2	166,77	97,84	**GFP-replicate 2**
MGAT1-replicate 3	55,39	0	**GFP-replicate 3**

Table C.2. RNA-Seq count numbers of BRI3 in three pairs of biological replicates.

	Count numbers of BRI3		
BRI3-replicate 1	14,32	0	**GFP-replicate 1**
BRI3-replicate 2	18,61	4,03	**GFP-replicate 2**
BRI3-replicate 3	34,77	29,92	**GFP-replicate 3**

APPENDIX D: RNA INTEGRITY NUMBERS (RIN) AND SPECTROPHOTOMETRIC ABSORBANCE RATIOS OF THE TOTAL RNA ISOLATED FROM TUMORS

Table D.1. RIN numbers and spectrophotometric absorbance ratios for the MGAT1 and GFP replicates. RIN numbers are depicted on a scale of 10, where 1 represents fully degraded RNA and 10 represents intact RNA.

	A_{260}/A_{280}	A_{260}/A_{230}	RIN
MGAT1-replicate 1	2,11	1,98	9,5
MGAT1-replicate 2	2,08	1,97	8,9
MGAT1-replicate 3	2,09	1,90	9,4
GFP-replicate 1	2,07	1,92	9,8
GFP-replicate 2	2,13	2,00	8,8
GFP-replicate 3	2,09	1,84	7

Table D.2. RIN numbers and spectrophotometric absorbance ratios for the BRI3 and GFP replicates.

	A_{260}/A_{280}	A_{260}/A_{230}	RIN
BRI3-replicate 1	2,09	1,87	8,8
BRI3-replicate 2	2,04	1,46	9,1
BRI3-replicate 3	2,09	1,93	8,8
GFP-replicate 1	2,09	1,96	9,5
GFP-replicate 2	1,96	1,15	8,1
GFP-replicate 3	2,08	2,04	9,8

APPENDIX E: RNA INTEGRITY ANALYSES BY AGILENT BIOANALYZER

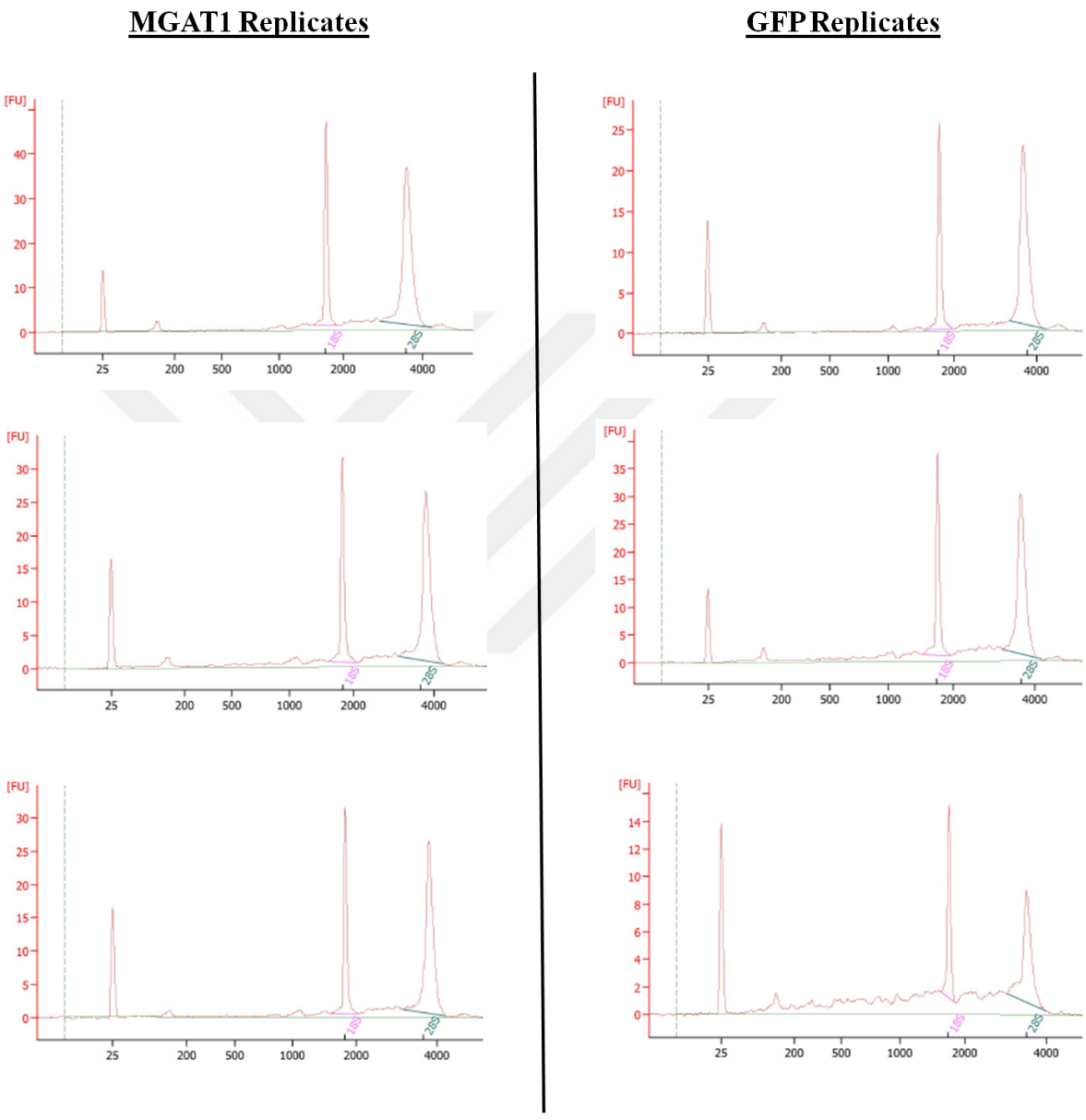

Figure E.1. Agilent Bioanalyzer results of total RNA extractions from MGAT1 and GFP tumor replicates.

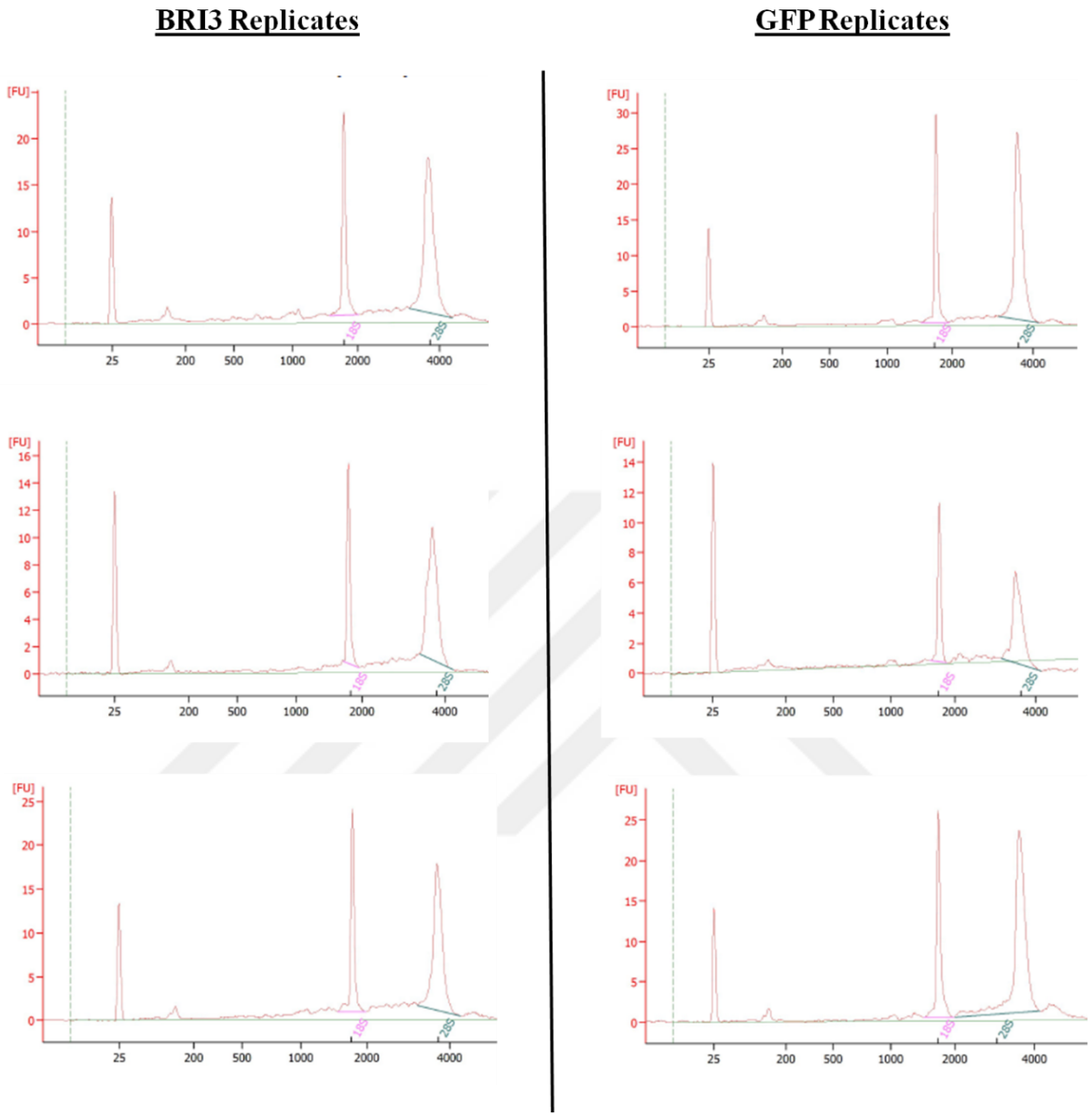

Figure E.2. Agilent Bioanalyzer results of total RNA extractions from BRI3 and GFP tumor replicates.